Study of the flight dynamics of a kite

Rogelio Lozano

UNIVERSITÉ DE GRENOBLE

THÈSE

Pour obtenir le grade de

DOCTEUR DE L'UNIVERSITÉ DE GRENOBLE

Spécialité : **Automatique-Productique**

Arrêté ministériel : 7 août 2006

Présentée par

Rogelio LOZANO Jr

Thèse dirigée par **M., Mazen ALAMIR**
et codirigée par **M., Ahmad HABLY**

préparée au sein **GIPSA-Lab, Département Automatique**
et de **Électronique, Électrotechnique, Automatique, Traitement du Signal**

Etude du vol d'un générateur cerf-volant.

Thèse soutenue publiquement le **30 Avril 2014**,
devant le jury composé de :

M., Frédéric BOYER
Professeur à l'Ecole des Mines de Nantes, Président

M., Luc JAULIN
Professeur à l'ENSTA-Bretagne, Brest, Rapporteur

M., Simon LACROIX
Directeur de recherche CNRS au LAAS, Toulouse, Rapporteur

M., Mazen ALAMIR
Directeur de recherche CNRS au GIPSA-lab, Grenoble, Directeur de thèse

M., Ahmad HABLY
Maître de conférence à l'ENSEEE, Grenoble , Encadrant

M., Jonathan DUMON
Ingénieur d'étude CNRS, GIPSA-lab, Grenoble, Examinateur

Table of contents

Acknowledgement

Cette thèse n'aurait pas existé sans la contribution de ma famille. C'est à eux que je dois la curiosité qui me fait étudier, questionner, remettre en question ce qui à première vue semble évident, chercher à comprendre et apprendre.

Enfant, j'ai passé la plupart de mon temps à construire des modèles réduits d'avions. J'ai eut la chance d'avoir eut des parents qui me prêtaient leur trousse à outils et leurs matériel artistique, malgré le fait que je perdais ou cassais la majorité des outils que j'utilisais. Mais mes parents ont cru en moi et ont continué à me prêter des outils et du balsa pour que je construise mes avions. Mes débuts dans l'aviation ont été une succession de crashs et de reconstructions. Mais avec de la passion, des livres, du courage et des efforts, mes avions ont de mieux en mieux volé et aujourd'hui, je vis de la mise au point de machines volantes innovantes. C'est cette passion qui est à l'origine des résultats actuels, et je la dois à mes parents. Merci.

Cette thèse m'a beaucoup apporté, et c'est principalement grâce à mon directeur de thèse, Mazen ALAMIR. Il est pour moi l'incarnation de la métaphore "une main de fer dans un gant de velours", en supposant que la main représente son raisonnement, et le gant, sa façon de l'exprimer. Mazen se distingue par la clarté limpide de son raisonnement, par ses explications, par sa façon de poser des questions, et par sa façon de s'exprimer. J'ai appris énormément à ses cotés.

Je voudrais remercier mon co-directeur de thèse Ahmad HABLY pour toute l'aide qu'il a pu m'apporter tout au long de cette thèse. Ahmad a toujours été là pour m'aider, me motiver et pour partager ses connaissances avec moi.

L'ensemble de l'équipe technique du gipsa-lab a beaucoup apporté à cette thèse. Jonathan DUMON m'a beaucoup aidé quand à la partie informatique et à l'instrumentation des prototypes. La qualité des mesures impacte directement la stabilité du système et c'est en partie grâce à lui si les expériences ont si bien fonctionné. Je voudrais remercier les frères BLANC pour tout ce qu'ils ont pu apporter au projet. Ils ont toujours partagé leur connaissances, leurs anecdotes et leur bonne humeur. Je voudrais aussi remercier Daniel REY, Laurent OTT, Ghatfan HASAN, Julien MINET, Pascal BELLEMAIN et Olivier CHABERT pour toute l'aide qu'ils ont pu m'apporter.

Parmi les professeurs qui m'ont le plus inspiré, je voudrais particulièrement remercier Marc MASSOT, professeur à l'ECP. Ses cours ont été pour moi la preuve que l'on peut enseigner des sujets très complexes, en étant à la fois très rigoureux, très pédagogue et très sympathique. Il est le professeur et le scientifique qui m'a le plus impressionné, motivé et donné confiance en moi. Les cours de Franck RICHECOEUR m'ont aussi beaucoup apporté, entre autre ils m'ont montré que les ailes classiques ne sont pas toujours la meilleure solution pour générer la portance, plusieurs de mes prototypes ont été mis pour la première fois sur le papier pendant, et grâce à ses cours.

Une autre partie de mes enseignements vient des pionniers de l'aérospatiale. Ils m'ont servi de preuve que l'on peut arriver à des résultats incroyables en partant de très peu. Ils sont mes modèles, mes sources d'inspiration et de courage. Je voudrais remercier Otto LILIENTHAL, Alberto SANTOS-DUMONT, Paul MACCREADY, Igor SIKORSKY, Etienne OEMICHEN, Rotislav ALEXEYEV, Werner VON BROWN et Sergei Pavlovich KOROLEV. Pour ceux qui ne les connaissent pas encore, arrêtez de lire cette thèse et lisez leurs biographies.

Mes amis ont toujours été là pour moi, je voudrais remercier chaleureusement Fanny, Quentin, Quendi, FX, David, Francois, Marie, Xavier, Pierre Loup, Jessica, Yo, Clem, Benoit, Lucie, Jordan, Germain, Valentina, Alexandra, Emerick, Claire, Luce, Thibault, Mihaly, Gérome, Lauren, Laurent, Amélie, Audrey, Anthony, Yayatte, James, Soheib, Ignacio, Tahar, Simona, Hamal et tous les autres... Les voyages, la musique, les soirées, les rencontres, les fous-rires ont été avec et grâce à eux.

Enfin, je voudrais remercier celle qui donne du sens au temps qui passe. Elle me démontre tous les jours que l'art et la science n'ont de sens que s'ils grandissent ensembles. Adela, sachant qu'un mètre cube d'hélium génère une poussée d'Archimède d'environ 1 Kg, combien d'hélium nous faudra-t-il pour faire un diner avec une vue imprenable sur la planète terre ?

Chapter 1

Introduction

Nowadays, nobody questions the need for progress in exploiting renewable sources of energy as oil and gas are running out too fast besides their dramatic impact on our environment. Nuclear energy is facing increasing serious questioning regarding its safety, its real long-term cost in terms of cleanliness and financial recycling budget.

Consequently, investigating renewable sources of energy is no more an option, but a real unavoidable necessity.

Wind is considered as an ideal source of renewable energy since it is infinitely sustainable and clean. Between 2000 and 2009, wind energy global production capacity increased more than nine-fold, growing from 17GW to 160 GW [2]. This makes wind not only the fastest growing renewable energy resource, but also the fastest growing electrical power resource of all.

A conventional wind turbine is a two/three blades rotor, that converts wind's kinetic energy into electrical energy. This is done by direct coupling with an electric generator or through a gearbox. The turbine is installed on the standard electric grid using a power electronics interface. The turbine power is controlled by the pitch and yaw blades angles. The whole conversion chain and the blades control unit are placed up next to the rotor hub, on the turbine tower. As for turbines size and rated power, in 2010 ENERCON has presented its E-126 wind turbine whose rotor diameter reached 126m, a tower height of 135m and a total mass of 6000 tons; this turbine's rated power is 7.5 MW (figure 1.1).

One aim of increasing turbines size is to reach higher altitudes where wind is known to be stronger and more stable. In fact, the amount of wind energy that is available for extraction increases with the cube of wind speed. The other objective is to increase the blades size and, consequently, the turbine working area, with which the available wind power increases linearly.

Wind turbine size is not expected to grow as dramatically in the future as it has in

Figure 1.1: The assembling of the E126 wind turbine.

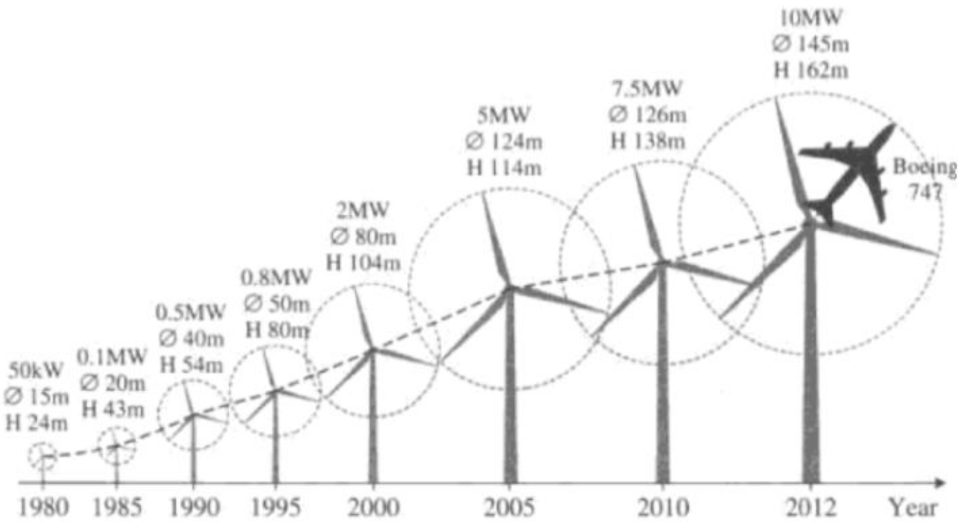

Figure 1.2: Evolution of the tund turbine size and respective power [3]

the past [4], for the cost which includes manufacturing, transportation and construction at some point starts growing faster than the resulting rated power [5]. At present, the highest wind turbine reaches 200m where the wind is still unstable with an acceptable speed. Nevertheless, strong wind could be present at higher altitudes with little or no wind at low altitudes. To overcome these limitations, high altitude wind kite concept has emerged and is currently heavily investigated by many research groups and emerging start-up companies.

For instance, for a 2MW wind turbine, the rotor and the tower weight is about 300 tons. For the same power range, 500 m^2 air foils and 1000m cable length would have a weight of approximately 2 tons.

This difference of weight/power ratio comes from the fact that most of the energy produced by wind turbines is produced by the tips of the blades, the rest of the structure being mostly used to support these blades.

Instead of using such a structure, the kite systems use a tether and a control system to make the kite follow the desired trajectory.

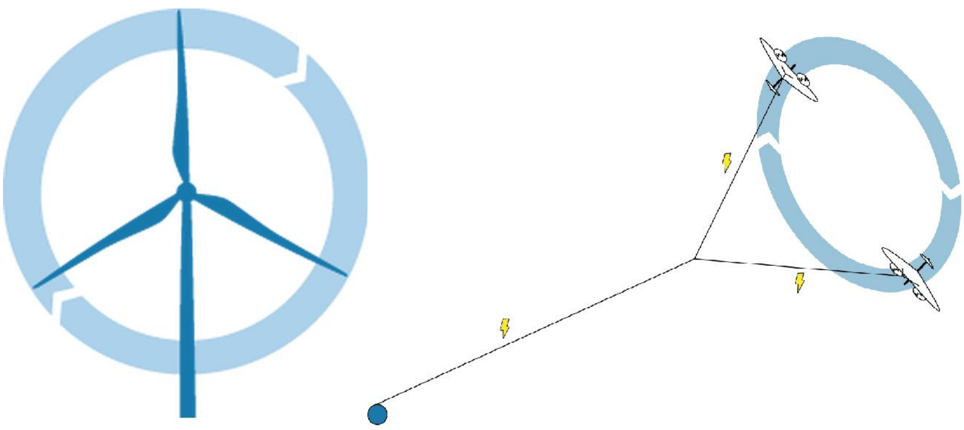

Figure 1.3: The wingtips of the windturbines produce most of the energy, kites systems propose to only use this blade section to harvest wind energy. Illustration by R.Paelinck [17].

A recent report [6] indicates that by 2015, fully autonomous kite-based systems, including start/land automation will be commercialized. These systems are expected to reach 75 percent of their capacity by 2021. These promising predictions reflect a rather optimistic view as many technical challenges are still to be addressed. Moreover, as it is described later on, there are still many available options regarding the design, the energy management and the trajectories to be achieved to cite just few items. This suggests that a maturation time is needed before a stabilized solution gathering a commonly shared acceptance from a technological, economical and safety point of view imposes itself. But maturation comes only with experiments and by facing the candidate solutions with reality. The present work aims at participating in this highly challenging and collective adventure.

1.1 How to produce energy with a kite?

The first paper describing the production of electricity with a kite was written by Miles L.Loyd in 1979 [7]. It was called crosswind kite power and described two different ways of producing energy using a kite. The first method was called "Lift mode": As the kite would fly in circular trajectories, the lift force produced by the kite would be used to pull a load. The "Drag mode" consisted in using small wind turbines placed on the kite to generate electricity that would be transferred to the ground by a conductive tether.

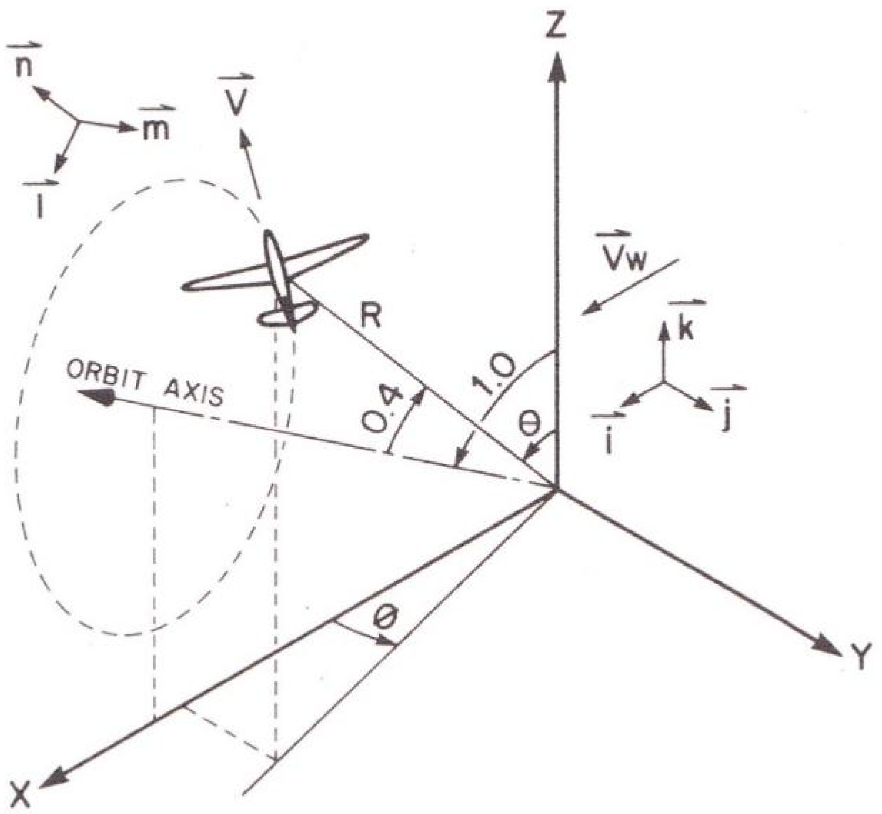

Figure 1.4: The scheme of the flight trajectory [7].

The results of his calculations are that with a wind speed of 10 meters per second, a kite of 576 m^2 of wing area and a Lift to Drag ratio of 20, the output power of the system would be 6.7 MW.

1.2 State of the art

From 2005 to 2013, the number of companies and university research teams grew from less than 10 to approximately 50 [8]. The kite systems that have been build and flown

will be here classified into 7 kinds of different solutions. The state of the art section will be divided into 2 subsections that will aboard the following topics:
- The first section will present the flying prototypes made by universities that work on this concept.
- The second section will present a part of the academic research, the studied topics, their proposed solution.

1.2.1 On-board power generation flying prototypes

1.2.1.1 Kite-based prototypes

The Makani company [9] has developed several flying prototypes that work with the following principle: The kite is a rigid wing structure equipped with four electric motors connected to propellers, see figure 1.5.

Figure 1.5: Makani's prototype in flight.

During the takeoff phase, the kite takes off vertically using its 4 brushless engines like a standard quadrirotor. Once it has reached a certain altitude, it starts flying following circular trajectories. At that moment the kite is propulsed by the wind and propellers are no longer used to provide trust but to generate electricity as small wind turbines do. The produced energy is transmitted to the ground using a conductive tether. The wing is used to provide wind speed to the propellers: "Due to its speed, the tip of a conventional wind turbine blade is the most effective part and is responsible for most of the energy produced. The Makani Airborne Wind Turbine (AWT) takes advantage of this principle by mounting small turbine/generator pairs on a wing that itself acts like the tip of a traditional turbine blade. The wing flies across the wind in vertical circles, fixed to the ground by a flexible tether". During the landing phase, the kite flies again like a quadrirotor and reaches back its base, see figure 1.6.

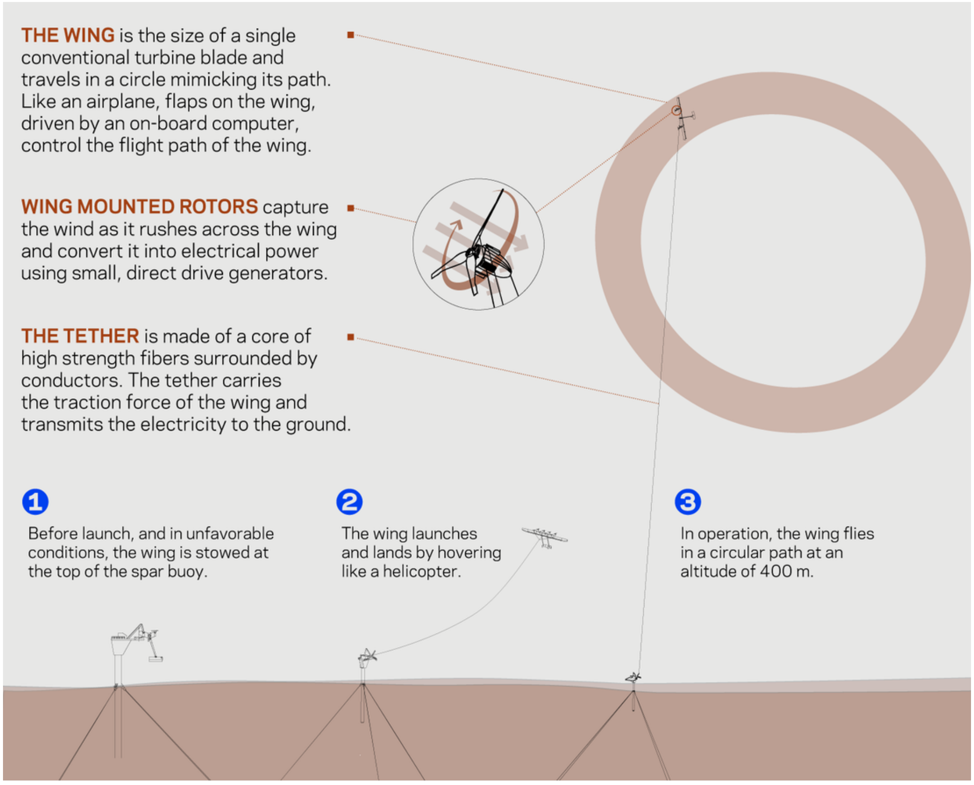

Figure 1.6: Makani's working principle [9].

This company was one of the first to perform autonomous flights. Their last prototype generates 30 kW with a wind speed of 11.5 m/s. Its wingspan is 8 meters and its operational altitude range is between 40 and 110 meters.

1.2.1.2 Autogyro based prototypes

The company Sky WindPower [10] developped a prototype that looks like quadrirotor of four flying wind turbines, see figures 1.7 and 1.8. As the wind passes through the rotor, the aerodynamic forces are used for both lifting the prototype and generating energy. The energy is sent to ground by a conductive tether. Up to now the team has built several flying prototypes.

1.2.1.3 Blimp based

Altaeros Energies [11] is developing a buoyant airborne wind turbine for remote power applications. The buoyant shell is designed to incorporate sufficient lifting gas volume to stay aloft in light winds while providing aerodynamic lift and passively stable flight characteristics in strong winds. In the middle of the blimp, a wind turbine generates the

Figure 1.7: Sky Windpower's prototype.

Figure 1.8: Sky Windpower's tests. The truck is used to generate windspeed and the structure is used to avoid crashes.

electricity that is sent down via the conductive tether to the ground, see figure 1.9.

1.2.2 Ground based power generation

1.2.2.1 Airfoil based generation

The concept has been developed by several companies and universities [12][13][14]. The kite is generally a paraglider, a kitesurf of a rigid wing, see figures 1.10, 1.11 and 1.12.

Paragliders and kitesurfs have some advantages regarding safety and tolerance to crashes. Moreover, many of them can be pourchased easily. Their flight performances are not as good as the rigid wings that have a greater Lift to Drag ratio.

For the paraglider and kitesurf-like systems, the control unit can be whether embedded or

Figure 1.9: Altaeros's flying prototype.

Figure 1.10: Enerkite's prototype.

on the ground. Embedded systems have two main problems, their energy consumption and the extra weight. The on ground control of kites uses the difference of length of cables to control the kite, see figure 1.13.

The performances of the Enerkite's prototype (see figure 1.14) are an output power of 30 kW [12], the operational altitude varies from 100 to 300 meters with a wind speed of 10 m/s, the kite is a paraglider of 21 m^2 of wing area that has a weight of approximately 7 kg.

Figure 1.11: Enerkite's prototype.

Figure 1.12: Ampyx power's prototype.

Figure 1.13: Enerkites' control winch system.

Figure 1.14: Enerkites prototype in flight.

1.2.2.2 Magnus effect based generation

The Magnus effect is a technique to generate lift by turning a sphere or cylinder. As the wind blows on the turning cylinder for example, it will produce a lift force comparable to the lift of a wing (see figure 1.15). This lift can be used for kite energy generation and is currently studied by the Omnidea company[15]: "The results of a demonstrator 16 meters in length and 2.5 m in diameter are provided as a proof-of-concept and current tests using a larger scaled-up version of 25 meters are discussed as a basis of a system that will deliver power in the MW range and be capable of operation at altitudes of about five km.". In order to work, the prototype needs to have an electric motor system that makes the cylinder turns and electric cables in order to supply power to the kite.

Figure 1.15: Omnidea's prototype in flight.

1.2.2.3 Traction of vehicles

The kite's traction has been used since very long time ago for transportation. Small boats, land buggies, surfboards, skis, sledges, etc. About ten years ago, the German company SkySails [16] has scaled up the kites and has developed a kite traction system for tanker boats, see figure 1.16. The last prototypes were able to generate an amount of traction equivalent to 2 MW.

Figure 1.16: Sky sails prototype in action.

1.2.3 Academic research

There are about 3 main teams that are active in the field of kite energy generation:
- The KU Leuven's team [17]
- The TU Delft's team [13]
- The Politechnico de Torino [18]

The Delft team has published many papers about the control of a kites system, from [38] to [52]. They have worked on many flying prototypes and on structural designs of the kite, specially on the aeroelasticity problem from [63] to [73]. They are known for their laddermill concept [53]. Initially, they proposed using rigid wings, but due to safety issues [54], they were soon changed by flexible light-weighted kites. Suggestions are made to improve this concept's maximal power by using multiple kites on the same cable (or set of cables). One can see in figure 1.17 two proposed structures. The first is to have a stack of kites, for instance the laddermill of Delft [55]. The second is to link two kites to the end of the same cable, which is useful to reduce the cable drag [34]. Both described structures will allow having the same traction force for a smaller space and less land requirements, but are more difficult to be modeled and controlled.

For early experiments, the delft team used commercial kites were used, such as the clark-y kite ($10m^2$) used in KiteGEN program [55], the Peter Lynn Guerilla ($10m^2$) Kite used by Worcester Polytechnic Institute (WPI) team [96], and the Peter Lynn Bomba ($8{,}5m^2$) surf-kite used by Delft team for their smallscale 2kW testing laddermill [56]. However, much bigger and more specialized kites must be designed and tested in the future.

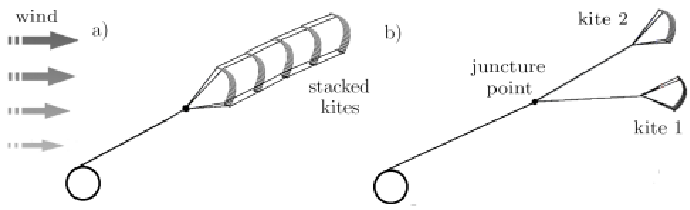

Figure 1.17: Multiple kite proposed structures [33].

The team of the KU leuven directed by Moritz Diehl developed many control techniques, specially MPCs, from [19] to [32]. They developed the concept of twin kites that increases the amount of produced energy [17]. The twin kites concept uses two kites and one rope that gets divided in two branches. On the end of each branch, one kites performs their flights. The first section of the cable has very few displacement with respect to the air, as a consequence, few energy is lost due to the the tether's drag. Recent work has been focused on rotational takeoffs [34] to [37], see figure 1.18.

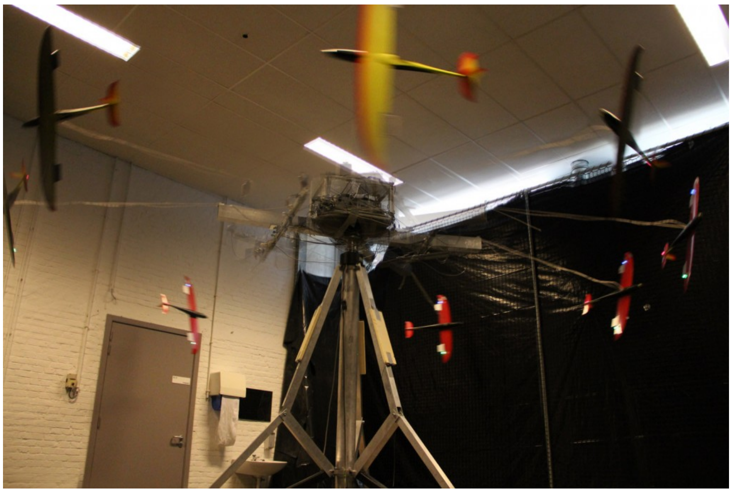

Figure 1.18: The rotational start system in action.

From the control point of view nonlinear model predictive control (NMPC) has made simulations that seemed to be convenient to generate the needed controls for trajectory tracking, though, [39] doubted the performance of this method, because it leads the solution to converge to different local optima depending on the initial conditions, and consume a lot of memory when it comes to application. Still NMPC was used in [74, 57, 90]. Other trajectory tracking suggested methods include neural network control [92], robust control [46], direct-inverse control [93], and nonlinear adaptive tracking control [39]. Two examples of control strategies are mentioned here. In T.U.Delft, a one-cable kite control is tested in simulation; the kite surface is 25m^2 with a mass of 50kg and the cable average length is 1000m. An optimal control is used to command the roll angle, attack angle, and the cable length variations rate. It uses different random guesses because there is no guarantee that the obtained solution is a global one. Also, for large scale kite-based systems, the cable model should be considered when controlling the system. A realistic model will take into account the cable weight and drag force, and includes its elasticity [42], [58].

1.2.4 Overview of the Contents

The following work will be divided in 6 chapters: The first chapter will present a study on the Aeronautic Pioneers work. It will describe how innovation was made in the aeronautics field. This work will be illustrated by some of the greatest breakthrough of the last century. This chapter will be by very far the most important of the manuscript for those who aim to do experimental work, proofs of concepts, new concepts and that aim to develop their companies on these concepts.
The second chapter will present the first kite prototype developed. The objectives of this work were to study the flight and the control of a flying prototype. The kite was flown indoors in a wind tunnel that was specially build for the experiment. Several control techniques were applied in order to control the kite's trajectory and the produced power. This chapter led to 3 papers [59][60][61]. The third chapter focuses on a technique used for keeping the kite flying as the wind diminishes without using an on board source of energy for propulsion. The advantages of this technique are that the kite can remain in flight as long as it the wind is too low to produce energy. Using this technique, the kite can avoid landings which require man handling, complex installations and that increase the probability of crash. This technique is called "reverse pumping" and led to the first paper dealing with this topic [62]. Several prototypes were build, many errors were made, the last prototype gave satisfying results.
The fourth chapter describes the outdoor prototype. The study is composed of calculations on the flight characteristics, the experimental setup description and the results of the flight tests. This experience gave the team technical knowledge on how to make outdoor tests on a 3 meters wide kite that flew at around 200 meters high.
The sixth chapter will briefly present three other prototypes that were build and that flew properly but that could not be more studied because of the lack of time.
The conclusion will sum up the manuscript. The reader will find in the annexes a list of some of the accidents that can be provoked in experimental work. The "carnet de vol" will give details of the flights of the 13 prototypes that were built during the PhD.

Note that several movies showing the experimental results can be viewed in [1].

Chapter 2

Pioneers study

2.1 Introduction

This PhD's objective is to develop a working system from scratch to the successful flight test. The system has to be defined as well as all the experimentation process in order to gain time. In such a study, there are huge amount of mistakes that can be done, the history of aviation proves it [78]. The objective of the study of the flight pioneers is to try to learn from their mistakes and successes in order to make more effective our work. Section II will give general motivations to study flight pioneers. Section III will illustrate some of the most important flight pioneer's ways to works in order to make successful projects. Often made mistakes will be presented in section IV and a conclusion will be presented in section V.

2.2 Motivations

The following paragraph will present the main reasons to study flight pioneers and not only the existing kites systems.

2.2.1 Standard aeronautics are a more complete source of information.

The literature on kite systems is few comparatively with standard aeronautics, moreover it does not give much information about the experimental parts, how to build kites, how to test them, how to implement such systems.

2.2.2 Existing kite energy concepts have not proved their maturity.

Kite systems started to be studied about approximately 10 years ago. None of the existing kite systems has gone through long time experimentation or commercialization process. The innovation work might have been done only for a fraction of some potential technological solutions. It is very likely that we are at the very beginning of a long development process and that nowadays prototypes are very different from what they will be in 10 or 20 years. Aeronautics has witnessed hundreds of different concept that went through serious studies, working prototypes, proofs of concept, somewhat like kites systems nowadays, but that were abandoned and forgotten because of some underestimated problem. One shall avoid unreasonable optimism on kite energy system's maturity.

2.2.3 Innovation needs a source of inspiration.

In order to find new concepts and working principles, one needs to find a source of inspiration. Flight pioneers works and experiences are a huge source of ideas. Kites can be seen as tethered airplanes, and airplanes as not tethered kites! Studying aeronautics can teach us a lot from the structural point of view to the flight characteristics, management of the project, the experimental protocols, etc.

2.2.4 Avoiding mistakes by learning from other experiment's failures.

Aeronautics is a domain in which one can do many mistakes that will dramatically slow down the research. By studying the mistakes done by others, we can try to classify them and make some general rules out of it in order to avoid failure. Many examples can be seen from the very beginning of aviation until the most recent researches. This can be resumed in fewer words: let's try to understand what are the differences between a project that succeeded and those which failed.

2.2.5 Learn how to deal with high complexity problems

The approach that pioneers used is very particular in the sense that the overall project treated many different problems. The management of such problems requires special skills of analysis that are more apparent in the history of aviation than in modern research papers. Probably one of the reasons of it, is that a lot of time is needed to have a proper view on the overall project.

2.3 Examples successful experiments

For each of the following aviation pioneer, one work has been selected in order to illustrate one particular way of working that lead to the fulfillment of the project.

2.3.1 Interpreting results one hundred years later

It is a complex work to judge the success of projects using the few material that can be found. Most of the documentation is made of books that were written long time ago, pictures and vintage movies. Trying to interpret such material is a work that certainly requires skills of a literary expert, historian, inventor, and experimental flying machines experience. At most, the author has some skills about experimental flying machines but the rest of the skills are certainly none of his competence. Before trying to analyze their work, the author would like to remind that he has an infinite respect for all the flight pioneers, from those who never got off the ground to the most successful of them. This work has only one aim, avoid to repeat mistakes and learn from other's experiences.

One easy way to know how successful was the work could be to ask "did everything worked as expected?". If the answer is:" Yes, absolutely ", the study is then a complete success, but from all the literature read about flight pioneers, it has almost never been the case when great levels of innovation were involved. The project that was the closest to that was probably the Gossamer Albatross project directed by Paul MacCready (see figure 2.1) [79][80].

2.3.2 Adding complexity step by step and choose the best environment to perform tests.

Otto Lilienthal developed some of the first gliders and made hundred of successful flights between 1890 and 1896 when died because of a crash [85]. His work was one of the major sources of inspiration for the Wright brothers, that made one of the powered and controlled flight in 1903 [77].

One of their common points is that both learned a lot from non motorized gliders, using slopes to make longer the flights. O.Lilienthal build his own hill with his workshop on the top of it in order to make simpler the experiments, he would takeoff from the top of the hill and land on its bottom. The Wright brothers build their workshop very close from the sand dunes where they made their glider flight tests, (see figure 2.2). Also,

Figure 2.1: The Gossamer Albatross in flight, crossing the english channel with the pilot Bryan allen, pedalling to make the propeller turn, 1979.

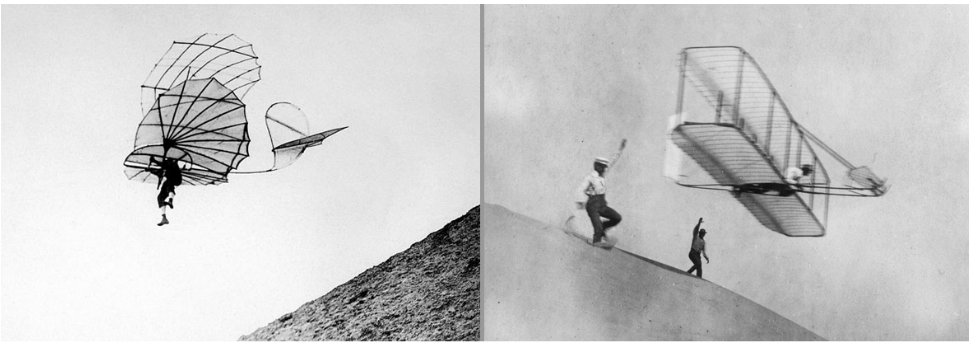

Figure 2.2: O.Lilienthal's flying from the top of his hill (left side). The wright brothers in action, in the sand dunes of Kitty Hawk (Right side).

O.Lilienthal built an aerodynamic forces measurement device, the "whirling arm", the Wright brothers built their wind tunnel (see figure 2.3).

In the case of the Wright brothers, it is very clear that they worked with growing levels of complexity: They started with kites, then one men would get on the kite, then the first flights were made on the slope. When the wind was strong enough, it would make their flight last much longer. Once they mastered the control of a glider, they started working on motorized versions. At the beginning, the power of the engine barely enough to perform flight but in order to solve this problem, they used a catapult. The controlled, self propelled flight was done in 1903 (see figure 2.4). Few time later, another version was made that did not needed the catapult.

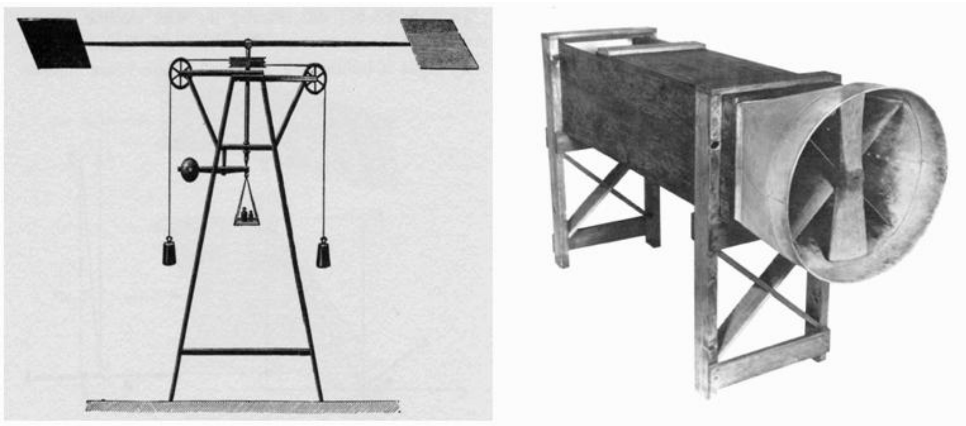

Figure 2.3: O.Lilienthal's whirling arm. As the aerodynamic surfaces would turn, the balance would measure the value of the lift (left side). The wind tunnel buit by the wright brothers (right side).

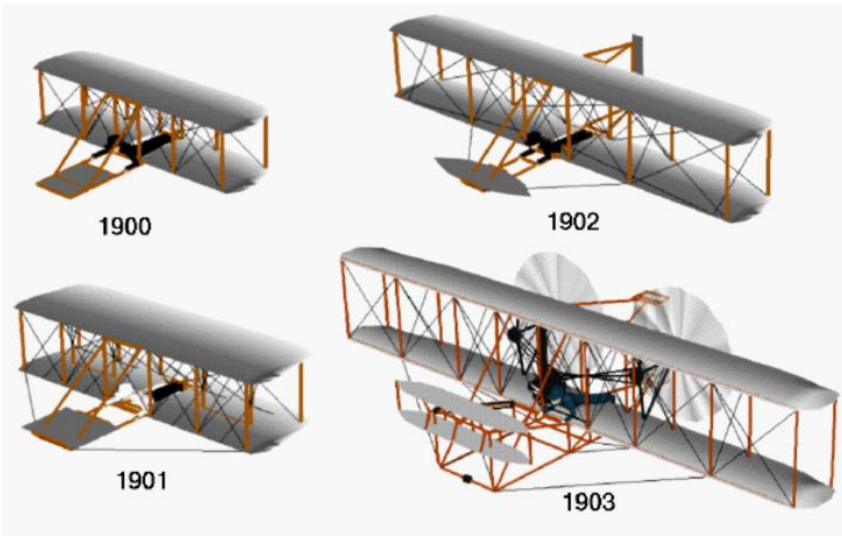

Figure 2.4: The progressive work of the Wright brothers.

The two guiding lines that these pioneers illustrated are that one should make efforts to make the tests as simple as possible and that the level of complexity should increase gradually.

2.3.3 Find targets that are close in results but more easily reachable

One of Victor Tatin's most interesting experiments was the *Aeroplane* that flew in 1879 (see figure2.5) [78]. It was a model airplane that flew using a compressed air motor. Back then, the stability of flight was a complex problem that made much more complex the flight. An unstable model could not prove flight was possible and could not be stabilized with the modern techniques, as the first automatic flight controllers appeared in the 1920's. Still, Tatin found a way to stabilize most of the degrees of freedom of the plane with a very simple process. He made the model airplane fly in circles, by doing so, he used the centrifugal force to fix control the yaw and roll. The remaining model was equivalent to a 2D model in which only the pitch, altitude and speed needed to be stabilized. Note that the model has two non co-axial propellers. Generally, this type of propellers need a high accuracy building in order to not destabilize the model. In this case, the stability due to the centrifugal force made their use more accessible. This prototype was one of the first ones to lift itself on his own power.

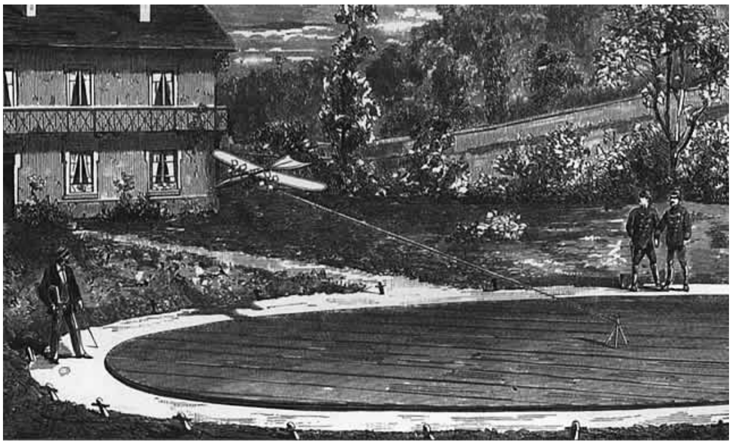

Figure 2.5: Tatin's *Aeroplane*, flying in circles.

Hans Von Ohain and Sir Franck Whittle (see figure 2.6) are the two co-inventors of the jet-engine. The story of how the jet engine was developed is an amazing source of knowledge [81][82]. One of many interesting facts will be exposed here. As Hans Von Ohain was developing the jet engine, he faced the problem that the mixture problems to ignite and had combustion instabilities. The project was financed by the Junkers aircraft manufacturer and they needed to prove that it was worth receiving more financial support. The combustion instabilities were solved by using hydrogen that ignites much faster than liquid fuel. The first prototype HeS 1 functioned with hydrogen in 1937. In 1939, the HeS 3 motorized the Heinkel He 178 airplane and made the first jet powered flight, using this time liquid fuel.

Figure 2.6: Frank Whittle (left) and Hans Von Ohain (right) with their respective jet engines pictures, 1978.

The principal guideline that the previous test illustrates is that, when unknown knowledge seems needed, there might be a partial solution that does not require to solve the problem, but that shunts it.

2.3.4 The right environment

Igor Sikorsky is one of the inventors of the helicopter, he founded the Sikorsky helicopter company that is nowadays still one of the world leaders in helicopters [84]. Studying his work is extremely interesting from all points of view. He developed hid first prototypes of helicopters in 1910 in Kiev, the prototypes could barely lift their own weight (see figure 2.7) He was sure that helicopters would fly one day, but that it was still too early given the low weight/thrust of his experiments.

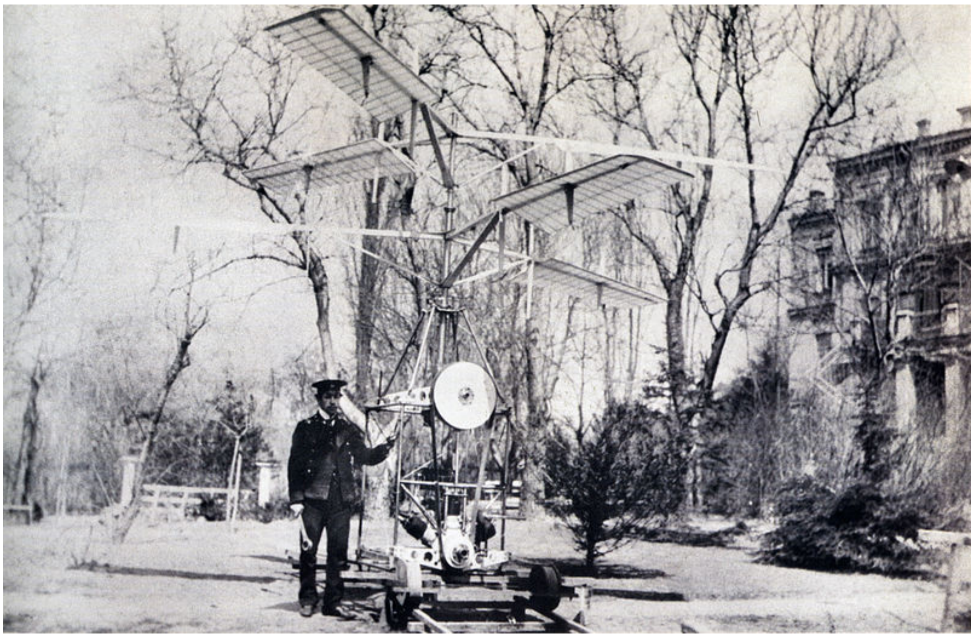

Figure 2.7: Igor Sikorsky with one ofhis early prototypes in Kiev, 1910.

In 1913, he built the S-21 *BolshoiBaltisky* that was the first twin motor airplane, it was also the biggest airplanes in the world. During the Bolshevik revolution, he had to leave Russia and after being in Paris and London, went to the USA. Once there, he spent his first year unemployed in New York. Then, he gave mathematics lessons in a night school for Russian immigrants and made conferences about the development of aircraft, until he put together enough money to open the Sikorsky Aero Engineering Corporation. He installed the workshop in an old chicken farm that a Russian friend lend him. With a few Russian workers, he started the construction of the S-29 A, a twin motor transport aircraft. Six years later, he had sold more than a hundred aircraft. Once that the economical problems were gone, he started again the research on helicopters and made successful flights of helicopters.

He said later that he found in the U.S.A. what he was looking for: "a strong country that was dynamic and that had a strong entrepreneurship spirit". This example shows how the development of such projects is dependent on its environment, the created opportunities. The other point is that the ambitions of the project have to be in adequation with the available technologies.

2.3.5 Innovating when the solution seems to be known and the easy to fix experiments

In 1959, the industrialist Henry Kremer established a series of monetary awards that were given to the pioneers of human powered flight [86]. The first Kremer prize of 50,000 pounds would be awarded to the first human-powered aircraft to fly a figure eight around two markers one half mile apart, starting and ending the course at least 10 feet above the ground.

Many teams joined the contest and built flying prototypes, like the PUFFIN human powered airplane (see figure 2.8). Its wingspan was 26 m for an empty weight of 54 Kg. One can see in the picture the complexity of the structure.

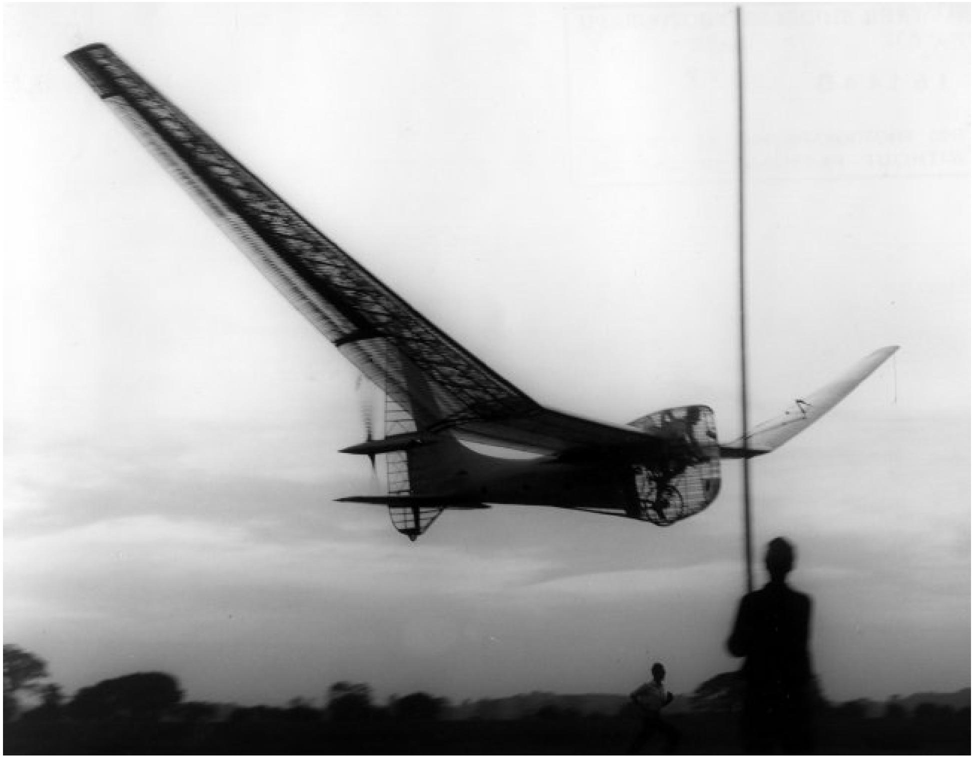

Figure 2.8: The puffin airplane in ground effect hovering.

Several teams made protoytpes that did fly but none had made prototypes that could turn. They would crash during the turns and a huge amount of time would be spent for repairing such complex structures. Their approach of the problem was basically to take as starting point the lightest existing sailplane and to modify it in order make it validate the requirements of the contest. Turning trials would fail and crash the model, the reconstruction would take time, and such prototypes have a very limited lifetime: after a certain amount of crashes, they would need to be rebuild from scratch. A lot of time was spent without reaching the requirements.

The approach of Paul MacCready's team was different by three principal guidelines.

- The first one is that they worked with a growing level of complexity. The first prototype tested was built in 10 days and tested in a parking, without pilot.The second was tested with a small pilot, Parker MacCready, (MacCready's son, see figure 2.9).
- The second point is that contrarily to the other competitors, their structure was made easy to repair. This led them to a huge gain of time.
- The third point is that the principle of working was designed specially for the prize, instead of adapting an existing concept. The turning problem, the construction, the aerodynamics and the global shape were adapted to the wining the prize and completely different from what could be done with the other approach.

After some flights, some crashes, and some other intermediary models, the Kremer prize was won.

Figure 2.9: The Gossamer Condor in flight with Parker MacCready as pilot.

Paul MacCready (see figure 2.10) continued his remarkable and exemplar career in aeronautics, and received the award of engineer of the century by the academy of achievement, and more than 50 other very prestigious awards.

Figure 2.10: Paul MacCready and a part of the brushless engine mounted on the Helios solar airplane.

2.4 The mistakes of Ikarus

The following section will present often seen mistakes that shall be avoided. Note that mistakes can be done by extremely experienced and skilled persons.

2.4.1 Too big too fast.

A very classic mistake is to start building flying machines by a huge, heavy, dangerous and extremely complex prototype. Validations on smaller prototypes are not made and the result is very often a non repairable crash. One example is the 1894's Hiram Maxim's *AirLeviathan* , see picture (see figure 2.11). Note that Sir Hiram Maxim's was the author of more that 200 inventions [78].

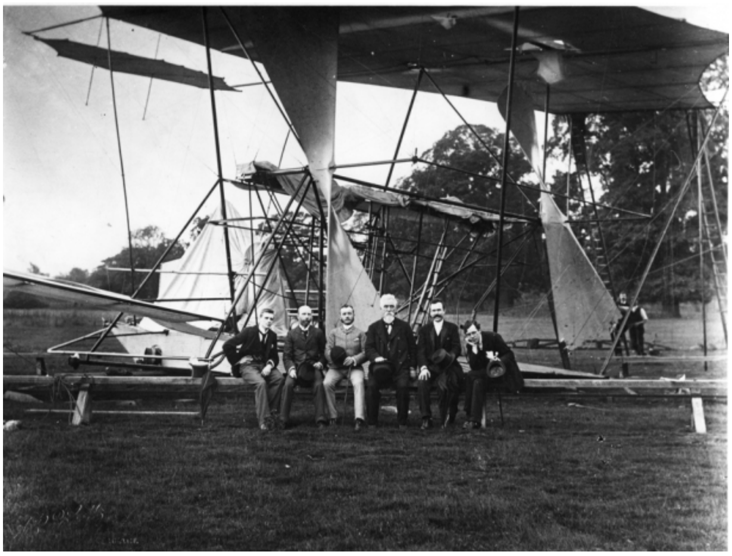

Figure 2.11: Sir Hiram Maxim's (fourth from the left) after an unsuccessful attemps of flight of the *AirLeviathan*.

2.4.2 The post flight experience.

Being a very talented inventor that brought incredible innovations does not guarantees to receive the deserved success. It also happened to many flight pioneers. For example, the Wright brothers had in 1903 a tremendous advance on the rest of the world. In Europe, the first comparable flights were made in 1906-1907 by Santos Dumont, in France [78]. Nevertheless, the Wright brothers stayed ahead of the game from the technological until roughly 1909, when Louis Bleriot crossed the channel. Still, during the years between 1903 and 1909, they received few funding to develop their projects, the army even said that aviation would not be useful for them. They lost their technological advance after 1910 and a few years later, they were no longer in the game. They were the first to build an actual airplane, but they never really got the success they deserved. As a conclusion, staying in the game require more skills than only invention.

2.4.3 The explorers of the unknown.

There are many cases known of persons that jump from great heights with very basic wings attached to their arms, trying to fulfill the dream of Ikarus. Most of them found death. Those persons might have a similar way if thinking than 15th century's sea explorers, heading to the unknown, thinking that the risk is worth the cause. They must have had many different kind of motivations. During most of last century, the idea of flying with wings attached to his arms was associated to madness. But once a sufficient level of experience was attained, these wings started to be improved and mastered. In may 2012, Gary Connery jumped from a helicopter with wings attached to his arms [88]. He flew and landed in a huge amount of card boxes settled to make the landing softer (see figure 2.12). He accomplished one of the dreams of hundreds that died trying to make the same flight.

The conclusion is that with the proper way of studying the problem, things that were seen as "impossible" become possible.

Figure 2.12: Gary Connery landing without parachte, 2012.

2.4.4 The modern researcher's mistakes

Some other kind of mistakes are often observed. Their origins are not well understood, but overconfidence and lack of experience seem to be involved often. They can be seen an effect of having a non rigorous, fuzzy way of thinking, they seem to diminish with experience and with the amount of crashes experienced, but it is not sure. The following list will try to categorize them and give some of the most frequent examples. These examples were heard or experienced by the author, from persons that are considered as specialists in UAVs.

- Over-sized optimism and underestimation of difficulties. It happens very often when people have few experience. As one starts to know more, he might still do this kind of mistakes but he will listen more when he will receive a warning about the error. The not experienced victims of over-sized optimism will not listen the good advise, probably because they are not aware of the difference between an experienced person and themselves. Example: "You will see, this thing will fly, we will study the aerodynamics later, once we have measured data in flight.".
- Generally accepted false beliefs and wrong analogies. Here are some examples:
  - "Coaxial helicopters are more efficient than standard helicopters."

- ”Helicopter’s are stable because the center of mass is situated below the rotor, just like a pendulum.”
- ”Paragliders are ”naturally stable” for the same reasons than round parachutes or helium balloons.”

One hint to recognize this kind of wrong ideas is that they often refer to terms that are odd mixes of therms from different topics that are linked by some unexplained analogical reasoning.

- Late discoveries of great mistakes. In aeronautics, some elements malfunctions can ruin a project or experiment. It can be the case of the engine, the remote control, servos, certain screws, the quality of the soldering, batteries, cable’s, etc. Sometimes, malfunctions could be quickly and easily tested but the working test are not done until it is too late, like a few minutes before supposed takeoff time. That is why elements shall be tested as soon as possible and checklists should be done. In the case of kite systems, one example is the legislation about flight altitudes. If kites systems do not get the permission to fly, most of the studies will have been made in vain. Not having a checklist can lead to forgetting something crucial. Attaching the seat belt of the pilot, checking the battery, the fuel, turning on some important devices are classic examples in aeronautics. Example: ”- Have you tested the servos? -No, they are brand new, why wouldn’t they work ? ”.

- Excessive trust in numerical simulations. This seems to be a direct implication of the lack of experiments made by the researcher. The difference between the experiments and the simulation is very often huge but it is not often visible because experimental validations are not always done. Simulations are a tool and shall not be seen as a proof of concept. The frontier between numerical simulations and Hollywood’s special effects is sometimes very fuzzy. Example:”As you can see, the simulations shows it will fly very well.”.

- Emotion and overconfidence. This phenomenon is well known in paragliding. When everything is doing fine, the level of attention goes lower and accidents may occur. It also happens due to fatigue. Example: ”- It works!!! let’s push it to max power!”.

- Solving a problem by adding complexity when it is possible to solve it by simplifying it. Generally, when two solutions seem to be roughly equivalent, one should choose the simplest and lightest one. One classic example is compensating a weight problem by adding a bigger motor instead of building a lighter model. In the extreme cases, the experimental protocol’s complexity becomes exponential and in the best case, it just does not work. In the worst cases, it can fly with uncontrolled trajectories, catch fire, or even explode. Example: ”The propeller does produce enough trust with the electric motor ? Replace the whole thing by a kerosene jet-engine! ”.

- An other related error that is seen very often is people who want to gain time by making many tests at the same time instead of trying one thing at the time. Working with incremental levels of complexity is very important. Example: ”- I cannot find the problem, the 10 programs won’t work together... - Have you tried them separately ? -Nope...”.
- The ”easy safety” device: a rope that attaches the prototype to avoid crashes or unexpected takeoffs, a sound emitter to localize it in case it crashes far away. Example: ”- Where is the quadricopter ? - I don’t know, it flew away !”.

2.5 Conclusion

This chapter is the most important part of the thesis. Having the knowledge necessary to know how to avoid crashes and projects failures seems unfortunately hard to be possible without experiencing failures. It is probably related to a certain optimism and to the lack of knowledge on our models. During the study, the initial interest for crashes changed and became more general: how to make a successful innovation and lead the project to the technical, and economical success. Having received a education mostly focused on the importance of mathematics and physics, this study brought a very new perspective. One of things that got clear is that these projects need as much scientific, technical, economical, psychological and management knowledge in order to work.

Chapter 3

The first experiments

3.1 Introduction

Energy kites systems have been studied for the last 10 years. There have been mainly theoretical works about the automatic control of the trajectory, from [89] to [93]. Few papers have validated their theoretical results with a flying prototype. The main reasons are that it is complex, costly and usually, prototypes have to be rebuilt once they crash. The presented system produces energy during cycles in which the kite moves away from, and returns to it's initial point, following a straight trajectory. As the kite moves away lifted by the wind, the wing's Angle Of Attack (AOA) is kept at an angle which produces an important lift force. The tether displacement makes a dynamo on the ground turn, which generates power. During the period when the kite is descending, the angle of attack is reduced so that the lift force is significantly smaller, and the dynamo is used as a motor for reeling in the kite to its initial altitude. As a consequence, few energy is used reeling the kite back and there will be a positive amount of energy generated at the end of each cycle. Most studies have focused on different kinds of trajectories, called crosswind flight, that maximizes the energy produced per kite. Its main drawback is that each kite requires a lot of room to fly, as it follows a 'figure-8' trajectory.

This chapter deals with the development of one of the simplest kite power systems (see figure 3.1) . The main goal is to make a study of the system that focuses on safety and on the accuracy of the output power control. As the kite flies in the wind tunnel that has been built at Gipsa-lab, the experimental set-up allows the simulation of wind gusts and operates at any desired wind speed with high precision. Therefore, kite energy generation is performed indoors independently of the weather conditions. This strategy makes the flight tests safer, faster, easier and brings precious knowledge for future outdoor flights. The proposed control strategy has led us to control the system output power with an accuracy of 99 %, with an unknown wind speed varying from 7 to 10 m/s. This prototype

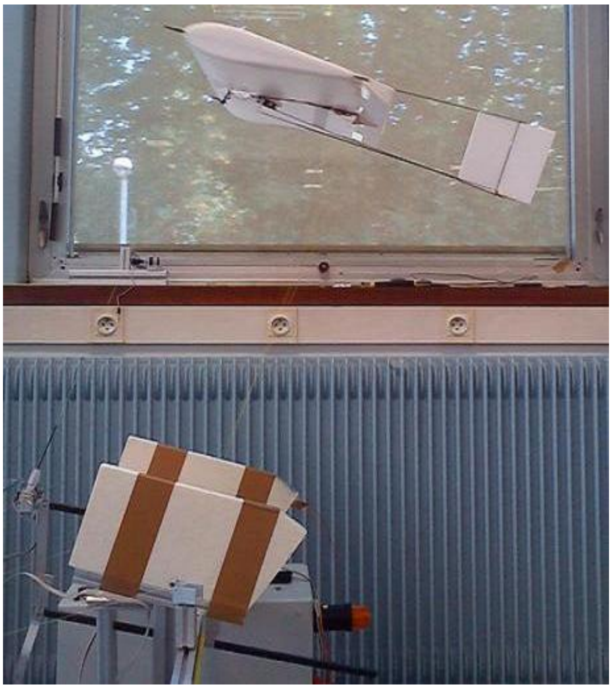

Figure 3.1: Flight test of the wind power system in the GIPSA wind tunnel (wind speed : 8 m/s).

can also fly safely in presence of very strong perturbations.

3.1.1 Studied flight plan

The system studied in this chapter has a kite that performs ascending and descending trajectories along the same straight trajectory. This system has two advantages over the 'crosswind kites' [7]. While it does generate a lower amount of energy per kite, since the flight space of each kite is a straight trajectory, one can put several systems in a very small land area. As a consequence, this system increases the amount of energy produced per used ground surface. It is better adapted to sites where the land used is a strong constraint that needs to be optimized. The second advantage is that it is safer: in order to have increased performances, crosswind kites need to have a larger aspect ratio. As a consequence, they need to have a strong structure that will be stiff and heavy. Our system does not need to have a high aspect ratio and can be built with soft materials. One has to remember that kite systems will not produce energy if they do not get a permit to fly. Building prototypes built out of soft materials has its importance as long as safety maters.

3.1.2 Objectives

The goal of this study is to increase the long term viability of our kite systems. This chapter has three main objectives:

- **Enhance safety**. It is a major key point for the system success because it has an obvious impact on reliability, ground handling, cost, etc. Wind gusts can be very brief and of enough intensity that they might cause loss of control of the kite before the actuators have time to react. For this reason, the flight plan and the stabilization of the system need to be studied so that the system becomes wind gust-proof.

- **Control the output power** so that the generated energy can be plugged into the grid reducing the need of batteries or supercapacitors. This has a direct impact on the cost of energy. The proposed control strategy will also extend the lifetime of the system as it depends on the strength of the aerodynamic forces. Reducing these forces makes the lifetime of our kites longer. As an example, aerobatic paragliders have a lifetime of around 100 hours because the materials are subject to very strong forces, whereas the lifetime is 300 hours in normal use. In the latter case the main cause of damage is due to U.V. sunrays.

- **To propose a methodology for those who would like to build their own prototypes.** This methodology has been inspired by aviation pioneers and UAV research.

Moreover, the previous points can be used for other kinds of kites systems.

3.1.3 Guidelines

As a result of the pioneer's study (see chapter 2), we will make special efforts to respect the following four research guidelines.

3.1.3.1 Testing in a wind tunnel experimental setup

Being independent of the weather conditions makes our research go much faster. We can control the wind speed, we can fly anytime and we do not have to transport the equipment far away to make fly tests. We can also make static flight, study the aerodynamic coefficients, simulate perturbations, block it with the hand, be next to it as it is flying, avoid crashes, etc.

3.1.3.2 Study of a simple prototype

Our aim is to work with a step by step growing level of complexity. As it is our first experience in the kite energy domain, we have chosen to study the simplest flying kite. Note that all of the principles explained in this chapter can be used as a basis for much more complex systems.

3.1.3.3 Minimal correlation of controls

Generally, flight parameters are correlated. For example, kitesurf's pitch angle depends on the angle of flight, its control accuracy depends on the relative speed of the kite, the length of the tether, etc. This kind of characteristics make the control of kite systems much more complex. This study tries to avoid this kind of correlations. For instance, the control of the pitch angle in the kite is independent of the angle of flight, a system of cables allows the kite to change the angle of flight without changing the pitch angle. Another example is that the angle of flight control could have been stabilized using the angle of attack, but this method would have provoked other problems for the control of the produced energy and the control of the the length of the rope. Instead of that method, the control of the angle of flight used a drag generator. this device passed tests to prove its influence on other the lift was delectable.

3.1.3.4 The 'crash proof concept'

Crashes seem to be an unavoidable part of experimentation. The faster we recover from a crash, the faster we learn to fly without crashing. We have chosen to design a very simple and robust prototype. Its robustness lies on the use of an inner structure of carbon fiber and foam sheets to give the external surface its aerodynamic shape. Its simplicity is such that in case of important damage, the kite can be fully reconstructed or modified within few hours.

To date, this prototype has experienced about 30 crashes, but none of them required more than half an hour to be repaired.

3.1.4 Chapter's organization

This chapter is organized as follows: The first part will briefly present the three first prototypes. Section 3.3 presents the fourth kite's main characteristics and some general information about the studied problem. Wind and wind gusts characteristics will be studied in section 3.4. These characteristics will be used in section 3.5 when we will study the main causes of crashes in order to avoid them. The aerodynamical model will be studied in section 3.6. Using the previous sections information, the flight plan will be designed for avoiding crashes in section 3.7. The energy production will be studied in section 3.8. The experimental setup in section 3.9 and the kite's control algorithms will be presented in section 3.10. Finally, the results and the conclusion will be held respectively in sections 3.11, and 3.12.

3.2 Early prototypes and wind tunnels

As a result of the previous guidelines, a wind tunnel and several kites have been constructed. The following study will focus on the 4th prototype (see figure 3.1). Four prototypes and two wind tunnels were built before arriving to the prototype that works, produces energy, autonomously, in presence of changing wind speeds. Here is a little sum up of what has been built.

The very first prototype was built in 2009 (see figure 3.2). It was the subject of study for the aeronautical research project at the Ecole Centrale Paris. The first tests of this wing were performed with a small electric engine. Once it showed it could fly, Tests were performed in the "Grande Soufflerie". It's objective was to stabilize the angle of flight using the spoiler's drag.

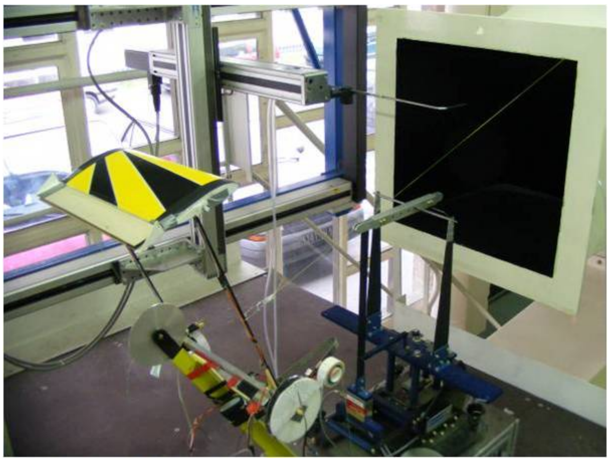

Figure 3.2: Flight test of the first prototype.

The wing was made out of a foam sheets, carbon tubes and balsa, the construction was made so that the angle of attack would remain the same regardless of the kite's angle of flight θ (see figure 3.7). Its angle of flight was its only degree of freedom.The control system was composed of two servomotors that would open the spoilers in order to increase the drag. The system had a proportional control algorithm that was implemented analogically. Tests showed that the control enhanced stability but the results still needed to be improved for the kite to have more degrees of freedom in order to produce energy.

The second prototype was build in order to test to control the angle of attack. One particularity of this prototype was that it was an extremely cheap study. The kite had to be build fast, with extremely few money. By that time, the laboratory did not have a wind tunnel. Making experimental validation of theoretical results is for me something very important, one solution had to be found to make a flight test. An air conditioning system was in the room, the choice has been made to transform it into a wind tunnel ! A duct was build and adapted to the fit the output of the air conditioning system (see figure 3.3). Its role was to redirect the airflow and to increase its speed by reducing its section. The kite dimensions were chosen so that the wingspan would be slightly smaller than the width of the airflow.

The prototype had a single cable that was attached to the control tube. The control tube would be actuated by a servo and would change its angle with respect to the wing's axis. As the wing's angle of attack would change, the tension of the cable would generate a couple that would bring the kite to its initial angle of attack. The control tube would roughly act as a proportional control an the angle of attack. A derivative component was brought by the aileron in the trailing edge, it would generate a torque that would damp the kite's rotation.

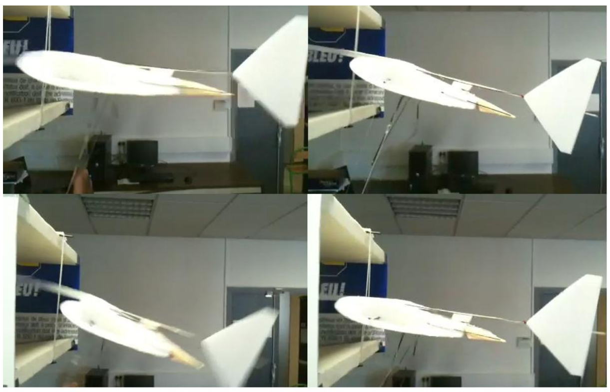

Figure 3.3: Second prototype in flight, in the "air conditioning" wind tunnel.

The kite's flight was stable, as it was a very cheap prototype, no measurement unit was implemented. Tests of stability were performed by disturbing the kite and comparing its reactions with the control system switched on or off. This method of testing gave results that were obtained quickly, with few means. One of its most interesting points is that it can give us interesting information about the possible problems we can face as we build a greater system. This experiment costed about a hundred euros but it made us be much more confident on the fact that building a greater prototype with much costlier devices would not be a lost of time and money because of some unexpected problem.

The early prototypes had the following characteristics:

Table 3.1: Carracteristics of the early prototypes

characteristic	kite n°1	kite n°2	kite n°3
mass	40 g	70 g	130 g
wing area	0.05 m^2	0.07 m^2	0.08 m^2
wingspan	0.3 m	0.36 m	0.4 m
control inputs	drag	pitch	drag and pitch
degrees of freedom	1	1	2
number of actuators	2	2	3

After the tests on the second prototype, the choice was made to build a wind tunnel in which more complete tests could be performed. The third prototype was build in order to fly in the wind tunnel. As the wind speed of the wind tunnel could go much higher than the one made with the air conditioning system, the third prototype was build with more actuators and with a total weight per wing area that was much greater than the one of the second prototype.

The objective of the third prototype was to control the angle of attack as well as the angle of flight. It had three embedded servos that would control the control tube's orientation, and every one of the two surfaces of the crocodile flap independently (see figure 3.6). Wind tunnel measurements showed that the torque and the opening of the flaps had a drag coefficient and a pitching moment that could be considered as independent. This allowed to increase the drag of the kite and to generate a torque that would be used for the angle of attack control.

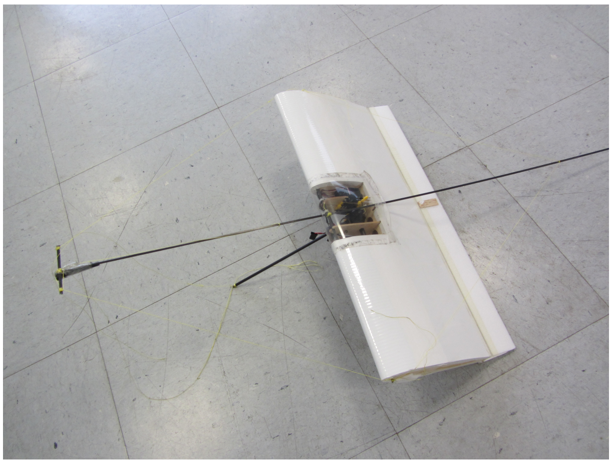

Figure 3.4: Third prototype.

The prototype was developed in order to be tested in the wind tunnel, that was able to

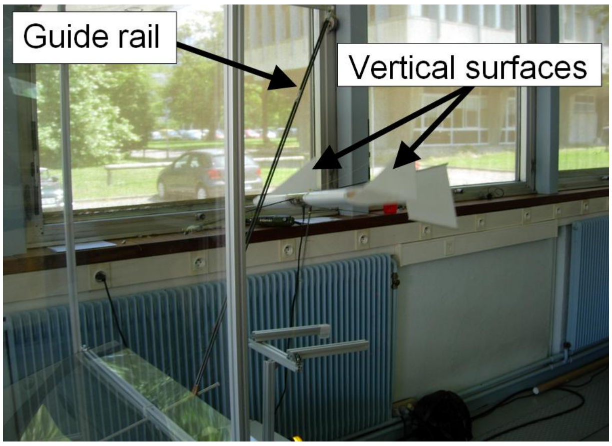

Figure 3.5: Third prototype in flight. A guiding system and vertical surfaces were used in order to reduce the oscilations arount the yaw axis.

generate a wind flow up to 11 m/s. As the tests started, is was found out that the wind tunnel generates a very perturbed flow as it goes to high speeds. The perturbations had variations of speeds on the horizontal and vertical axis. Their variations of speed were extremely strong and quick. They would generate very strong changes on the lift force and the servos were not quick enough to respond to such high speed variations. As a consequence, the kite would have great lift variations and stall problems that would lead to losses of control.

Some small improvements were made in order to make it fly in a more stable way, a honeycomb structure was added to the wind tunnel in order to make the windgust's amplitude smaller. The result was that it strongly reduced wind gusts but it also reduced the maximal speed of the flow to around 9 m/sec. The flight of the prototype did not get much better because its weight could barely be supported by the lift. The choice was made to build a new prototype that could fly with lower wind speeds.

3.3 Description of the fourth kite prototype

3.3.1 The aerodynamical structure

Two main changes were made after the relatively poor results brought by the third prototype. The fourth prototype (see figure 3.6) was build much lighter, with a controlled rudder that enhanced greatly the lateral stability. The weight of the prototype was reduced of 40 percent (80 grams), the wing area was made 75 percent greater (0.14 m^2). The NACA 0018 airfoil has been chosen for two main reasons, stall propagation is very progressive and the airfoil has enough room for the embedded electronics. The wing has

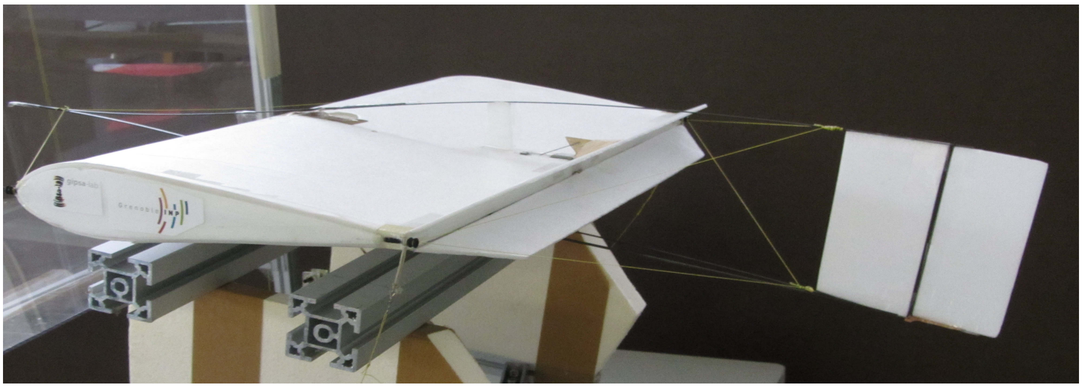

Figure 3.6: The wing with the spoilers in a medium drag position. Note the rudder used for the yaw angle stabilization.

a constant cord, a symmetrical airfoil, 2 embedded actuators that control the tail rudder and the spoilers that increase the amount of profile drag. The Angle Of Attack (AOA $= \alpha$) is controlled using a servo on the ground that pulls a rope attached to the leading edge of the wing and two other ropes that are attached to the trailing edge. This rope system makes the AOA independent of the angle of flight. This system made possible the use a heavy set of actuators in order to control very quickly and precisely the angle of attack, without adding extra weight to the prototype. It is composed of four Hitec servos that have a speed of 0.1s/60 degrees and a torque of approximately 30 N/cm each.

3.3.2 The two dimensional flight concept

Like Tatin (see chapter II), we have focused on an equivalent of a two dimensional flight. We have chosen to lock the roll angle, the lateral position and the yaw angle. The roll axis is blocked by the lift and a rope system connected to the sides of the wing. The lateral position is as well stabilized by the lift force. The yaw axis is stabilized by a PID controller that acts on the tail rudder.

3.3.3 The production cycles

This kite system can produce energy with very simple flights. It is based on a tethered kite driving a dynamo on the ground, see Figure 3.7. As the kite moves upwards lifted by the wind, the wing's angle of attack is kept at an angle which produces an important lift force and the dynamo generates power. During the period when the kite is moving downwards the angle of attack is smaller so that almost no energy is used bringing the kite back to its lowest altitude. As a consequence, there will be a positive amount of energy generated at each cycle.

3.3.4 The control problems

The trajectory of the kite and the produced power need to be controlled. The trajectory is composed of the flight angle θ and the rope's length r as depicted in Figure 3.7.

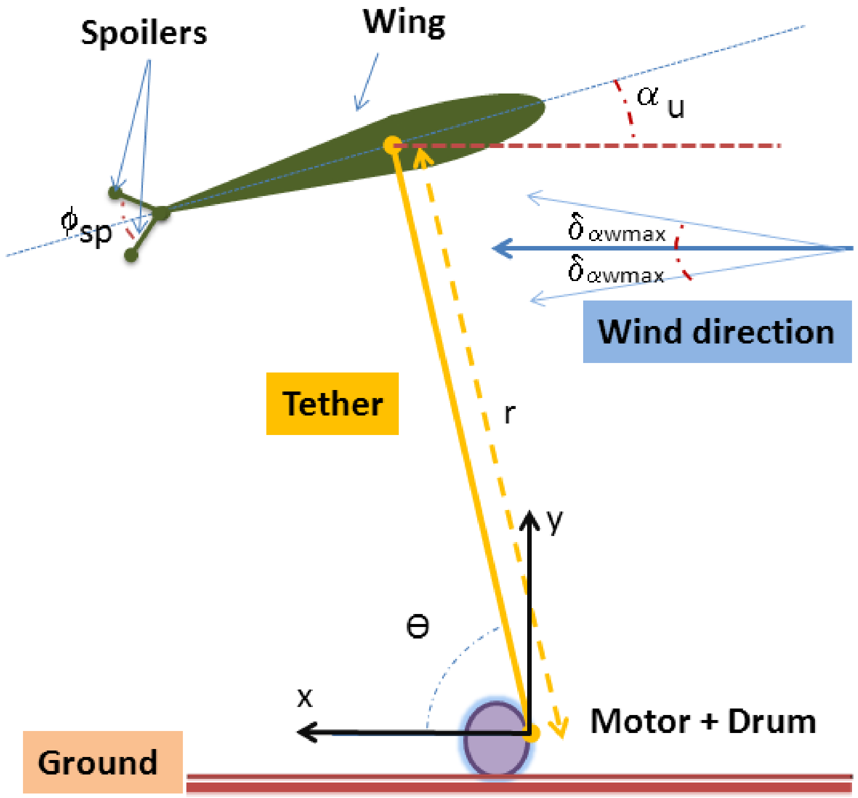

Figure 3.7: The whole wind power system (wing+tether+motor) in airflow

It has been noticed that at high angles of attack, some very strong perturbations (Figure 3.8) might appear on the θ axis.

If they are not properly controlled, these oscillations can lead our kite to crash. The same kind of oscillations can appear on the rope's length r control. The angle of attack α needs to be controlled as well, it will have to adapt to changes of relative wind speed and orientation. The angle of attack will be here defined as the sum of the pitch angle α_u measured with respect to the horizon, the relative wind orientation α_w and its perturbation $\delta_{\alpha w}$ (2.5.18) due to wind gusts.

$$\alpha = \alpha_u + \alpha_w + \delta_{\alpha w} \tag{3.3.1}$$

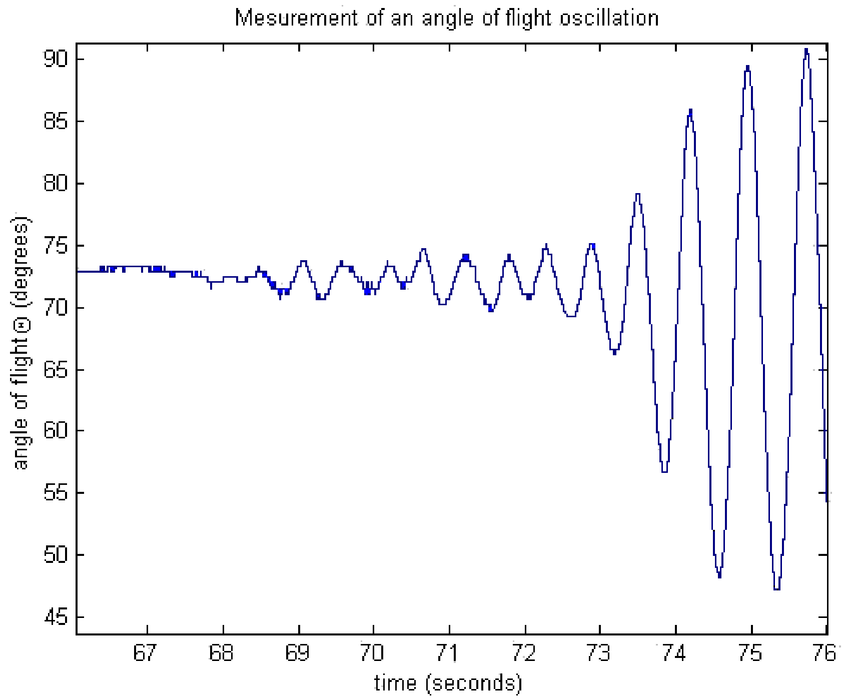

Figure 3.8: Oscilations observed on the angle of flight θ, when no control systems are used.

3.4 Wind characteristics

Wind gusts can make the orientation and the strength of wind change, they can be very brief and intense. They are one of the biggest causes of crash in aeronautics, kitesurf and paragliding. If the wind gust makes the angle of attack lower, the lift change can provoke a phenomenon similar to the one known as 'frontal collapse' in paragliding. On the contrary, if the wind gust rises the AOA, it can provoke stall.

The wind gusts also make the windspeed value change, once combined, both phenomena can lead to great variations of lift. In order to reduce the probability of crash due to a wind gust, some statistical data about the wind gusts is needed.

The wind speed V will be here modeled as the sum of a controlled main stream speed $\overline{V}$ and uncontrolled variations of intensity δ_V. This wind blows horizontally but the wind gusts can change its orientation of an angle $\delta_{\alpha w}$.

3.4.1 The mean wind speed control

The wind tunnel's mean wind speed $\overline{V}$ obeys to a first order system that is controlled by the control input U_V.

$$\dot{\overline{V}} = \beta_V \left(U_V - \overline{V} \right) \tag{3.4.1}$$

Nine brushless motors generate a wind speed that goes up to 9 m/s with a response time of approximately 0.5 s. This control will be used to simulate wind gusts along the x axis. During the tests , $\overline{V}$ values will be of 7 , 8 and 9 m/s.

3.4.2 The wind gusts

The propeller's turbulence provokes some perturbations that can not be controlled. Normally, their characteristics depend on the ground's surface, shape, the temperature differences, the presence of other flying machines, etc. In this study, wind perturbations will be approximated them by a simple model where one only knows that their amplitudes are bounded as follows.

$$\| \delta_V \| < \delta_{Vmax} \tag{3.4.2}$$

$$\| \delta_{\alpha w} \| < \delta_{\alpha wmax} \tag{3.4.3}$$

The Gipsa-lab wind tunnel has values of $\| \delta_V \|$ that are smaller than $\delta_{Vmax} = 0.5 m/s$ and the $\| \delta_{\alpha w} \|$ value is bounded by $\delta_{\alpha wmax} = 3$ degrees. In this specific case, the lateral wind gusts have a very low impact on the system so they will not be taken into account.

3.5 Analysis of crash causes

3.5.1 Two different approaches of unknown aerodynamics

Most of aerodynamics models are studied in a reduced flight domain. For example, their lift coefficient C_L, moment coefficient C_M and drag coefficient C_D are generally studied for AOA values between -20 and 30 degrees. Beyond these limits, most control algorithms will loose their effectiveness and kite's trajectories will look chaotic, like falling leaves. Avoiding this kind of loss of control can be done by two means: expanding knowledge of the flight domain or restricting our flight domain by staying in a well known flight domain. The classic way to avoid these problems is to avoid the unknown aerodynamics by restricting the flight domain. This study follows this strategy.

Nevertheless, it is important to remember that expanding models can have great advantages. To illustrate this, one can mention that regular planes pilots avoid to fly at high AOA to avoid loss of control due to stall. On the contrary, the Sukhoi engineers enhanced their aerodynamic models in order to be able to do the 'cobra' figure where the angle of attack goes up to 120 degrees. Both approaches are made to avoid loss of control.

The expansion of models brings a lot of new possibilities. For example, acrobatic paragliding is full of complex figures that could be very useful for our kites systems. One can cite the 'helicopter' figure, the 'ears', the 'big ears', etc. None of these Figures fit the standard aerodynamic models.

3.5.2 Causes of crashes and safe flight conditions

The control algorithms must be designed so that the kite respects the 4 following safe flight conditions.

3.5.2.1 Condition 1: Dynamic stall

The angle of attack α must never be greater then the stall angle α_{stall} . This dynamic stall condition must be taken into account for the worst possible value of $\delta_{w\alpha}$, i.e. when it is at its maximal value.

$$\alpha = \alpha_u + \alpha_w + \delta_{w\alpha} < \alpha_{stall} \tag{3.5.1}$$

3.5.2.2 Condition 2: Frontal collapse and loss of tension

Frontal collapse can happen to paragliders when the lift coefficient suddenly becomes too small or negative. If it happens, classic paraglider's airfoil lose their shape and the lift changes its orientation which leads to a total loss of control. It is the first cause of crashes in paragliding. The second kind of problem happens to kites that need a minimal rope tension in order to have effective controls. It is generally the case when the actuators are not embedded.

These two phenomena should lead to two different conditions, one on the minimal tension, and one on the minimal angle of attack. In this study, the minimal needed rope tension is very small and we will approximate both conditions by the following one. The kite must never fly with an angle of attack lower than $\alpha_{min} = 2$ degrees.

$$\alpha > \alpha_{min} = 2 \text{ degrees} \tag{3.5.2}$$

3.5.2.3 Condition 3: Overload

Our systems lift $\overrightarrow{L}$ and drag $\overrightarrow{D}$ forces must respect the structures maximum load F_{max}. Beyond the maximum value, the kite, the rope or the dynamo get destroyed.

$$\| \overrightarrow{L} + \overrightarrow{D} \| < F_{max} \tag{3.5.3}$$

This inequality must be respected in the worst case, i.e. when the wind gusts δ_V and the δ_α are at their max value. This study's kite maximum load is 10 N.

3.5.2.4 Condition 4: Minimal lift

The projection of the aerodynamic forces on the vertical axis $\overrightarrow{z}$ has to be greater than the weight Mg in the worst case, i.e. when the wind gusts diminish the V speed and the relative wind angle to their minimum value.

$$\| (\overrightarrow{L} + \overrightarrow{D}) \cdot \overrightarrow{z} \| > Mg \tag{3.5.4}$$

3.6 Aerodynamic model

This section presents the aerodynamic model of a kite wind power generator system as depicted in Figure (3.7). The following formulas are taken from [83].

3.6.1 Forces

From Newton's second law we obtain the following nonlinear dynamical system:

$$\ddot{\theta} = \frac{1}{r}\left[-2\dot{\theta}\dot{r} + \frac{F_t}{M}\right] \tag{3.6.1}$$

$$\ddot{r} = \frac{1}{M + M_{IM}}\left[r\dot{\theta}^2 M + F_r - T\right] \tag{3.6.2}$$

where r is the rope length from the kite to the dynamo on the ground, θ is the angle the rope makes with respect to the horizontal line, M is the mass of the kite, $M_{IM} = \frac{I}{R^2}$ with I the inertia of the rotor and R the radius of the drum, T is the tension on the rope, F_r and F_t are respectively the radial and tangential forces acting on the kite due to aerodynamical forces and the weight $w = Mg$.

The aerodynamical forces can be expressed in terms of the lift L and the drag D as follows:

$$F_r = L\sin(\theta - \alpha_w + \delta_{\alpha w}) + D\cos(\theta - \alpha_w + \delta_{\alpha w}) - w\sin\theta \tag{3.6.3}$$

$$F_t = L\cos(\theta - \alpha_w + \delta_{\alpha w}) - D\sin(\theta - \alpha_w + \delta_{\alpha w}) - w\cos\theta \tag{3.6.4}$$

The angle of relative wind speed will be here approximated by $\alpha_w + \delta_{\alpha w}$. When the kite speed is very high respectively to the wind gust values, one has to take into account the speed of the kite, its orientation and the behavior of the wind speed V.

The norms of the lift and the drag amplitude obey the following equations:

$$L = \frac{1}{2}\rho S v_r^2 C_L \tag{3.6.5}$$

$$D = \frac{1}{2}\rho S v_r^2 C_D \tag{3.6.6}$$

where ρ is the air density, S is the wing surface, v_r is the relative wind speed and the lift coefficient C_L and the drag coefficient C_D are

$$C_L = \frac{\partial C_L}{\partial \alpha}(\alpha_w + \alpha_u + \delta_{\alpha w}) + C_{L0} \tag{3.6.7}$$

$$C_D = \frac{C_L^2}{\pi e \lambda} + C_{D0} + k_{sp}\phi_{sp} \tag{3.6.8}$$

where C_{L0}, C_{D0} are constant coefficients, e is the Oswald's efficiency factor, λ is the aspect ratio. The pitch angle α_u in controlled via the input U_α, see equation (3.6.10). The amount of added drag is $k_{sp}\phi_{sp}$ where $k_{sp} = \frac{\partial C_D}{\partial \phi_{sp}}$ is the drag derivative with respect to the angle of opening of the flaps ϕ_{sp}. The flap is opened via the input U_θ and obeys to equation (3.6.11).

3.6.2 Control inputs and actuators dynamics

The systems has three control inputs, U_α, U_θ and U_r. Equations (3.6.9), (3.6.10) and (3.6.11) represent the first order dynamic response of actuators used in the experimental platform to control respectively the torque of the motor, the pitch angle of the wing and the angle of opening of spoilers.

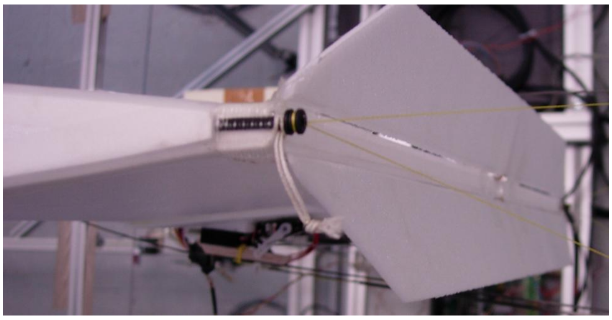

Figure 3.9: Close up of the spoilers in the maximum drag position.

$$\dot{T} = \beta_T\Big(U_r - T\Big) \quad (3.6.9)$$

$$\dot{\alpha}_u = \beta_a\Big(U_\alpha - \alpha_u\Big) \quad (3.6.10)$$

$$\dot{\phi}_{sp} = \beta_{sp}\Big(U_\theta - \phi_{sp}\Big) \quad (3.6.11)$$

Note that U_r controls the length of the cable using the torque of the dynamo/motor. The dynamo/motor will act as a motor or as a dynamo depending on whether it is generating power or pulling the kite down to restart a duty cycle.

3.6.3 Use of the spoilers

The spoilers are used to generate drag to stabilize the kite at the desired angle of flight θ_D, the value of the opening can vary from 0 to 160 degrees (Figure 3.9). The standard position is 80 degrees. Our tests revealed that the amount of generated drag can be approximated as proportional to the angle of opening ϕ_{sp}.

For every combination of AOA, $\overline{V}$, $\dot{r}$ and U_θ, there exists one corresponding angle of flight θ value for which the kite tangential acceleration $\ddot{\theta}$ is equal to 0, if the flight is possible. This particular value is named the natural angle of flight θ_N.

The value of this angle is controlled by the vertical forces VF and the horizontal forces HF:

$$\arctan\frac{VF}{HF} = \theta_N \quad (3.6.12)$$

with :

$$VF = \| (\overrightarrow{L} + \overrightarrow{D}) \cdot \overrightarrow{z} - w \| \quad (3.6.13)$$

$$HF = \parallel (\overrightarrow{L} + \overrightarrow{D}) \cdot \overrightarrow{x} \parallel \tag{3.6.14}$$

As we want to reject perturbations and follow the desired angle θ_N in case of change of mean wind speed $\overline{V}$, one needs to be sure that there is a value of U_θ that can satisfy $\theta_N = \theta_D$ and that this value of U_θ still have enough resources to reject perturbations. It has been experimentally noticed that the kite can reject perturbations using 50 percent of U_θ. As a consequence, the values of θ_D have to be chosen in the intervals between the value of θ_N corresponding to $U_\theta = 0.25\%$ and $U_\theta = 0.75\%$. This makes that for every θ_D, the kite has still enough range.

3.6.4 Relative wind

The horizontal relative wind speed (3.6.15) and the vertical airspeed (3.6.16) depend of the movements of the kite and are given with respect to V. In order to simplify equations, we will express the relative wind speed as the sum of the wind gust and the value of relative wind speed that would be seen by the kite with no wind gust.

In the absence of wind gust, the horizontal v_h and the v_v are given by:

$$v_h = \overline{V} + r\sin(\theta)\dot{\theta} - \dot{r}\cos(\theta) \tag{3.6.15}$$

and

$$v_v = r\cos(\theta)\dot{\theta} + \dot{r}\sin(\theta) \tag{3.6.16}$$

Using (3.6.15) and (3.6.16) we obtain the wind angle α_{w0} which is the angle of the wind velocity vector measured with respect to the horizon, and the kite's relative wind velocity v_{r0}.

$$\alpha_w = -\arctan\frac{r\cos(\theta)\dot{\theta} + \dot{r}\sin(\theta)}{\overline{V} + r\sin(\theta)\dot{\theta} - \dot{r}\cos(\theta)} \tag{3.6.17}$$

$$v_{r0} = \sqrt{(r\cos(\theta)\dot{\theta} + \dot{r}\sin(\theta))^2 + (\overline{V} + r\sin(\theta)\dot{\theta} - \dot{r}\cos(\theta))^2} \tag{3.6.18}$$

Adding the wind gusts perturbations, v_r is bounded as follows:

$$v_{r0} - \delta_{Vmax} < v_r < v_{r0} + \delta_{Vmax} \tag{3.6.19}$$

3.7 Flight plan design strategy

The flight plan has to be designed so that it respects the 4 safe flight conditions and be able to follow the desired trajectory. The proposed strategy for designing the flight plan will consist in computing all the possible trajectories and choose one that satisfies the safety requirements, i.e. avoid the crashes studied previously. The possible trajectories will be categorized in three different domains:

- The static flight domain when the kite does not move.
- The constant speed flight domain for all the straight trajectories at constant $\dot{r}$ speed.
- The accelerated trajectories will be studied in the transitions flight domain.

This particular way of studying the flight can be extended to flights with more degrees of freedom. For instance, when a kite is turning following a figure of eight trajectory, the two wingtips have different wind speeds. The angle of attack on each wingtip depends on its speed. Proving that none of the wingtips is stalling would be interesting in order to make the flight safer. This is a simple example whose calculation can be done very quickly adapting equation (4.3.6). When the systems become more complex, many other phenomena can change the values of aerodynamic forces and can lead to losses of control due to the lack of comprehension of the flight dynamics.

3.7.1 Static flight domain

Using the safe flight conditions, we can compute the values of AOA and relative wind speed that respect the 4 conditions (3.5.1), (3.5.4),(3.5.3) and (3.5.4) when the kite is static (Figure 3.10).

This domain gives a first idea of the restrictions one must consider. The values of AOA and mean wind speed must remain in the 'safe flight domain'. One can see that the size of the safety margins reduce a lot the possibilities for flight and that the safe flight domain is surrounded by the 4 causes of crash. The size of the safety margins increases with the values of δ_{Vmax} and $\delta_{\alpha w}$

3.7.2 Constant speed flight domain

In order to set a flight plan and compute the output power, we need to find out what are the possible values for the angle of flight θ depending on the $\dot{r}$ speed and on the wind

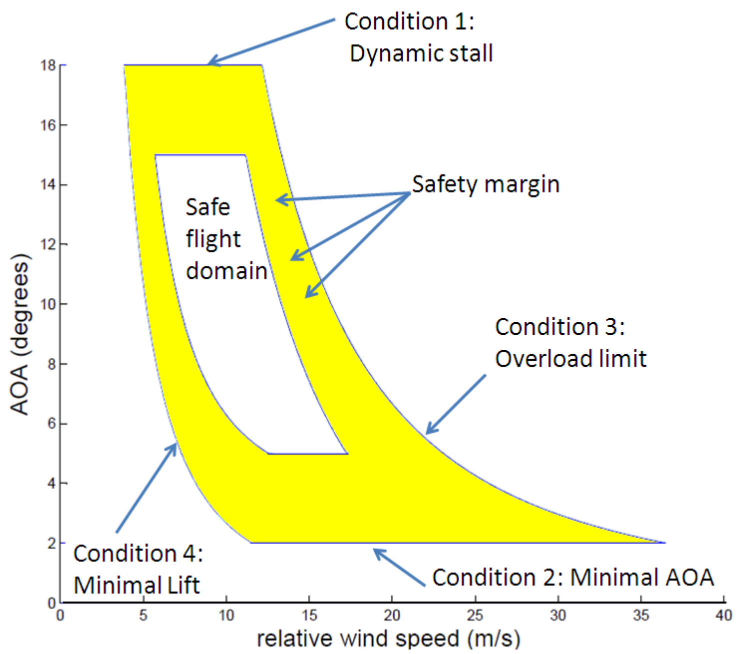

Figure 3.10: Static flight domain for the fourth prototype.

speed. The basic flight trajectories are straight trajectories at constant angle of flight θ and $\dot{r}$ speed. These trajectories must be followed in case of mean wind speed change, for example when $\overline{V}$ goes from 8 to 9 m/s , and in case of AOA change. The kite has to be able to keep the same angle of flight θ using less than 50 percent of the spoilers total rate, as explained in section 4.2. In case of wind gusts, the kite must be able to regain the desired trajectory after the transition period.

3.7.2.1 The constant flight angle condition

The fifth condition is that the kite must be able to stay at the desired angle of flight θ_D for different values of AOA and mean wind speed V using only the U_θ control. This condition reduces the size of the flight domain, but it is a first approach that guarantees the flight safety.

Figure 3.11 shows the possible angles of flight corresponding to a $\dot{r}$ =0.5 m/s, mean wind speeds of 8 and 9 m/s. Wind gusts are set at their less advantageous values. For each graph, the upper curve corresponds to the θ_N value corresponding to $U_\theta = 0.25\%$ and the lower to the θ_N value corresponding to $U_\theta = 0.75\%$.

We can see that in this particular case, the θ_D value can take any value between 58 and 65 degrees. This condition makes some flights at constant angle of flight impossible. The following graph has been plotted for a 3 m/s value of $\dot{r}$ (Figure 3.12).

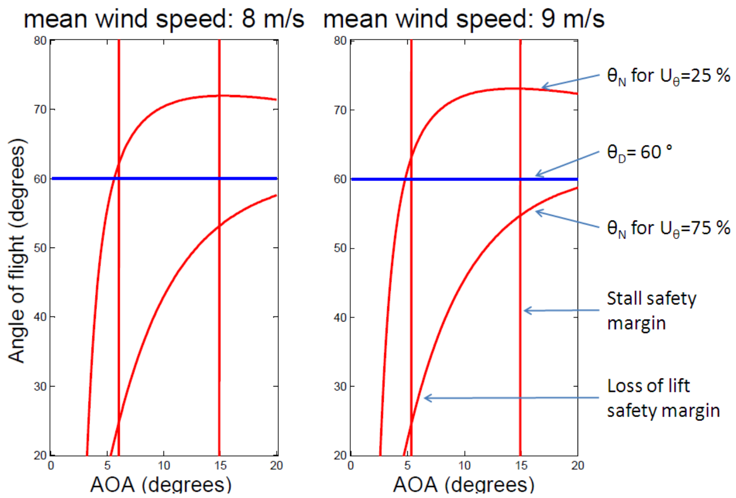

Figure 3.11: Possible angle of flight θ values depending on the AOA value, for $\dot{r} = 0.5$m/s.

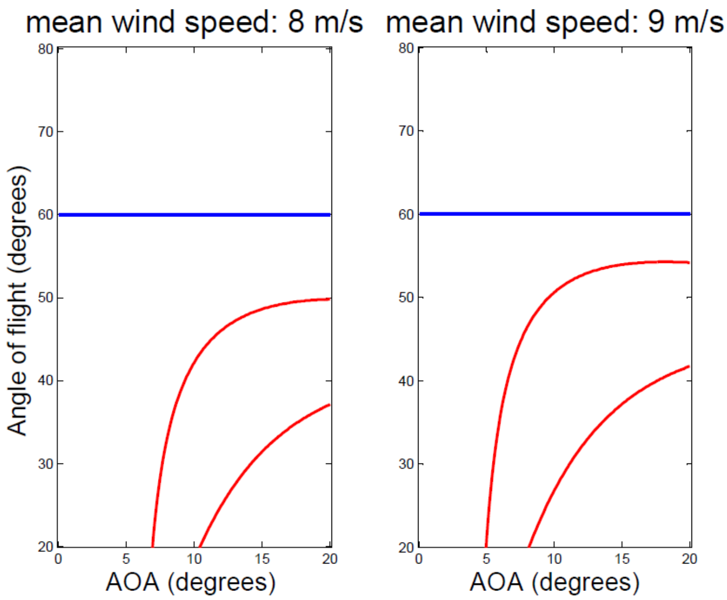

Figure 3.12: Possible angle of flight θ values depending on the AOA value, for $\dot{r} = 3$ m/s.

One can see that the system is no longer able to keep a constant flight angle in case of a change of $\dot{r}$. Note that these kinds of phenomena also happen when the kite is flying with low wind speeds. These situations are likely to produce a crash because there is a wide interval of angle of flight values for which the angle of flight can no longer be controlled because there is no U_θ value that satisfies the equation $\theta_N = \theta_D$. When the U_θ control can no longer stabilize the angle of flight, because the θ_D is out of reach by the kite, one possible solution could be to change the value of θ_N using $\dot{r}$ as a control input. This solution will not be studied in this manuscript. Note that this kind of control problem is one of the main causes of crashes in kitesurf, when experimented kitesurfers try to make the kite takeoff in the 'max power zone'. The θ_N value is very high and the kites accelerated and as the kites accelerates very quickly, the kitesurfer gets pulled so hardly that he almost immediately takes off the ground.

3.7.2.2 Safe flight conditions respect

Vertical lines in Figure 3.11 are the limits on AOA to respect condition 1 and 2 (see section 3.5.2). Taking into account the safety margins, the angle of attack has to be greater than 5.2 degrees for 8 m/s of mean wind speed, and 6 degrees for 9 m/s. The 15 degrees line represents the limit on AOA to avoid stall. For these ranges of wind speeds and AOA, the conditions 3 and 4 are respected as well.

3.7.3 Accelerated flight domain

This study will focus constant angle of flight trajectories. In order to keep a tense tether, One needs to satisfy the two following condition.

3.7.3.1 The maximal $\ddot{r}$ value condition

The sixth condition is that when the $\ddot{r}$ value is positive,the maximal rate of acceleration of the rope must be inferior to the kite's acceleration rate. Otherwise, the cable will go loose. The kite acceleration rate can be approximated by $\parallel \overrightarrow{L} \parallel /M$ This condition can be written as follows:

$$\ddot{r} < \frac{\parallel \overrightarrow{L} \parallel}{M} \tag{3.7.1}$$

3.8 Maximum energy production

The maximum energy production is studied to obtain the reachable values for the desired output power. The energy consumed during the transition phases will be neglected in this section since its value is very low compared to the total energy production.

The amount of energy generated during a cycle depends of the flight plan. In order to maximize it, one has to use the maximal safe value of α in order to maximize radial force F_r during the production phase, and to reduce the angle of attack to its lowest possible value during the recovery phase. In order to optimize the power production, two main inputs, the angle of attack α and the $\dot{r}$ speed are used.

A basic flight plan can be defined by 6 parameters that are : the speed $\dot{r}_1$ during the production phase, the radial force F_{r1} of the kite during the production phase, the speed

$\dot{r}_2$ during the recovery phase and the radial force F_{r2} of the kite during the recovery phase. Finally r_{min} and r_{max} are the minimum and maximum rope length attained at the time t_1 and t_2.

The amount of energy produced during a cycle of this flight plan is then given by:

$$E(t_0, t_1, t_2) = \int_{t_0}^{t_1} F_{r1}\dot{r}_1 dt + \int_{t_1}^{t_2} F_{r_2}\dot{r}_2 dt \tag{3.8.1}$$

the first term is the produced energy during the production phase, the second is the consumed energy for reeling in the kite.

The mean power can be written as:

$$P(t_0, t_1, t_2) = \frac{E(t_0, t_1, t_2)}{t_2 - t_0} \tag{3.8.2}$$

Note that this simple flight plan and the energy expression do not take into account the loss of energy due to energy losses during the transition phases, the efficiency of the motors and actuators,the rope's weight, friction losses.

3.8.1 Ideal recovery phase

The ideal recovery is very short and consumes very small amounts of energy. The fastest the kite will go, the smaller will be the induced drag. As a consequence, the kite's tension will no longer be generated by the lift but by the drag due to its C_{D0} coefficient. With an appropriate control and an appropriate flight plan, the kite should have a straight trajectory, with an AOA close to zero, just like the flight of an arrow.

Supposing the kite could follow this kind of trajectories, the output power would be given by Figure 3.13. This kite could have a maximum production of 40 W/m^2 with a mean wind speed of 8 m/s. Note that the $\dot{r}$ speed during the recovery phase has a value of 15 m/s.

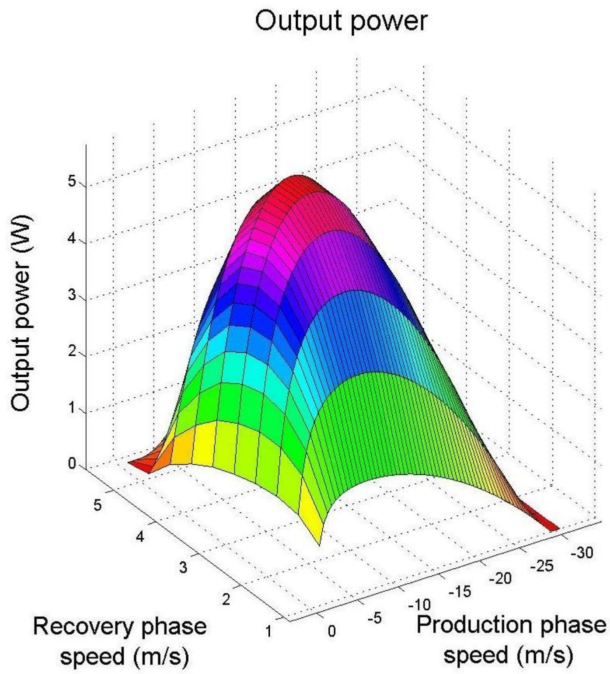

Figure 3.13: Maximum energy production correponding to an ideal recovery phase and a mean speed wind of 8m/s.

3.8.2 Experimental recovery phase

The experimental setup has a maximum rope's length r value equal to one meter, as a consequence, it can not reach high values of $\dot{r}$. The maximal values that can be reached are about 0.3 m/s. The performance of recovery phases with these values of $\dot{r}$ are quite low, and one needs to keep a minimal angle of attack of approximately 6 degrees. As a result, the following flight plan has been design (Table 3.2). It respects all the safety conditions and leads to a maximal output power of approximately 0.3 W.

Table 3.2: Coefficients of the experimental set-up

Variable	production phase	recovery phase
$\dot{r}$	0.1 m/s	0.2 m/s
α	15 degrees	6 degrees
r	1 m (max value)	0.2 m (min value)
θ_D	65 degrees	65 degrees

3.9 Experimental setup

3.9.1 The wind tunnel

In order to validate the proposed control strategy, an experimental set-up has been built in the Gipsa-lab laboratory for testing the proposed wind power system presented in the previous sections. This experimental setup allows to test our prototype independently of the weather conditions (see Figure 3.14). The air flow is produced at speeds up to 9 m/s. The wind tunnel is composed of 9 brushless motors of 800W each distributed on a surface of 1.2 m^2.

3.9.2 The control platform

Controllers are implemented on the experimental set-up using the xPC target real-time toolbox of Matlab. The ground station sends U_r control variable to a dynamo-motor system Maxon 2260L DC 97W driven by a 4 quadrants amplifier Maxon ADS 50/10. Two incremental encoders provide measurement of flight angle θ and rope length r. Control outputs U_θ and U_α are sent to servomechanism via a RS232 communication and a torque sensor provides an accurate measurement of tension of the cable T.

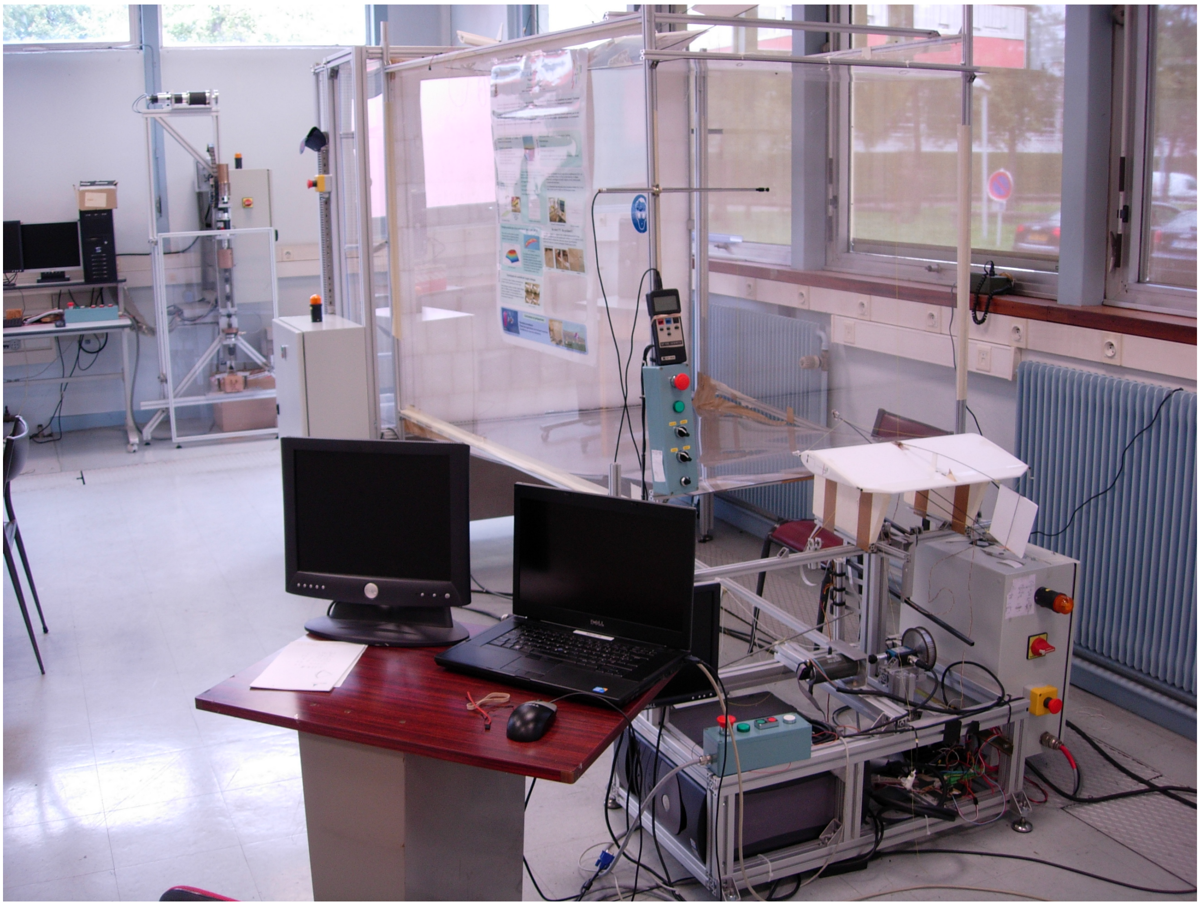

Figure 3.14: The Gipsa-lab wind tunnel system, including the 7.2 kW wind tunnel, the wing, the ground station and the control computer.

3.10 Kite's control algorithms

During last decade, kite systems have been studied by many different automatic control teams. Nonlinear model predictive control (NMPC) has been applied in ([74, 57, 91]. Trajectory tracking methods including neural network control [92], robust control [46], direct-inverse control [93], and nonlinear adaptive tracking control [89] has been also proposed.

This study highlights the fact that respecting some conditions on flight mechanics and using simple flight plans can make possible the use of simple control algorithms. This method does not give the maximal values for output power, it can be improved by finding solutions to reduce the losses due to the safety margins. This can be done by two main methods: enhancing the response time of the kite to reject perturbations, or studying methods to keep the control of the kite when we do not respect the safe flight conditions. The last method has been studied since the 70's, by the development of high performance aircraft.

Two methods will be here proposed, the first one will use a state feedback technique that will use the angle of flight sensors. The second one will use an observer based method and will perform a control of the output power.

3.10.1 Table of coefficients

Both proposed control strategy were first validated in simulation using values of coefficients of the experimental set-up given in the following table.

Table 3.3: Coefficients of the experimental set-up

Symbol	Name	Value
M	mass	0.08 Kg
M_{IM}	rotor's mass	0.0481 Kg
ρ	air density	1.225 $\mathrm{Kg/m^3}$
S	wing area	0.14 $\mathrm{m^2}$
e	Oswald's factor	0.7
λ	aspect ratio	2.5
$\frac{\partial CL}{\partial \alpha}$	lift derivative w.r.t. α	0.07 deg^{-1}
C_{D0}	zero lift drag	0.01
C_{L0}	lift coefficient at $\alpha = 0$	0
V	mean air speed	8 - 9 m/s
k_{sp}	drag derivative w.r.t. ϕ_{sp}	0.0031 deg^{-1}
β_{sp}	inverse of the time constant	100 s^{-1}
β_a	inverse of the time constant	100 s^{-1}
β_T	inverse of time constant	14.28 s^{-1}

3.10.2 State feedback control strategies

3.10.2.1 Control of the angular position θ

We first study the control strategy for the angular oscillations on θ which will be stabilized using the spoilers u_θ. We have noticed that without spoilers it is very difficult to stabilize the angular position θ because there exist sever oscillations, see Figure 3.8. Such oscillations have been damped by introducing spoilers on the wing. To analyze the system we have to rewrite (3.6.1) in such a way that the spoiler control input u_θ appears in the equation. Injecting (3.6.4) (3.6.5), (3.6.6) and (4.3.4) into (3.6.1) leads to

$$\ddot{\theta} = \chi + Q u_\theta \tag{3.10.1}$$

where

$$Q = \frac{\rho S v_r^2 \beta_\theta \sin(\alpha_w - \theta)}{2Mr} \tag{3.10.2}$$

$$\chi = -\frac{2\dot{r}\dot{\theta}}{r} - \frac{L\cos(\alpha_w - \theta) - w\cos\theta}{rM} + \frac{\rho S v_r^2 (\frac{C_L^2}{\pi e \lambda} + C_{D0})\sin(\alpha_w - \theta)}{2rM} \tag{3.10.3}$$

The objective is to propose a control law for u_θ such that the closed loop system behaves as

$$\ddot{\theta} + 2\dot{\theta} + \theta = \theta^d \tag{3.10.4}$$

where θ^d is the desired value for θ which is typically $60°$. Using Laplace transform the above equation can be expressed as

$$(s+1)^2\theta(s) = \theta^d$$

This means that the desired closed loop system has two real poles at -1. Introducing (3.10.1) into (3.10.4) it follows that the required control input is

$$u_\theta = (-2\dot{\theta} - \theta + \theta^d \ - \chi)/Q \tag{3.10.5}$$

The above control input linearizes the system (3.10.1) using a state feedback technique and guarantees that $\theta \to \theta^d$. The desired angular position θ^d can be also computed to maximize the generated energy.

3.10.2.2 Control of the rope length r

In this section we propose a control strategy such that the rope length r tracks a sinusoidal trajectory. We have chosen a sinusoidal trajectory in order to smooth the displacement of the kite. Notice that the kite velocity is zero, i.e. $\dot{r} = 0$, when the kite reaches its highest and lowest altitudes. Suppose for simplicity that we wish r to follow the desired trajectory:

$$\begin{aligned} r_d &= A\sin\omega t \\ \dot{r}_d &= A\omega\cos\omega t \\ \ddot{r}_d &= -A\omega^2\sin\omega t \end{aligned}$$

where A and $f = \omega/2\pi$ are respectively the amplitude and frequency of the desired oscillation.

Let us introduce the error

$$e = r - r^d$$

and let us assume that we wish the closed loop system to behave as

$$(s+1)^2 e(s) = 0$$

Therefore

$$\ddot{r} = \ddot{r}_d - 2(\dot{r} - \dot{r}_d) - (r - r_d)$$

From (3.6.1) and the above it follows that the control input T should be chosen as

$$T = M\left[-\ddot{r}_d + 2(\dot{r} - \dot{r}_d) + (r - r_d) - r\dot{\theta}^2\right] + F_r$$

The above control law is a state feedback control law which linearizes system (3.6.1) and forces it to track a sinusoidal trajectory. The amplitude of such a control input normally increases as A or f grows.

3.10.2.3 State feedback control's tests

We have observed experimentally that the control of the yaw angular displacement ψ works properly. Furthermore, for a fixed rope length r, we have observed that for a given angle of attack α, we can see on figure 3.15 that the rope angle θ reaches an almost constant value. The small oscillations are due to the fact that the wind in these experimental conditions is very turbulent.

This kind of perturbations might seem over sized, but one has to keep in mind that in case of a loss of control, the tether might give great perturbations to the kite. These are the tests that kites systems must pass in order to be considered as a safe system.

The control of the rope length r works quite well, as it can be seen in Figure 3.16 and in Figure 3.17. We have noticed that in the case of very low speed displacements, the behavior of the system has some problems due to the system's static friction.

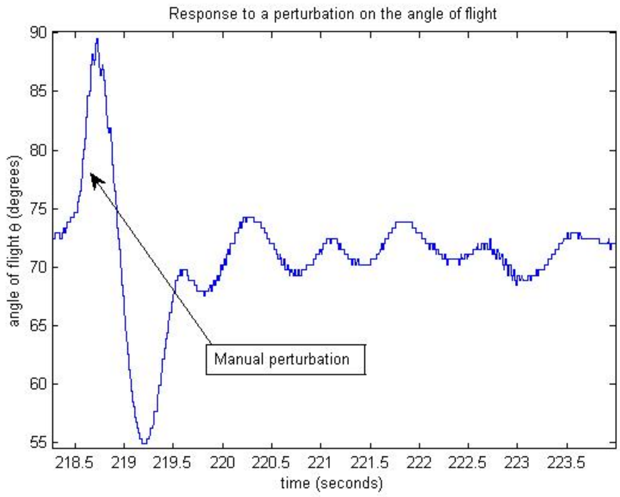

Figure 3.15: Response to a manual perturbation on the closed loop system.

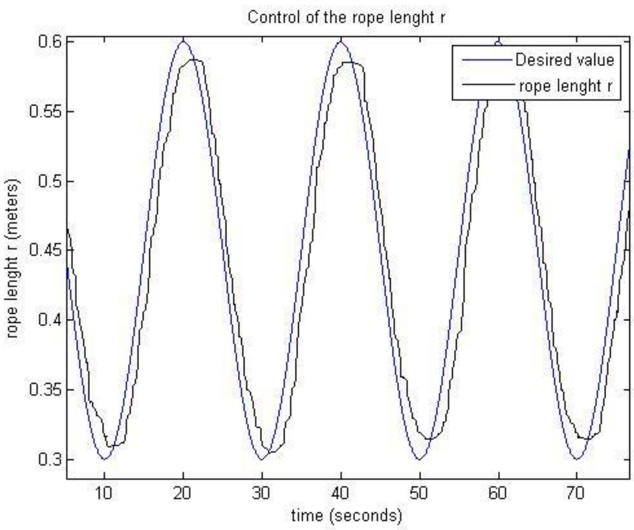

Figure 3.17: Sinusoidal trajectory tracking with torque control.

This experiment was the first time we produced energy, the energy curve can be seen in Figure 3.18. Though the energy production was positive, its value would change according to the wind value and to the perturbations. The precision on the amount of generated energy was low and needed to be improved.

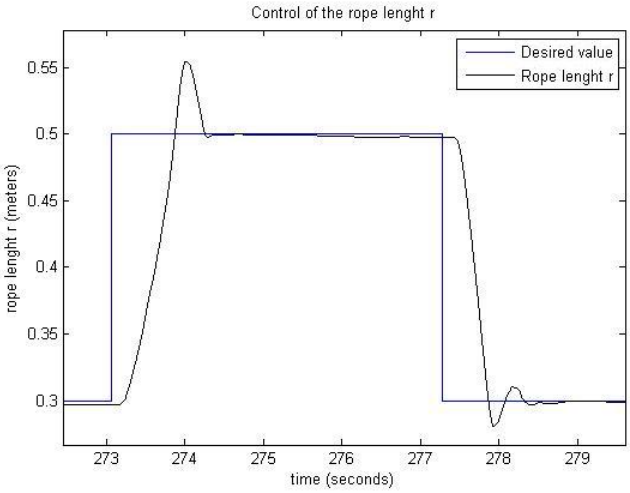

Figure 3.16: Desired position tracking with Torque control .

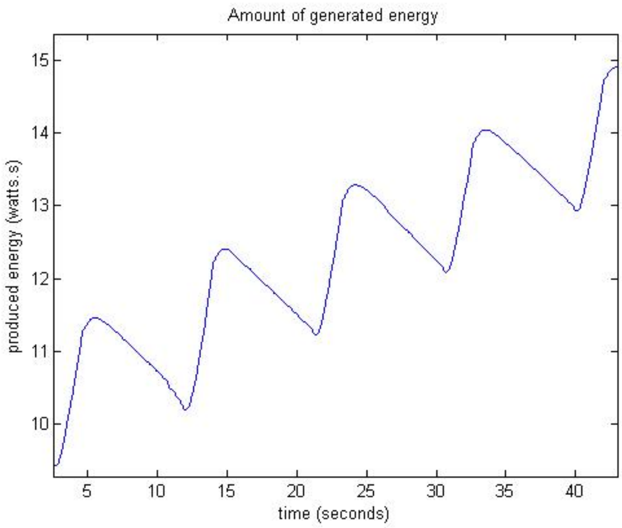

Figure 3.18: Generated energy.

3.10.3 Observer based control strategies and output power control

The second control algorithm proposes a different approach for stabilizing the kite and a method to control the output power production.

In a near future, kites system will probably be used in wind power farms with great constraints about the closeness to neighbor kite power systems. The management of the position of the kite and the timing of the energy production phases will have a great importance. That is why choice has been made to design a control strategy that allows us to control better the the kite's position and the amount of energy that is generated. This section will propose a control strategy that, once the $\dot{r}$ and the θ values are properly controlled, can control the output power using as only input the angle of attack control U_α.

The general control scheme is showed in Figure (3.19)

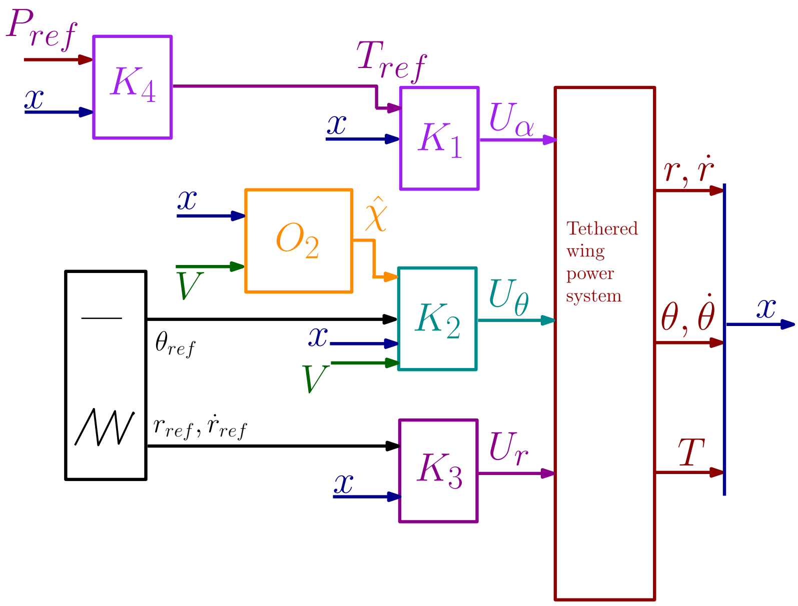

Figure 3.19: The complete system: O_2 is the observer of χ. K_1, K_2, K_3 and K_4 are respectively feedback controlers for α ,θ, r and P.

3.10.3.1 The control of angle of flight θ

The control of the angle of flight can be done with simple control algorithms if the θ and $\dot{\theta}$ values are accurate enough. If the sensor is not very accurate, or if it gives a numerical signal that can not be easily used for the stabilization of the angle of flight θ, the proposed solution reconstitutes the θ and $\dot{\theta}$ using the following observer based strategy.

Note that the equation (3.6.1) can be rewritten in the following condensed form:

$$\ddot{\theta} = \chi + QU_\theta \tag{3.10.6}$$

where χ represents the *relatively badly known* term

$$Q = -\frac{\rho S v_r^2 k_{sp}}{2Mr} \sin(\theta - \alpha_w) \tag{3.10.7}$$

$$\chi = -\frac{2\dot{r}\dot{\theta}}{r} + \frac{L\cos(\theta - \alpha_w) - P\cos\theta}{rM} - \frac{\rho S v_r^2 (\frac{C_L^2}{\pi e \lambda} + C_{D_0}) \sin(\theta - \alpha_w)}{2rM} \tag{3.10.8}$$

This suggests that χ can be estimated using the following Luenberger estimator based on the sole measurement of θ:

$$\hat{\chi} = \begin{pmatrix} 0 & 0 & 1 \end{pmatrix} \hat{X}_1 \tag{3.10.9}$$

$$\dot{\hat{X}}_1 = (A_1 - L_1 C_1)\hat{X}_1 + B_1 U_\theta + L_1 \theta \tag{3.10.10}$$

where the observer's state is $X_1 = [\theta \; \dot{\theta} \; \chi]$ and

$$A_1 := \begin{pmatrix} 0 & 1 & 0 \\ 0 & 0 & 1 \\ 0 & 0 & 0 \end{pmatrix} \; ; \; B_1 := \begin{pmatrix} 0 \\ Q \\ 0 \end{pmatrix} \; ; \; C_1 := \begin{pmatrix} 1 & 0 & 0 \end{pmatrix} \tag{3.10.11}$$

while L_1 is the observer gain obtained for instance using LQE design. This gives the control law given by (3.10.9)-(3.10.10) together with

$$U_\theta = -\frac{1}{Q}\Big[\hat{\chi} + \lambda_{1_\theta}(\dot{\theta} - \dot{\theta}_{ref}) + \lambda_{2_\theta}(\theta - \theta_{ref})\Big] \tag{3.10.12}$$

where θ_{ref} and $\dot{\theta}_{ref}$ are respectively some desired angle and angular velocity while λ_{1_θ} and λ_{2_θ} are some design parameters. Note that feedback law (3.10.12) only needs the estimation of θ, $\dot{\theta}$ and χ and does not need any particular knowledge on the drag force expression.

3.10.3.2 The K_3 rope's length r control

The rope's length r control works like a servo motor using a torque control as input. This control is much more accurate than the one presented in the previous study (see figure 3.20). A PID has been chosen to perform this control. Nevertheless, it must be adapted so that it can respect the two following conditions. It must respect the condition 6 (3.7.3.1) on the maximal $\ddot{r}$ value.

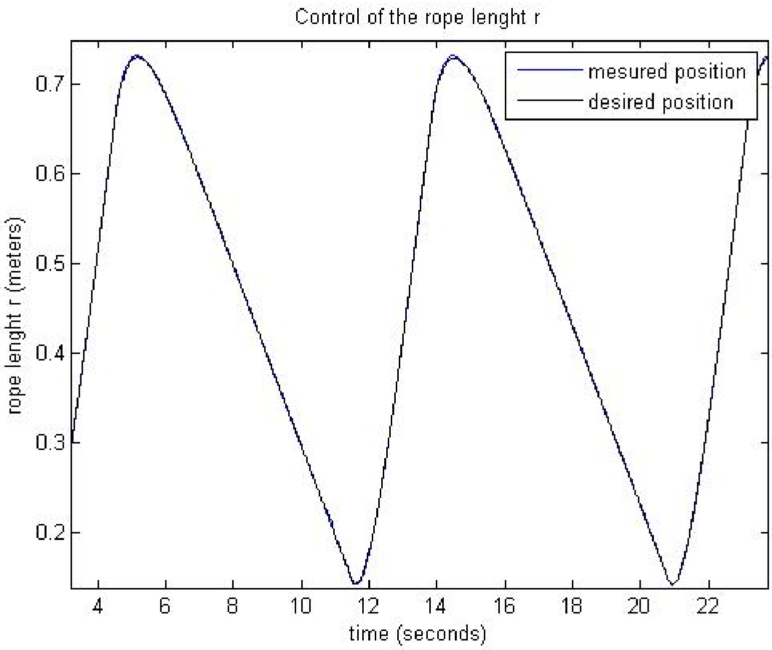

Figure 3.20: The control of the r rope length using the motor as a PID controlled servo motor.

3.10.4 Ouput power control

The proposed output power control uses the controller K_4 that computes the desired tension, which is controlled by the K_1 controller using U_α. This method allows to control with a great precision the tension and therefore the amount of generated energy.

3.10.4.1 The desired tension K_4 calculator

This kite system can not produce a constant desired output power P_{ref} because it consumes power during the recovery phase. The aim of this algorithm will be to control the produced amount of energy of each cycle.

The cycle duration is t_{cycle}, the produced energy is E_{cycle}. For simplicity matters, P_{ref} will be supposed constant, but this algorithm can be adapted to changing values of P_{ref}.

The proposed algorithm will control the desired energy E_{real} in order to reach the desired energy E_{des} defined by the following definition:

$$E_{des} = P_{ref} t_{cycle} \tag{3.10.13}$$

$$E_{real} = E_{rec} + E_{prod} \tag{3.10.14}$$

E_{prod} is the energy produced during the production cycle and E_{rec} the energy consumed during the recovery phase.

The proposed algorithm :
1) As the kite does its recovery phase, the consumed power is measured.
2) At the end of the recovery cycle, The E_{prod} value needed to satisfy $E_{real} = E_{des}$ is: $E_{prod} = E_{des} - E_{rec}$
3) Produce the desired amount of energy at the end of the production phase, the traction force has to be $T_{des} = (E_{des} - E_{rec})/\dot{r}$

3.10.4.2 The K_4 traction force controller

The traction force is measured by a torque sensor, the traction force is equal to the torque divided by the radius R of the drum. The traction force can be approximated as proportional to αv_r^2. The v_r values are steady enough to use a simple PID controller. Nevertheless, it must be bounded so that it respects the 4 safe flight conditions.

3.11 Results

3.11.1 Angle of flight θ control

This control is very important when the angle of attack is very high because of the beginning of stall propagation that provoke oscillations. One problem that has been noticed is that every phase change provokes perturbations that can be seen in Figure 3.21.

Two other problems that can be seen in the Figure 3.21. The θ angle seems to have constant error during each phase and, as a consequence, the value of U_θ tends to have a value that is too far from the standard 50% value. This might be explainable by the rope's friction, some undesired displacement of the application point of the aerodynamic force force vectors, but the answer is not clear yet. Nevertheless, the proposed control strategy proved its utility during some very intense perturbations test sessions and showed a great level of stability.

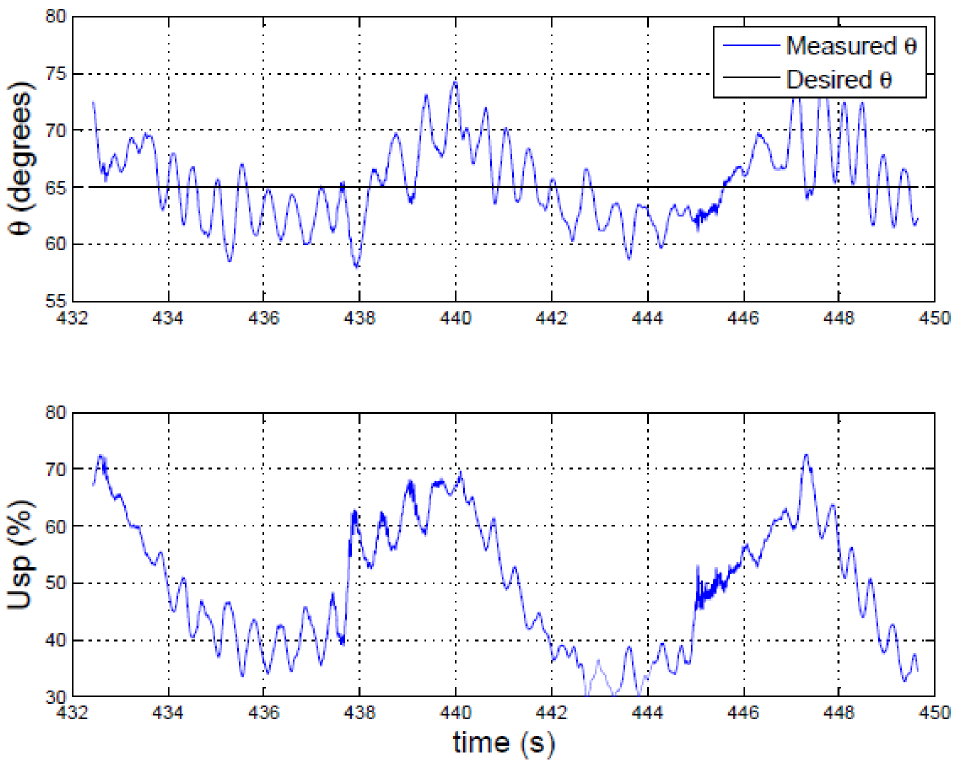

Figure 3.21: The angle of flight value and the input U_θ.

3.11.2 Rope's length r control

The r control works very properly, it follows the desired trajectory with no particular problem (Figure 3.22). The configuration of the system makes this control very stable.

3.11.3 Angle of attack control

The system has to keep the desired trajectory and produce the desired output power in presence of the changing values of wind (Figure 3.23). One can see the value of the angle of attack adapting to the wind speed changes and to the amount of generated energy.

3.11.4 Output power control

The output power control works pretty well, simulations results seem to be confirmed by the experimental validation. The experimental setup measures have shown that the amount of energy generated at every cycle's end has a mean value of 99 % of the desired output power, see Figure 3.24. The level of accuracy of the experiments fits the results that were obtained in simulations, see Figure 3.25.

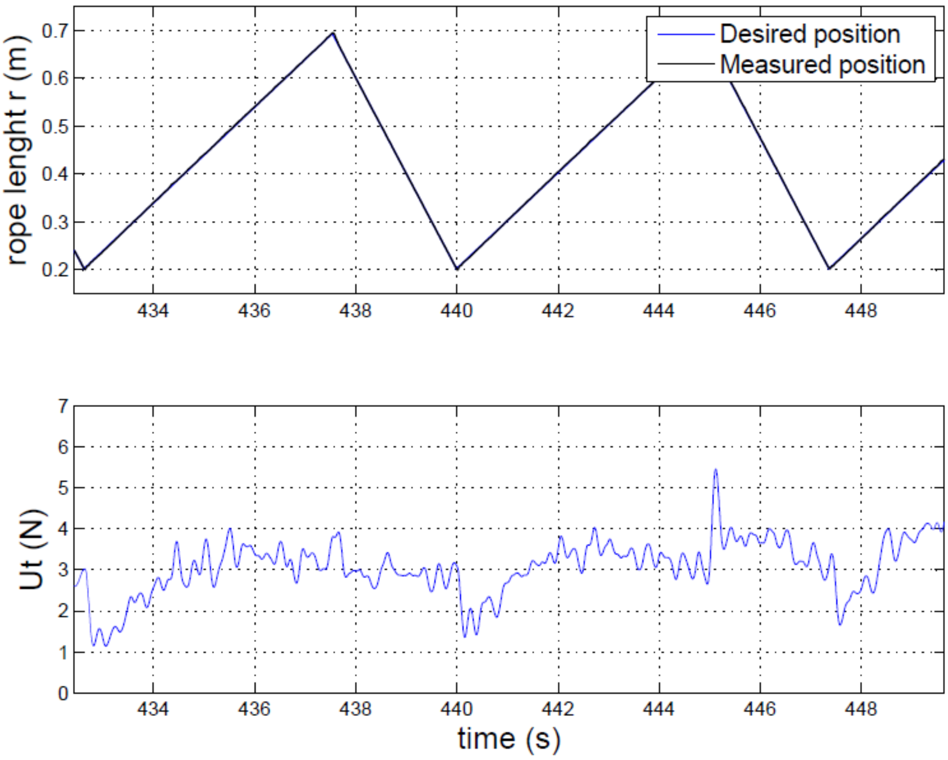

Figure 3.22: The rope lenght value (top) and its U_t value (bottom).

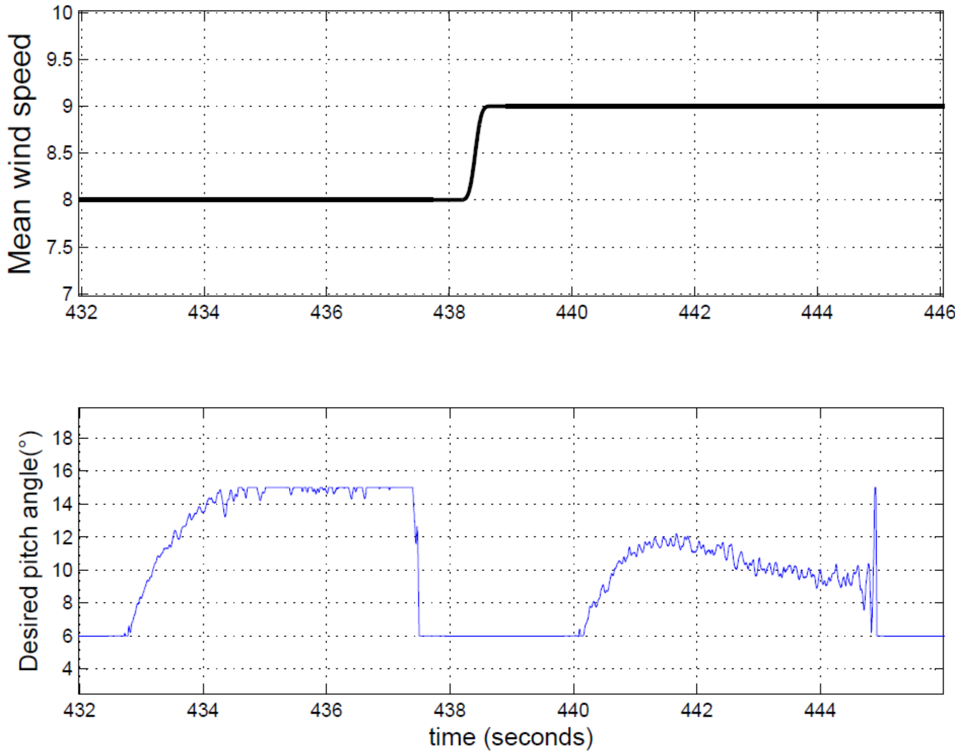

Figure 3.23: Wind speed rise from 8 to 9 m/s (top) and the U_α reaction. Note that the controller reduces the AOA to avoid an overproduction of energy.

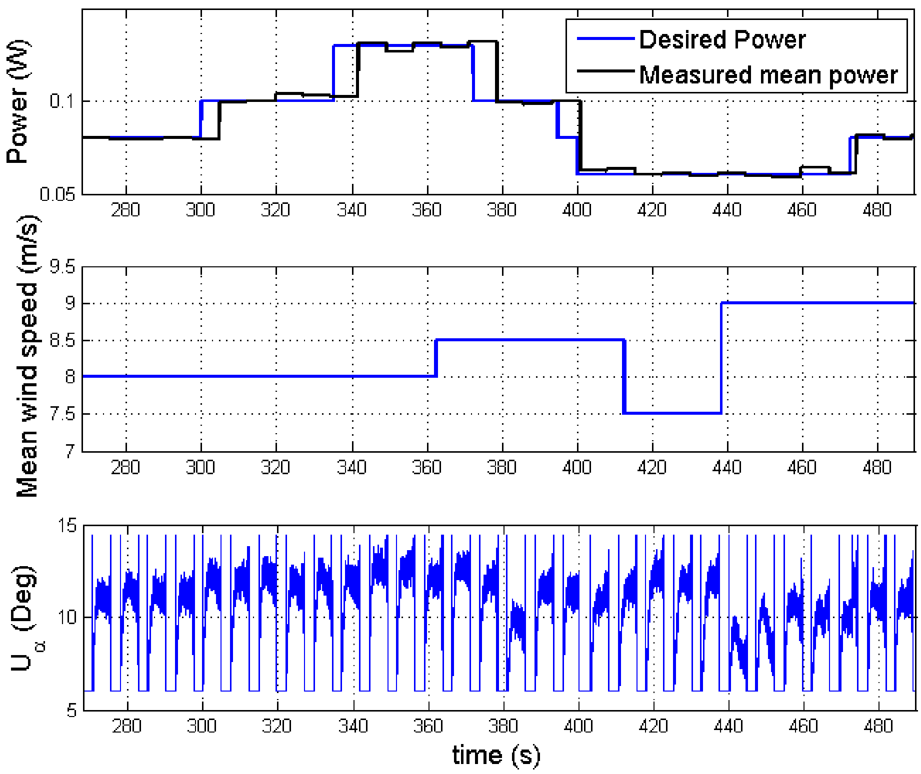

Figure 3.24: Measurement of the output power, tracking a variating desired power in presence of a wind speed that goes from 7.5 to 9 m/s.

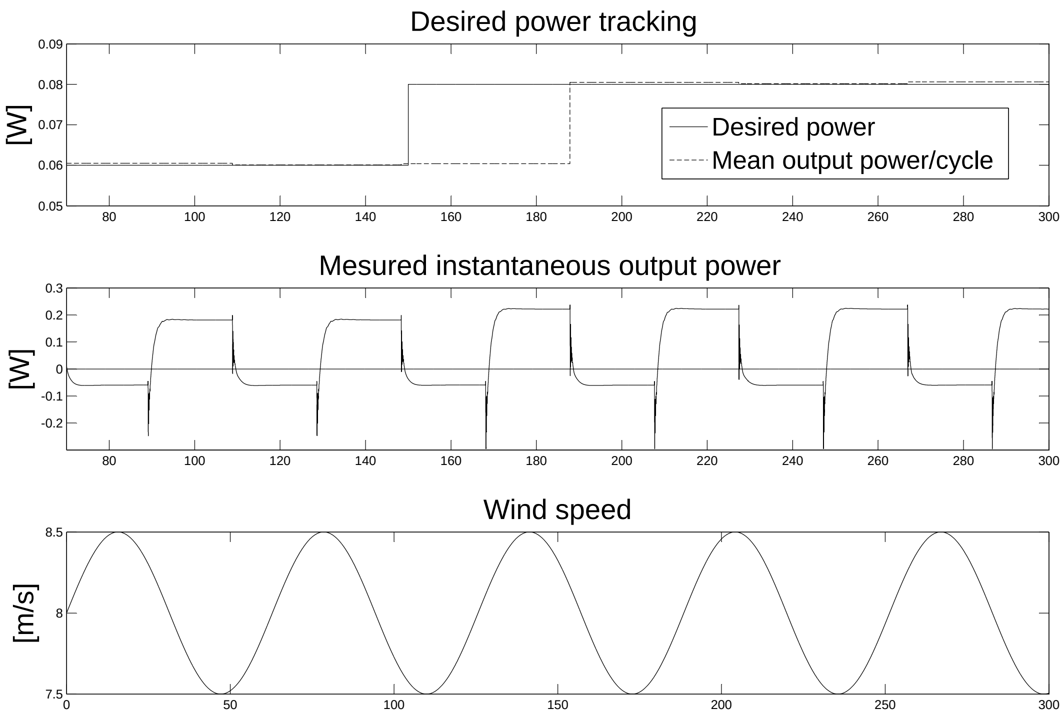

Figure 3.25: Simulations of the output power, tracking a step function in presence of a wind speed that follows a sinusoidal value.

3.12 Conclusion

In this chapter we have studied a wind power generation system mainly composed of a wing attached to a dynamo with a rope. The wing subject to airflow generates a lift force which drives the dynamo on the ground to generate power. We have focused our interest in such a configuration because it is less expensive than current wind power systems and could be used in rural areas without infrastructure. We have presented an aerodynamical non linear model of the wind power generation system. We have introduced spoilers in the wing so that damping introduced into the system cancels oscillations in the displacement of the wing. We have also proposed two different control strategy to stabilize the wing displacement and the rope length. Such control laws were based on state feedback linearization and an observer based control techniques. A method has been developed for controlling the output power, the accuracy of the control is 99 percent in presence of changes of wind speed. An experimental set-up has been built including a wind tunnel, a wing with spoilers and a system for controlling the wing angle of attack. The experimental prototype has been used to test the control of the yaw angle, the angle of attack and the angle of the rope. The indoor testing made the tests much faster, safer, with more accurate results than what could have been done in an outdoor experiment. The simulations and the experimental results fit quite well, which validates the aerodynamical model and the effectiveness of the proposed control algorithms.

Nevertheless, the proposed approach for rejecting perturbations does limit the energetic performance. This is due to the size of safety margins and to the response time of the actuators. In order to be competitive, safety margins will have to be reduced. Kite systems will face wind gusts that will appear faster than the response time of the actuators, as a consequence, they will probably lose control. The control system role will no longer exclusively be to avoid chaotic situations but also to be able to regain control of the kite once it is in a chaotic situation.

Chapter 4

Reverse pumping

4.1 Introduction

Most kite wind power systems have a great drawback that wind turbines do not have: they cannot stay in the air if the wind is not strong enough. As a consequence, most of the kite systems need to land when there is no wind, and to take-off once the wind is strong enough. These maneuvers are quite risky because generally the wind gets weak and turbulent close to the ground's surface. Moreover, as the wind can be strong enough at high altitude and weak close to the ground, it might lead to losses in energy production. From a material point of view, ”classic” landings and takeoffs need a landing zone, ground handling or infrastructure (such as pylons) that reduces the advantages of kite systems. Some ideas, such as embedded motors or helium balloons, might solve this problem, but they have their own drawbacks such as the weight of the motor and its battery, the necessity of a conductive cable or the need to refill the balloons.

This chapter studies a solution called ”reverse pumping”. It basically consists of providing kinetic energy to the kite by pulling the kite with a rope. This kinetic energy is then transformed into potential energy by gaining altitude. This technique allows to keep the kite airborne in total absence of wind. This chapter will explain the reverse pumping principle, the constrains on the aerodynamical model, flight simulations and will present the experimental setup used to validate the theoretical study.

4.1.1 Basic principle

The following technique is not intuitive at all. It consists of maintaining the kite in the air, by pulling it with a force directed to the ground. These kinds of phenomena are in fact somewhat common, for example, the classic yo-yo game can use a force directed

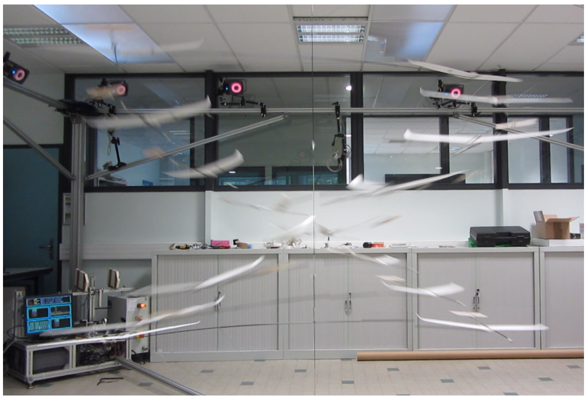

Figure 4.1: The experimental protocol in flight.

to the ground to maintain a mean altitude over many up and down cycles that remain constant. In the case of the yo-yo, the force used to push the yo-yo to the ground is then converted in kinetic energy, and is then reused by the yoyo to regain altitude. In the case of the kite system, the basic principle is similar, but the system is more complex as it has various control inputs that can be used to optimize the energy consumption, and it obeys aerodynamic forces that depend on the state of the kite and on the wind perturbations. The following study uses only the tension of the rope to transmit energy to the kite. This allows the system to not need an on-board source of energy which reduces the prototype's weight, and to use a source of energy that is on the ground. Therefore, the kite can stay in flight as long as one provides energy to the on-ground system, without needing a conductive cable. If the control of the kite in embedded, it consumes some energy, but this energy could be generated on-board by some small wind turbines, this system would not limit the flight time.

4.1.2 Objectives

The main objectives of this chapter are :
- To study the influence of the aerodynamic characteristics on performance.
- To propose a flight plan for performing reverse pumping.
- To study the cost of maintaining the kite in flight with this technique in order to state whether it is more profitable to use this reverse pumping technique.

The chapter is composed of a theoretical investigation of reverse pumping, numerical simulations applied to a twin kites system and finally, validation of the numerical simulations on an experimental setup.

4.1.3 Chapter's organization

The chapter is organized as follows: section 4.2 introduces the studied models, section 4.3 presents the aerodynamical model of the last prototype. The description of the principle of reverse pumping is described in section 4.4 and the performances are described in section 4.5. The control algorithm will be described in section 4.6, the experimental protocol in section 4.7 and the results will be described in section 4.8.

4.2 Studied models

This chapter would have been incomplete without an experimental validation. As a consequence, it was needed to study a model that we could build, with a position which could be measured and controlled properly. It is a difficult task that is unfortunately often skipped, as simulations tend to be presented as a proof of concept.

4.2.1 Early models

During the first year of PhD, two different prototypes were build with roughly the same working principle. The simulations that were done showed good results, but the experimental setups gave results that were much less positive. During the second year, the efforts were concentrated on other experiments. During the third year, a radical change of experimental setup was made and three different prototypes were build. The third and fourth prototypes gave hope and the fifth prototype showed that the reverse pumping principle works.

4.2.1.1 The *Satellite I and II*

The idea of reverse pumping came from some videos where some people would make kites fly indoors for a kite contest. It had nothing to do with the energy production, its aim was purely artistic. Nevertheless, these people were able to make a kite fly without wind, without moving their foots, just by pulling and releasing the kite's rope. Few time later, simulations showed that this concept could make a kite fly just by pulling and releasing the rope.

The first idea in order to prove that the reverse pumping was possible was to build a kite that would look pretty much like a standard kite, see Figure 4.2. This kind of flight seemed too complex to be done because it would have needed to measure 6 degrees of freedom, control 3 actuators for the kite's orientation and the rope's pulling would have needed a complex mechanical structure. An other difficulty would have been due to the fact that there are few accessible places where the the room would have been big enough for this kind of flights. The only wide space that was available was a room of 9 meters by 9 meters with a ceiling at 2.5 meters.

Figure 4.2: An indoor kite contest.

To sum up, this kind of kites would have had too many degrees of freedom, and would have needed too much room to fly it. The solution was found thanks to the work of Victor Tatin, see chapter 2. The choice was made to develop a prototype that would fly in circles. The left wing tip was attached to a pole in order to do so. It had its propulsion system and a control unit to control its altitude. The kind of flight was very close to the ones of control line model airplanes, see Figure 4.3 .

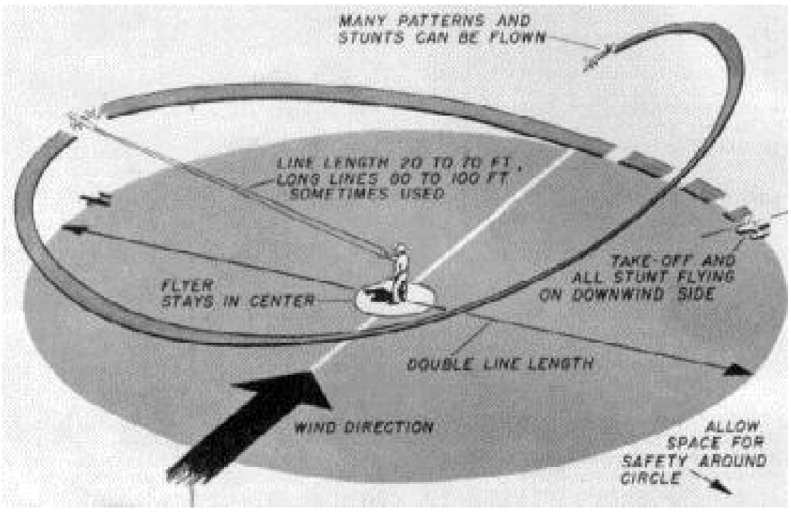

Figure 4.3: Flight path of a standard control line model airplane.

The centrifugal force acting on the flying model locked the two axis of rotation equivalent to the roll and yaw. In other terms, the direction of the rope and the axis between the attachment point and the center of mass of the flying machine are almost tend to be aligned. In order to separate the lift that would compensate weight from the lift that would accelerate the flying speed of the prototype, a second wing was added on the prototype (see figures 4.4 and 4.5).

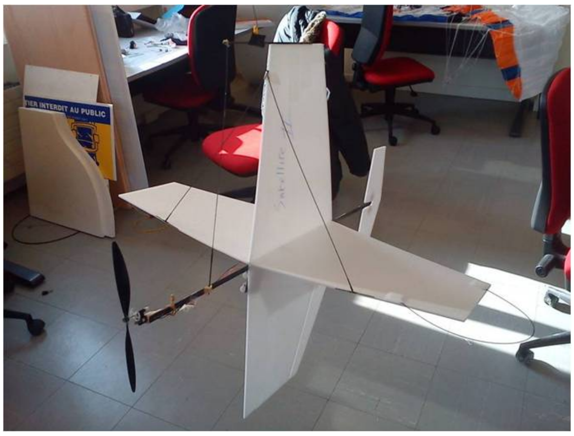

Figure 4.4: The "Satellite I", first prototype for reverse pumping.

Figure 4.5: The "Satellite II", improvements were made to build a prototype that would be lighter, stiffer and with a lower amount of drag.

This wing's objective was to generate the lift necessary to accelerate the kite independently of the horizontal wing. During the acceleration phase, the propulsion engine would be shut down and the cable would pull the kite so that the vertical wing would generate a lift force that would accelerate the kite. Both built prototypes flew but the results were not convincing. The main cause of failure was that the prototype was still too complex, the two wings were not independent enough, and drag was generated by the propeller and by the results of an excessive elasticity. The project was abandoned until a new idea for the experimental setup was found. One year later, some studies about helicopter's auto-rotations brought the idea of using a helicopter's swashplate mechanism in order to perform reverse pumping. An example of autorotation can be seen in Figure 4.6. Both flight paths would be very similar: energy would be accumulated by the blades-kites during the descent. The same accumulated energy would then be used to regain altitude by changing the angle of attack of the blades-kites.

Figure 4.6: S-70i helicopter performing an autorotation.

The second change was that more hardware was available. All the equipement used in the experiments of chapter 2 was available, and a Vicon mesurement unit got acquired by the lab. The new experimental setup gained a lot from these equipment. The third and fourth prototypes brought hope and interresting results and the fifth proved that the reverse pumping principle works.

4.2.2 New construction guidelines

Taking into account the restrictions due to the construction of a working prototype and the gained experience, the last three prototypes were designed using the following guidelines:

1) The model's state will be measured using a Vicon optical tracking system. Therefore, it needs to be able to perform reverse pumping flying in a space of 3x3x3 meters, which is the flight domain in which the Vicon system can perform the measurement.

2) Aerodynamical forces obey to equations that become very complex if they are not studied in the correct domain. We will try to reduce the error due to the model as much as we can. Therefore, the shapes of the kite will be simplified, compared to standard kites, but it will greatly enhance the accuracy of the model and therefore the study's relevance.

3) For simplification, we will only control the inputs that are necessary to perform reverse pumping, i.e. the angle of attack and the rope's length. Many freedom axes will be locked as the wings will be fixed.

As a result of these guidelines, the three last experimental protocols were built, they corresponds to a simplified model of the twin kites [34]. The main difference is that the kites have much simpler movements (see Figure 4.7). The construction of the protocol makes that they can only fly turning symmetrically around a vertical axis, keeping a constant distance from each other. The two inputs are the pitch angle control U_α, which is the same for the two kites and the control of the main rope's length U_r. R is the distance between the center of rotation and the tip of one wing, z is the height of the system.

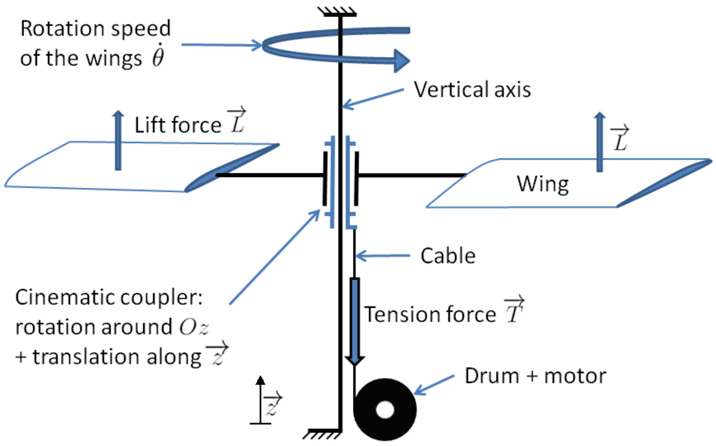

Figure 4.7: Scheme of the experimental setup.

4.2.3 Inspiration

The kite system has been inspired by the Otto Lilienthal's 'Whirling arm', (see Figure 4.8). It was probably the first aerodynamic forces measurement machine [85].

Using the knowledge brought by this machine, Lilienthal built many different kinds of gliders that made successful short flights. He died in 1896, when a wind gust made him lose the control of his machine. He is now considered the father of Aeronautics. One hundred and twenty years later, Lilienthal's sense of simplification and his experimental techniques are still used for experimental aeronautical research and has led to major innovations (see chapter II).

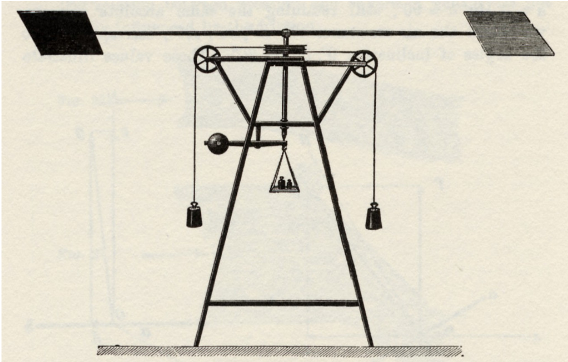

Figure 4.8: The Lilienthal's 'Whirling arm'.

4.3 Aerodynamical model

Standard kites can be studied with the classic airplanes equations of flight mechanics. Our system is a bit different because as the kites fly in small circles, they pass through their own downwash and generate a wake that has a vertical speed V_w, that can be described by the basic equations of a hovering helicopter. This wake's speed tends to greatly diminish the performance of our system, but it will probably not exist in outdoor models, as the kites pass less quickly by the same point. In this case, they can be studied using the standard flight mechanics equations. Other phenomena make it complex to study, like the non constant wind speed along the wingspan, the strong ground effect, etc. In order to reduce the model's errors, the first study will be done with the helicopter equations to study how to design the experimental setup so that it can be studied with the classic airplane's flight dynamics equations. The experimental setup will be designed using the knowledge brought by helicopter theoretical equations.

4.3.1 Helicopter Theory

By studying helicopter theory equations [87], one can see how design parameters act on the system. As the two wings turn around an axis, they define a rotor disc that generates lift and a wake (see Figure 4.9). From this point of view, the system is similar to the rotor disk defined in standard helicopter theory. However, there are still some differences between the initial assumptions of helicopter theory and the ones of our experimental setup: the blade's length are smaller than the radius of the disc, the system flies in presence of ground effect and some "roof effect", the rotation speed of the rotor is low. The wake generated by the downwash reduces the efficiency of the system because it changes the angle of relative wind speed and makes the lift turn backwards. As a consequence, the torque generated by the lift decreases as well as the general efficiency of the system.

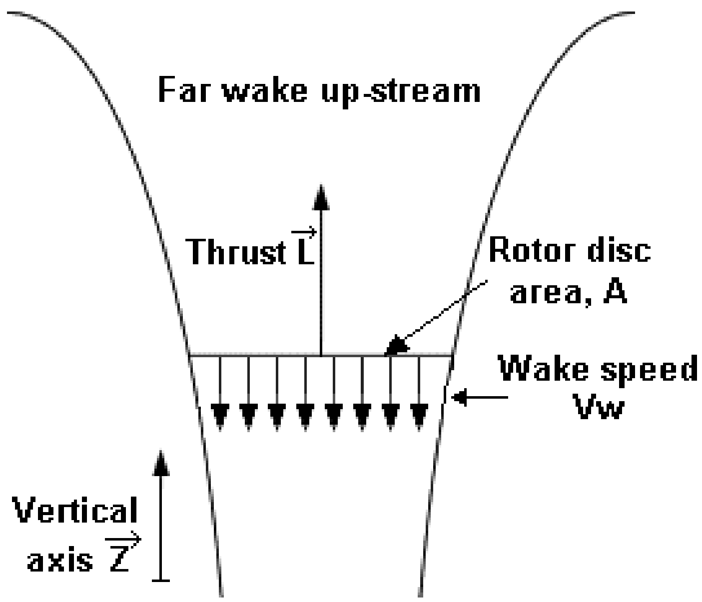

Figure 4.9: Side view of the rotor disc and it's wake.

Considering a rotor disc that generates a lift force L, has a rotor disc area A, an air density ρ, constant climbing speed V_c along the vertical axis $\overrightarrow{Z}$, the speed V_w of the wake that passes through the rotor disc is given by (4.3.1):

$$V_w = -\frac{V_c}{2} + \sqrt{\left(\frac{V_c}{2}\right)^2 + \frac{L}{2\rho A}} \tag{4.3.1}$$

Using the mean values of the lift over a cycle, we can get an approximate idea of what the value of the wake will be. Additionally, ground effect tends to diminish V_w by a factor $K_G = 1 - (R/4z)^2$, where R is the rotor's radius and z it's height. Note that in order to remain in flight, the lift force L needs to be greater or equal to the weight of the prototype. As a conclusion, in order to reduce the value of downwash, one needs to build a prototype that is very light, and at the same time, has a large diameter to increase the disc area A. These two characteristics are obviously hard to conciliate.

4.3.2 Flight Mechanics Approach

A standard flight mechanics approach to the problem will be done to try to model the behavior of the kite. The results will be then compared to experimental results. In this section, the wake V_w is assumed to equal zero. The trajectories and the study of the system will be calculated taking as a basis the following equations. The forces applied to each wing wing are described in Figure 4.10. Note that the aerodynamical forces acting on both wing have the same strength. For the sake of representation, half of the traction force $T/2$ and half of the weight $W/2$ are sketched in Figure 4.10, permitting us to draw the acceleration, lift and drag vectors corresponding to only one of the two wings. The total lift force is $2L$, total drag is $2D$ and acceleration rate is $2a$. The equations of lift $\overrightarrow{L}$

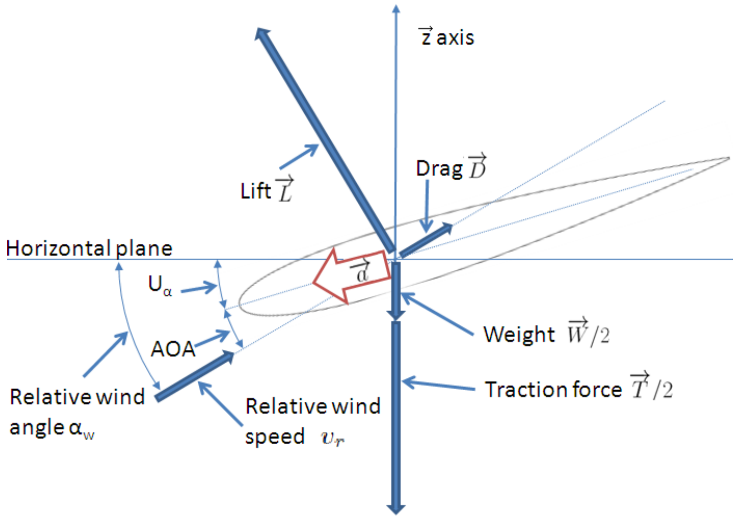

Figure 4.10: Forces diagram for each wing.

and drag $\overrightarrow{D}$ are defined for each wing using standard notation, i.e. the drag is directed in the same direction as the relative wing angle, and the lift applies orthogonal to it, in the direction of positive angle of attack (AOA $= \alpha$) as depicted in Figure 4.10. The strength of each force is described in (4.3.2),

$$L = \frac{1}{2}\rho S v_r^2 C_L \quad ; \quad D = \frac{1}{2}\rho S v_r^2 C_D, \tag{4.3.2}$$

where ρ is the air density, S is the surface of each wing, v_r is the relative wind speed and the lift coefficient is C_L (4.3.3) and the drag coefficient C_D (4.3.4) are:

$$C_L = \frac{\partial C_L}{\partial \alpha}(\alpha_w + U_\alpha) + C_{L0} \tag{4.3.3}$$

$$C_D = \frac{C_L^2}{\pi e \lambda} + C_{D0} \tag{4.3.4}$$

where C_{L0} is the lift coefficient at null AOA, λ is the aspect ratio and U_α is the pitch angle. The zero lift drag coefficient C_{D0} will take into account the drag of the structure. In this case, Oswald's efficiency factor e should not be defined as it usually is because the distribution of lift along the chord is not symmetric [83]. This e factor is normally used to calculate the AOA that leads to the best L/D ratio but in this case, we will not use e and directly work with the L/D ratio. Also, note that when the kite is performing a non accelerated flight at a constant speed $R\dot{\theta}$ with $T = 0$, its corresponding glide slope is $GS(\alpha) = -\arctan C_D/C_L$. At that moment, the sum of the lift and drag vectors is vertical, compensates the weight of the kite, and the kite's acceleration is equal to zero. This gliding slope $GS(\alpha)$ is an important parameter because it defines the minimal gliding slope needed in order to perform reverse pumping. The classic way to reduce the value of this gliding slope $GS(\alpha)$ is to make λ greater. The second way is to fly with the optimal AOA, which in this case will more complicated as it will be used for control purposes.

4.3.3 Relative Wind Speed

Relative wind characteristics will be defined, assuming the air is still. The relative wind speed will be approximated by the sum of the horizontal speed v_h and the vertical speed v_v (4.3.5).

$$v_h = \dot{\theta}R \quad ; \quad v_v = \dot{z} + V_w \tag{4.3.5}$$

In the equation (4.3.5), the radius R is the distance between the rotation axis and the middle of the wing. Note that in this case, the horizontal windspeed v_h is an approximation because it is not constant along wingspan. In our experiment, for each wing, the relative wind speed difference from the right wingtip to the left wingtip is approximatively of 4. If the radius R would be much greater than the wingspan, the horizontal windspeed v_h over one wing could be approximated as constant and equal to $R\dot{\theta}$, and one could use the e factor and the equation 4.3.4 to calculate the L/D ratio.

Using equation (4.3.5) we obtain the wind angle α_w (4.3.6), which is the angle of the wind velocity vector measured with respect to the horizon. The wing's relative wind velocity is given by v_r (4.3.7).

$$\alpha_w = -\arctan\frac{\dot{z} + V_w}{\dot{\theta}R} \tag{4.3.6}$$

$$v_r = \sqrt{(\dot{\theta}R)^2 + (\dot{z} + V_w)^2} \tag{4.3.7}$$

Note that when $V_w = 0$, the gliding slope GS is defined by the relative wind angle $\alpha_w = -\arctan\frac{\dot{z}}{\dot{\theta}R}$.

4.3.4 Acceleration Rates

This system can have two kinds of accelerations: vertical and rotational. The vertical acceleration $\ddot{z}$ is given by equation (4.3.8):

$$\ddot{z} = \frac{L\cos(\alpha_w) + D\sin(\alpha_w) - w - T}{m} \tag{4.3.8}$$

The rotational acceleration $\ddot{\theta}$ is given by (4.3.9):

$$\ddot{\theta} = 2\frac{Ra}{J} = 2\frac{RL(\sin\alpha_w) - RD(\cos(\alpha_w)}{J}, \tag{4.3.9}$$

where J is the moment of inertia. Its value will be approximated by $J = mR^2$, where m is the mass of the system. These two equations will be used to study the model's performances and behaviors depending on the L/D ratio and on the gliding slope.

4.4 Basic Principle of Reverse Pumping

The basic principle of reverse pumping lies in the exchange of energy during two different phases: the "kinetic energy charge" phase and the "potential energy transfer" phase. Kinetic energy charge happens between time t_0 and t_1, when the kite will convert the energy provided by the rope's tension into the kite's kinetic energy. Potential energy transfer happens from time t_1 to t_2, when the kite transforms the kinetic energy into potential energy by acquiring height. For simplicity matters, the efficiency of the transitions during the phases will not be studied here, they shall be studied in future work to improve the results. We differentiate four different kinds of energy. The energetic cost ΔE_t is the energy brought by the rope's tension T. Its value can be written as:

$$\Delta E_{t\,t_0\to t_1} = \int_{t_0}^{t_1} T\dot{z}dt. \tag{4.4.1}$$

The variation kinetic energy of the kite is:

$$\Delta E_{c\,t_i\to t_j} = 0.5m(V(t_j)^2 - V(t_i)^2), \tag{4.4.2}$$

and the variation potential energy is (4.4.3):

$$\Delta E_{p\,t_i\to t_j} = mg(z_j - z_i). \tag{4.4.3}$$

During the kinetic transfer phase phase, $i = 0$ and $j = 1$, and during the potential transfer phase, $i = 1$ and $j = 2$. These energy variations obey the following equations:

$$\Delta E_t = \Delta E_c + \Delta E_p + \Delta E_{lost} \tag{4.4.4}$$

where ΔE_{lost} is the loss of energy due to drag.

There are several ways to transmit energy during the kinetic energy phase, such as using a constant tension T, a constant slope, or changing angles of attack. This study will focus on a technique using constant slope and constant angle of attack. Its main advantage is simply that its simpler to explain and study. For the potential energy transfer, the study will consider flight with a constant angle of attack. Note that the novelty of the study lies on the first phase.

4.4.1 Initial Conditions

The initial conditions correspond to a non accelerated flight of the kite with rope tension T equal to zero. The initial speed V_0 is chosen such that the sum of the lift and drag vectors compensates the weight vector mg, and therefore $V_0 = \sqrt{\frac{2mg\cos GS(\alpha)}{\rho SC_L}}$. The angle of attack is kept constant, and the corresponding gliding slope is $GS(\alpha)$. At that instant, the kite's acceleration is equal to zero and it behaves like a glider in non accelerated flight. The initial height is greater than z_0.

4.4.2 Kinetic Energy Charge Phase

The kinetic charge phase starts when the glider's height is equal to z_0. A tension T will force the system to follow a straight trajectory with a forced slope where the value will be less than the gliding slope $GS(\alpha)$. The forced gliding slope is defined as $FS = GS(\alpha) - \Delta_{GS}$, where Δ_{GS} is the slope added by pulling the kite. As a consequence, the sum of $\overrightarrow{L}$ and $\overrightarrow{D}$ will no longer be aligned with the weight and generate an acceleration vector that will increase $R\dot{\theta}$ and therefore the kite's kinetic energy. The horizontal component of the acceleration vector is the one part that increases the horizontal speed $R\dot{\theta}$ and its acceleration is given by (4.3.9). The end of this period t_1 happens when the kite reaches its lowest height z_1, while respecting its maximum speed V_{max}. If this phase is effective, the kite's energy $\Delta E_c + \Delta E_p$ is greater at t_1 than at the initial time t_0.

4.4.3 Potential Energy Transfer Phase

At the beginning of the potential energy transfer phase t_1, the potential energy of the kite is $E_p(t_1) = mgz_1$, where z_1 is the glider's altitude at t_1. During this phase, the transmitted kinetic energy $\Delta E_{ct_0 \to t_1}$ will be transformed into potential energy by gaining altitude. The tension T of the cable is set to zero during the entire phase. When all the gained kinetic energy will be transferred, its value will reach back its initial value, and as a consequence, the kite's speed will be V_0 and this moment will define the time t_2. This allows to calculate the amount of gained energy using only the difference of potential energy between t_0 and t_2.

In order to have the same gliding slope at t_2 than at t_0, The kite will transform its kinetic energy into potential energy by gaining altitude until the kites reaches it's maximal height or it's speed goes below the initial speed V_0. This flight can be done with different flight plans. The two principals are flying with a constant AOA, of flying with a constant gliding slope, that is controlled by acting on the AOA. The end of this phase happens when the kite has regained its original flight speed V_0. The reverse pumping is effective if the height z_2 is greater or equal to z_0.

4.4.4 Standard flight plan

To sum up, a classic flight plan looks like figure 4.11. In this particular case, the end of the potential transfer phase happens when the kinetic energy reached its initial value, and the final height is much greater than the initial value.

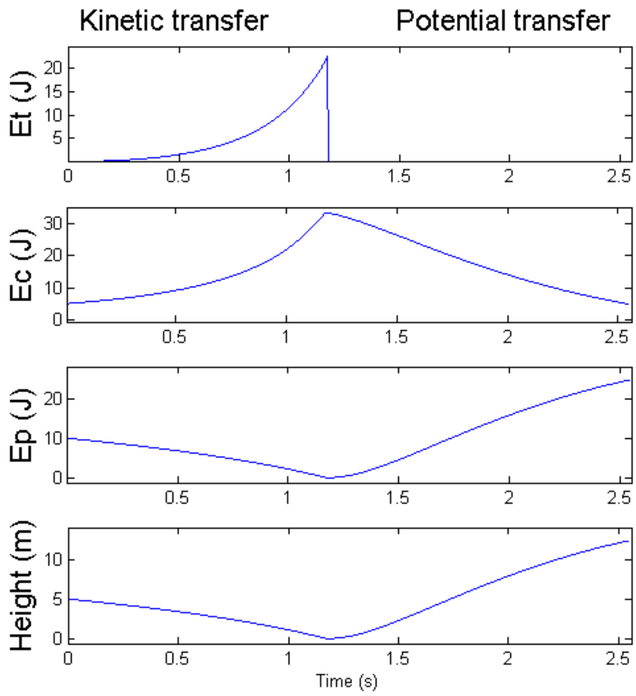

Figure 4.11: Example of the energy variations during the *kinetic charge* phase and the *potential transfer* phase. Note that the final height is greater than its initial value. (L/D =20 , Δ_{GS}=20 degrees)

4.5 Performances of the system

In this study, three different characteristics will be analyzed and we will try to study their relation with the L/D ratio. The most important factor is ξ, the variation of kinetic energy per loss of altitude during the kinetic charge phase, given by equation (4.5.1). Its value must be greater than one to make the reverse pumping possible. One can see in Figure 4.12 that ξ increases with the L/D ratio and the Δ_{GS} value. Note that if $\Delta_{GS} = 0$, ξ is necessarily equal to zero and the reverse pumping is not possible.

$$\xi = -\frac{\Delta E_{ct_0 \to t_1}}{\Delta E_{pt_0 \to t_1}} \tag{4.5.1}$$

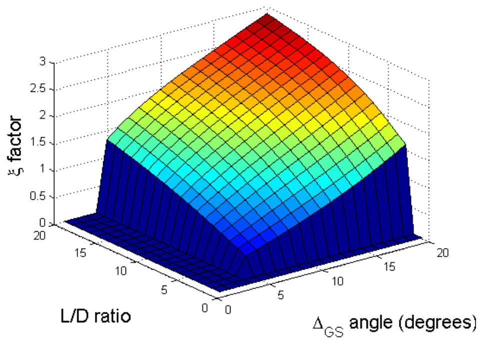

Figure 4.12: Variation of kinetic energy divided by the lost potential energy during the *kinetic charge* phase.

The factor η_1 characterizes the efficiency of the transfer during the kinetic charge phase. Its expression is given by equation (4.5.2) and plotted in Figure 4.13. Note that this parameter gives information about how much it will cost to make a kite stay in the air. The cost worthiness depends of many other parameters that are quite hard to estimate, like the risk of crashing, how long the wind speed is going to be low, etc.

$$\eta_1 = -\frac{\Delta E_{pt_0 \to t_1} + \Delta E_{ct_0 \to t_1}}{\Delta E_{tt_0 \to t_1}} \tag{4.5.2}$$

The η_2 parameter characterizes the efficiency of the potential transfer phase, i.e. the efficiency of the energy transfer from the gain kinetic energy E_c to the potential energy E_p, see equation 4.5.3. As the L/D ratio increases, η_2 gets closer to 1, see Figure4.14.

$$\eta_2 = -\frac{\Delta E_{pt_1 \to t_2}}{\Delta E_{ct_1 \to t_2}} \tag{4.5.3}$$

The reverse pumping increase of energy per cycle can be characterized by the energy gain $\xi\eta_2$ value plotted in Figure 4.15. Note that in order to be effective, $\xi\eta_2$ has to be greater or equal to 1, the design of the flight plan and the kite's characteristics must respect this condition. One can see that in this case, many combinations of low values of L/D and Δ_{GS} cannot satisfy the requirements of reverse pumping.

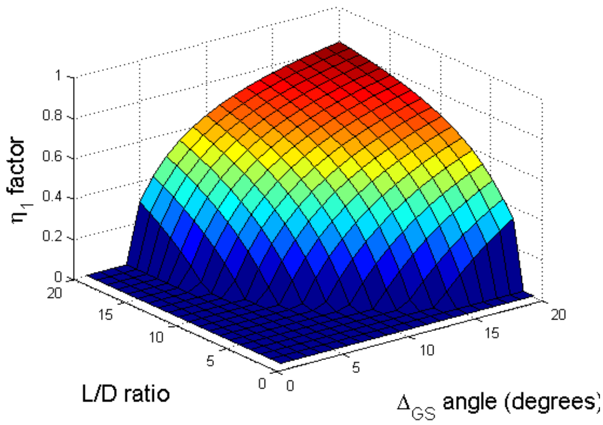

Figure 4.13: Efficiency of the *kinetic charge* phase.

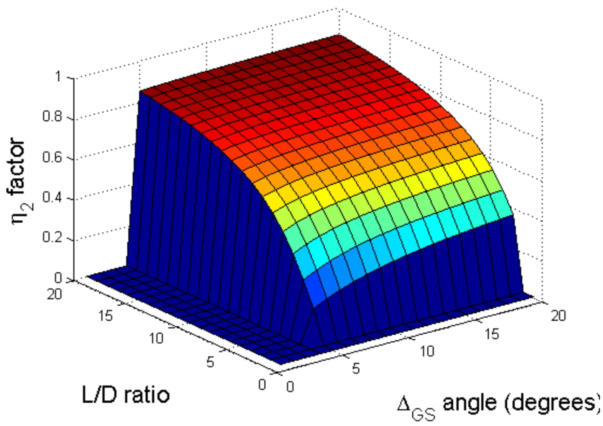

Figure 4.14: Efficiency of the *potential transfer* phase.

Note two limits are not taken into account in the previous plots: the fact that the motor that pulls the kite has limits on its performances and the maximum load of the kite system. As this study is made for a constant angle of attack, the maximum speed has a limit that can be calculated using the maximal load of the kite and equation (4.3.2).

4.5.1 Cost of the flight time with the reverse pumping technique

In order to know if it is worth using the reverse pumping technique, one has to compute its cost, and compare it to the cost of making the kite land and then takeoff that depends on the kite type. This section will present an approximated formula in order to compute the cost of the flight time.

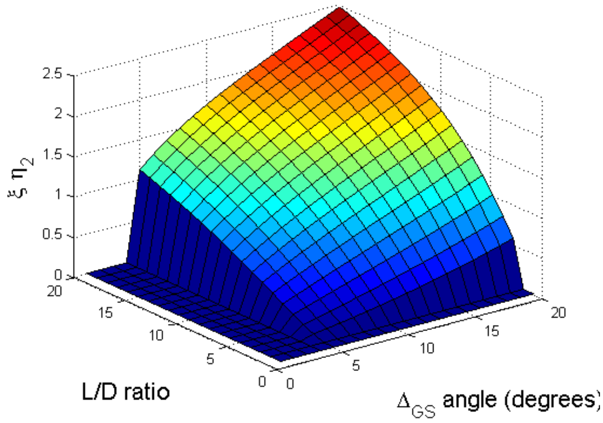

Figure 4.15: Increase of energy per cycle. Note that it increases with the L/D ratio and Δ_{GS}

During a cycle, the consumed energy is ΔE_t. The end of the potential transfer phase can be defined as the moment when the kite's kinetic energy reaches back its initial value, i.e. the kite's speed reaches V_0. In order to concatenate easily cycles of kinetic charge and potential transfer, the flight slope should also be the same between the end of the cycle and the beginning of the next cycle. In order to do so, the kite should modify its trajectory from going up to going down with the initial gliding slope. This maneuver has an energetic cost that will be here neglected and therefore, the end of the potential transfer phase will be defined as the moment when the kite's speed is V_0 and that all the maximum height has been reached. In this case, the maximal height value is $z_{max} = z_0 \xi \eta_2$. The height between z_0 and z_{max} can be spend by the kite gliding until it starts another cycle of kinetic charge phase. The flight time FT will be approximated by the gliding time, neglecting the kinetic charge and potential transfer phases lengths. Like the initial condition, the flight speed is V_0 and the gliding slope being $GS(\alpha)$, the vertical speed is then $V_z = V_0 \sin GS(\alpha)$. The cost of the flight time in Watts will be named X, and is given by equation (4.5.4):

$$X = \frac{\Delta E_t}{FT} \quad ; \quad FT = \frac{z_0 \xi \eta_2 - z_0}{V_0 \sin GS(\alpha)} \tag{4.5.4}$$

In this special case, for values of $L/D = 20$ and $\Delta_{GS} = 20$ degrees the cost of the flight time is approximately 1.8 W. A standard flight with an embedded propulsion system like a propeller would consume approximately 0.5 W, see [83].

4.6 Control of the system

4.6.1 Control architecture

The system is composed of 4 main parts. The kite system includes the two kites with an embedded control unit that controls the tail position so that the angle of attack of the wing takes the desired position. The position is then measured with a Vicon motion capture system and sent to a real time computer that makes the control loop for the altitude control (4.6.3) and transmits the orders to the ground station. The ground station has a motor and a controller used to pull the kites down with the desired position.

4.6.2 The angle of attack control

The angle of attack of the kite can be controlled with different techniques. Some experiments have used the length of the cable or their attachment point to control it. This experiment will use a method that is classically used in airplanes; a tail has been mounted on the wing to control it. The major advantage of this method is that the angle of attack has a stable value that depends on the angle of attack of the tail [83]. Normally, a PID controller is enough to reject perturbations and allows proper control of the AOA. The main use is to reduce oscillations, the D parameter is then the most important. In this particular case, the control could not be implemented because of the short length of each cycle.

The total response time, from acquisition of the position to the stabilization of the AOA could not be done within the duration of a the kinetic charge phase, as its duration is approximately 0.2-0.5 seconds. The acquisition and calculation of control were done at a frequency of 200 Hz but the main problem was the response time of the servo that would have a response time of around 0.2 seconds. The passive stability of the system was used, but led to an approximate control of the AOA.

4.6.3 The altitude control

A rope and a servo motor are used so that the kite follows the forced gliding slope FS during the kinetic transfer phase. The value of FS is controlled by $FS = GS(\alpha) - \Delta_{GS}$ and GS is approximated by $-\arctan \frac{\dot{z}}{\dot{\theta} R}$. The $\dot{\theta} R$ value is controlled by aerodynamic forces and the value of $\dot{z}$ is computed so that it follows $-R\dot{\theta}\tan(FS)$. To do so, a PID controller has been implemented to control the motor's position. More complex algorithms could be used to diminish the consumption of the motor. The reduction of consumption comes as a more complex work that does not seem relevant before the reverse pumping functions properly.

4.7 Experimental setup

A movie showing the experimental results can be viewed in [1].

4.7.1 The kites

The third and fourth prototypes had an angle of attack that was directly controlled by a servo fixed to the carbon tube. This led to a low accuracy on the AOA control because the main carbon tube had the tendency to twist over the longitudinal axis.

The control of each wing's AOA had to be more accurate and the system had to be light, so the chose has been made to use auto stabilized wings; the tube does not need anymore to have a axial stiffness. The control of the AOA got enhanced, but the stabilization system would have needed lower response times in order to be really effective.

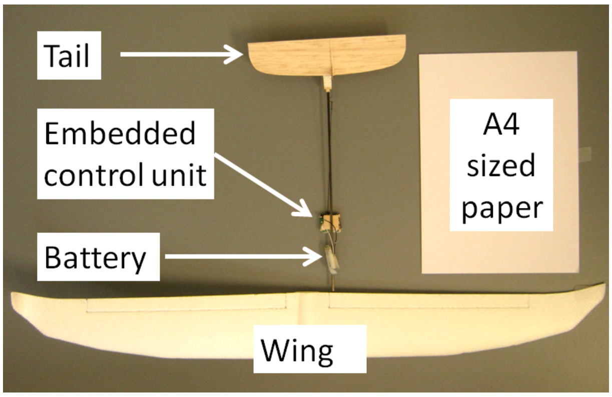

Figure 4.16: The wing.

The kites wings are built with a mix of EPP foam and a carbon fiber tube that is used to hold the tail (see Figure 4.16). The most important characteristic of this wing is that its aspect ratio is 10. The tail is a piece of balsa wood controlled by the embedded control unit AR6400 SPECTRUM receiver that has two build-in linear servos. The total weight of each wing is 40 grams. Having a low weight allows to have very low flight speeds, which is a very important characteristic. On the other hand, light structures are less resistant to shocks and to aerodynamic forces. These wings showed us that they start twisting as the wind speed reaches 8 m/s and their properties change a lot in these conditions.

4.7.2 System's characteristics.

The built prototype has the following characteristics, see Table 4.1:

Table 4.1: Coefficients of the experimental set-up

Symbol	Name	Value
M	mass	0.15 Kg
R	radius	1.2 m
ρ	air density	1.225 Kg/m^3
S	wing area (each)	0.065 m^2
e	Theoretical e factor	0.9
λ	aspect ratio	10
$\frac{\partial CL}{\partial \alpha}$	lift derivative w.r.t. AOA	0.05 deg^{-1}
C_{D0}	zero lift drag	0.01
C_{L0}	lift coefficient at AOA=0	0
L/D	L/D (simulations)	3 to 20
L/D	L/D (measured)	5.5
GS	gliding slope (measured)	10 degrees
V_0	initial air speed	6 m/s
V_{max}	max speed	8.5 m/s
z_0	initial altitude	1.5 m
z_1	min altitude threshold	0 m

4.8 Experimental results

4.8.1 Experiments vs simulations

The first flight tests had the objective to determine the L/D ratio. The wings that were used usually have a L/D ratio that can go up to 20. The tests revealed that the whole system could not have a L/D ratio greater than 5.5. The main reasons are that the wind speed along the wing is not constant, which has an effect equivalent to reducing the value of the e parameter. The second reason is due to drag and friction forces; the carbon structure that unites the two wings seems to be a great source of drag, although it is made out of a carbon tube of only 4 mm of diameter. Friction forces also made the L/D ratio go low, even using ball bearings in every single rotating part. The low value of L/D ratio made the tests much more complex than expected as it led to great losses of energy.

The second difference is that the wings had a tendency to twist as aerodynamic forces got too strong. It has been noticed that high frequency oscillations appear in the wing tips, which made the AOA have great variations, instead of staying constant at 10 degrees.

The last great difference is that the displacement over z has a range of only 1.5 meters, whereas it has a value of 5 meters in the simulations presented in previous section. As a consequence, the system can not reach high values of ξ that are needed to perform reverse pumping. The acceleration $\ddot{z}$ also had the tendency of generating big variations on the AOA value. Depending of the value of the acceleration, it could generate oscillations that would increase the AOA, making greater the acceleration of the system, and leading to some results greater that what was expected, see Table 4.2.

4.8.2 The kinetic charge phase

As a consequence of the low L/D ratio and of various friction forces, only the kinetic charge phase could be studied. Table (4.2) gives the result for the ξ values depending on the Δ_{GS} values.

The first thing that must be seen is that this experimental setup led to a maximum value of $\xi = 2.72$. This means that reverse pumping is possible as long as the kite system can have an η_2 value that is greater than 0.36, in order to satisfy $\eta\xi_2 \geq 1$. One can see on Figure 4.15 that this value of η_2 can hardly be reached with a L/D ratio of 6. Adding the friction due to the the kinematic coupler (see Figure 4.7) and the approximate control of the AOA, the needed η_2 can not be reached. Note that the mean error ratio between the measurements of ξ and the simulations goes from 0.37 to 1.45 . The first thing that comes to mind is that the level of precision is not very high. The general lack of accuracy on the control of the AOA can be seen as the main reason for the unexpected results. The ξ values corresponding to $\Delta_{GS} = 30$ and 35 degrees are greater than theory because of the bad control of the AOA, instead of having a value of 10 degrees, their value was measured with peaks up to 25 degrees, which generate an acceleration that explains such values of ξ.

Figure 4.17 shows the kinetic and potential energy variations for Δ_{GS} of 25 degrees. One can see that the beginning and the end of the kinetic charge phase do not have the

Table 4.2: Results for the ξ parameter

Added glide slope Δ_{GS} (degrees)	Theoretical ξ value	Measured ξ value
10	0.69	0.26
15	0.91	0.41
20	1.11	0.49
25	1.32	0.92
30	1.56	1.86
35	1.87	2.72

desired trajectory. The trajectories need to be smoothed in order to avoid mechanical shocks that would harm the structure.

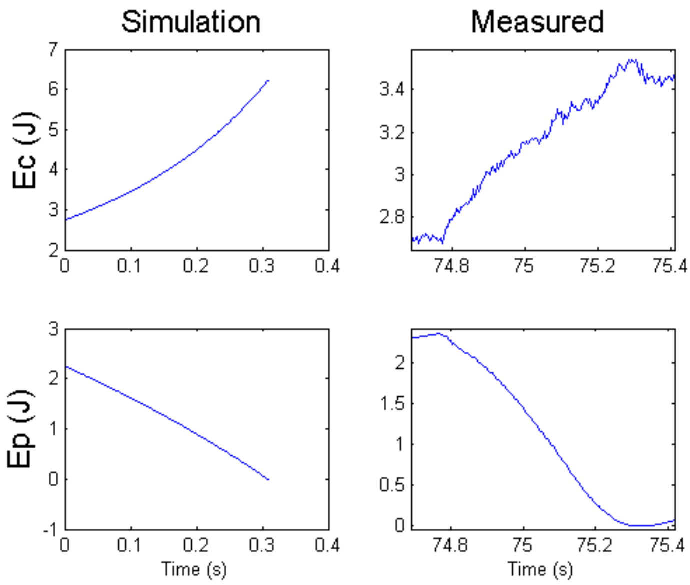

Figure 4.17: Comparison between the theoretical results and te measured results. The difference between the two values of E_c led to a percentage of error of 40%.

4.9 Conclusions

This study shows that the reverse pumping is possible as long as the L/D ratio and a max speed are great enough. The kite system does not have stability and aeroelasticity problems. One of its important knowledge brought by this study is that theoretical and practical work can give quite different results when the practical part has problems. It reminds us the importance of developing simple prototypes that are as close as possible to the theoretical model, or the importance of studying accurate models. The study provides general information that could be seen as a basis for more detailed studies. Every different phase can have many ways of being optimized, the most important and innovative part seems to be the kinetic transfer phase. Future work shall be done on more performant kite systems.

Chapter 5

The outdoor prototype

5.1 Introduction

The final aim of the overall work being to generate great amounts of energy and as the indoor prototypes flew properly, the decision was made to build our first outdoor prototype. By that time, about 5 companies had prototypes that could fly autonomously, except for take off and landing [9, 14, 15, 16, 18]. This prototype had three major goals:
- Build a prototype that could produce energy in real conditions.
- Get knowledge about the development of large prototypes.
- Perform automatic flights in real outdoor conditions.
The two first objectives were attained, as many prototypes were build, a lot of time was dedicated and the remaining time was not enough to allow us to perform automatic flights on the outdoor prototype.

5.1.1 Constrains on the prototype

The team had some experience in the development of autonomous helicopters and experimental vertical take off and landing UAVs. The most important issue was about the safety rules. It could be summed up in these three guidelines:
-Safety and Crash proof concept: the system had to have mostly soft parts in order to reduce the risks of hurting someone in case of crash, the hard parts had to be hardly reachable in case of contact with the kite. Therefore, rigid structure solutions were put aside. Inflatable kites presented a very nice solution from this point of view.
-Easily available components: the construction of a kite has been experience by the past and the conclusion is that it takes a lot of time to sew, adjust, test. The choice was made to buy a standard commercial kite and to adapt it, in order to gain time. To avoid complex embedded electronics, the model would be tele-operated with standard

material from RC airplanes.
-Easy first tests: the kite's first flights were planned to take place in a small park next to the lab. This made the first tests of the kite much easier as the workshop was very close to the flight park. As the park had roughly the size of a square of one hundred meters of side, the size of the kite had to be small enough to be able to be controlled with a rope of 50m of length (see figure 5.1) . We chose one of the smallest inflatable kite available, the *UNO* kitesurf produced by the OZONE company. An other important point was that the kite had to have the capacity of flying without wind and to take off vertically. The solution was brought by the implementation of an electric propulsion system on board. This added another problem, the kite's weight would be 3.6 Kg.

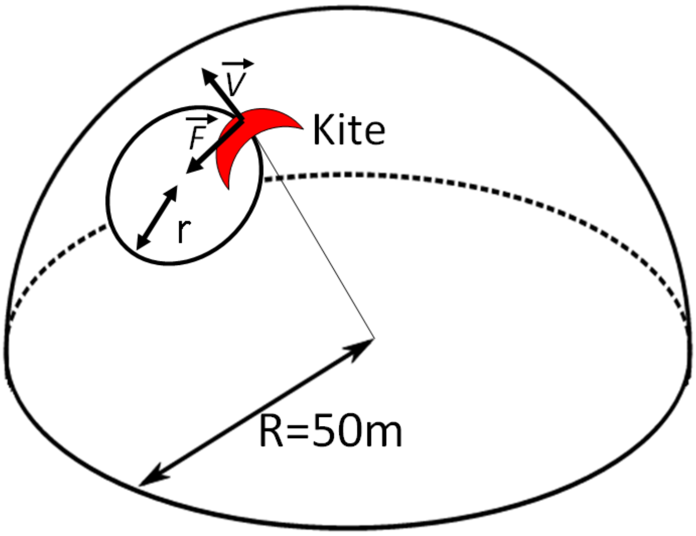

Figure 5.1: Scheme of sphere in which the kite can fly (R = 50m), the small circle corresponds to the trajectory followed with a gyration radius of 15m.

As the kite was a beginners kite, the original version could be flown easily, even with the response time of the servos. As this original version would be modified, we needed to study two question:
- Would the second version of the model's radius of gyration r be small enough to fly with a rope that would define a sphere of $R = 50$m? (see figure 5.1).
- Would the kite be perform able to perform lateral flight, in which the lateral aerodynamic forces compensate the weight ? (see figure 5.2).

Figure 5.2: Lateral flight of the kite, the weight is only compensated by the lateral aerodynamic force.

5.2 The studied model

The chosen kitesurf has a classic shape, by pulling the control lines, one twists the shape of the kite in order to generate a lateral force that modifies the trajectory of the kite. The tethers can be distinguished in two kinds, the control tethers and the front lines. The control tethers are attached to each trailing edge, at the wingtip, (see figure 5.3). Their role is to pull the trailing edge in order to increase the angle of attack of each side of the kite. The front lines are attached to the wing's leading edge, they hold most of the lift force.

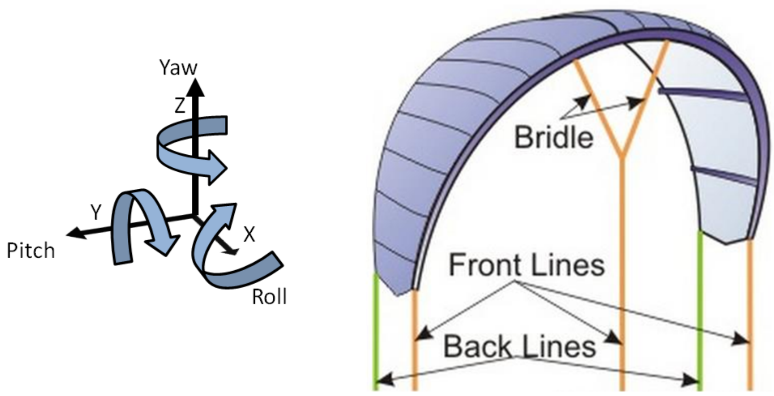

Figure 5.3: Line scheme of the Uno kitesurf and axis notations.

5.2.1 Passive stability

The chosen kite has the interesting specificity that is that the yaw axis align is passively stable in the sense that is aligns to the direction of the wind. This stability is due to the relation between the center of mass and the point of application of aerodynamic forces, the principle is the same than the longitudinal stability of an airplane in standard flight theory [83], or like an arrow.

By construction, the roll angle is fix with respect with respect to the axis of the tether (see figure 5.3). The front cables are attached on each wingtip, therefore the movements of the kite around the roll axis can be neglected for this kite. More precisely, the roll axis keeps almost a constant value of 90 degrees with respect to the main rope direction.

The longitudinal stability would not be changed because the propulsion motor was positioned so that the traction force generated by the propeller is aligned to the center of mass of the hole kite, therefore it would not generate any longitudinal torque. Moreover, the center of mass of the kite was put in front of the kite so that the model would have longitudinal stability, for more details, one can read [83].

5.2.2 Radius of gyration and lateral flight.

The classic way of calculating the radius of gyration of such kites would be to make a simplified model of the lateral aerodynamic forces, and then to calculate how would the kite turn with such lateral forces. This method leads to errors of approximations because the aerodynamic forces are hard to estimate because they depend on the sweep of the wing, on its angle of attack, of the aerodynamic airfoil, etc. None of these parameters is constant along the wingspan, all of them are complex to measure, and on top of that, there are two wings that interfere with each other and they might be other complex phenomena involved. The proposed solution consists on testing the kite and deducing the parameters from measures. Once done, these calculations will tell us if the kite can satisfy the two conditions.

As a kite flies in circle (see figure 5.1) , its lateral motion obeys to the following equation (5.2.1) if the weight force is neglected.

$$a = \frac{V^2}{r} \tag{5.2.1}$$

where a is the lateral acceleration, $\overrightarrow{V}$ is the speed of the kite and r is the gyration radius. The lateral force that makes the kite turn $\overrightarrow{F}$ being an aerodynamic force, its magnitude will be approximated by:

$$F = kV^2 \tag{5.2.2}$$

Standard models could give k a classic aerodynamic notation like $1/2\rho SC_l$, but we won't write it like this because it might make the reader think that its aerodynamics are similar to a standard wing, which would be false. From the two previous equations, one can see that the radiation radius is independent from V^2 can be written as $r = \frac{m}{K}$.

From measurements made on the wing, it was able to have a radius $r = 4$m at a a constant speed of $V = 15$m/s with a mass of 1.2 Kg. With these values and the previous equations, one can see that r increases to 12m and that $F = 65$N. Which is also enough to perform lateral flight because the force is greater than the weight $w = 35$N.

5.3 The experimental setup

The experimental setup was build at the Gipsa-lab with the help of two undergraduate students, Pierrick AZOU that helped with the development of the flying prototype and Kevin Das Nieves Domingues that helped with the ground station. The choice was made to develop an embedded control system in order to have a single tether that would be connected to the ground station, which makes it much easier to build.

5.3.1 The wing

The wing was modified in order to receive the control elements and the camera. An aluminum tube was adapted to match the kite and supported the electric engine, the battery, the controller, the receiver and the camera. Two servos were modified in order to build winches (see figure 5.4). As the servos would both diminish the size of the control line, the angle of attack of the kite would increase. When only one servo is pulled, it will increase the angle if attack of the one side that is pulled, generating a lateral increase of lift [8].

The winches were positioned one on each corner of the training edge and were fixed directly to the fabric material of the kite. Each one had its own battery in order to reduce voltage drops in long cables going from the the center of the kite to its extremities.

5.3.2 The ground station

The ground station's objectives were to perform measurements of the trajectory of the kite, of the tension on the rope and to be able to reel-in and reel-out the cable. In order to reel-in the cable, the system was equipped of an electric motor. A brake system, a coder and a torque-meter were mounted on the axis of the motor in order to perform measurements. The position and trajectory of the kite were estimated by tracking the

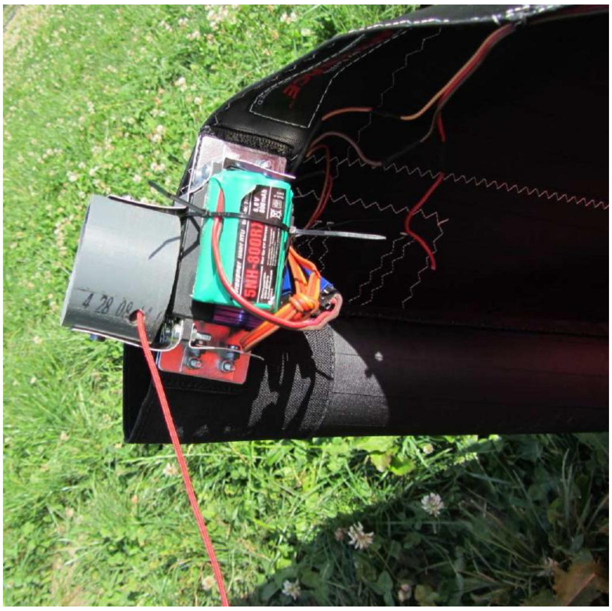

Figure 5.4: The servo winch system addapted to the kitesurf. The winch can pull about 10 Kg at a speed of 30 cm per second.

Figure 5.5: The wing in flight.

orientation of the cable with a dual axis coder.

5.3.3 The flights

Three different sessions of tests were done in an undesired quasi total absence of wind. The electric propulsion system was used and flights could be performed. A great amount of time would have been lost if the motor had not been implemented.

Figure 5.6: The ground station.

The management and planning of the flight tests was complex to do. One of the conclusions of these tests is that having a flight site next to the workshop is a significant advantage. The last tests were done about 200 km away from the workshop, in a zone that was supposed to be windy and in which we had a permission to fly. The management of the displacement, the lack of material, the problems due to the lack of electricity, the transport, the lack of infrastructure and many other elements made these tests complex to perform.

5.3.3.1 The takeoff

This phase phase was not easy at the beginning with such a prototype. The main difficulty was that the response time of the servos was extremely long. As a consequence, the most important point of the takeoff phase was to reach a high speed as fast as possible. The kite had a weight of 3.5 Kg and a trust of about 5 kg. After a few trials, 3 takeoffs out of 4 would succeed. It would take about 2.5 seconds to have proper control on the kite.

5.3.3.2 The Flights

The performances of the flight were very satisfying. The gyration radius seemed to correspond to the calculated values, the kite would be able to perform lateral flights, see figure 5.7. Once in a field, we had no more cable length restriction. The cable length varied from 50 meters to 200 meters. Basic production cycles were performed, the generated output power reached peaks of 200 W.

Some unexpected reactions were noticed during the flights at high speeds and low angle of attack. The airfoil would start waving as the tension of the wing's surface would

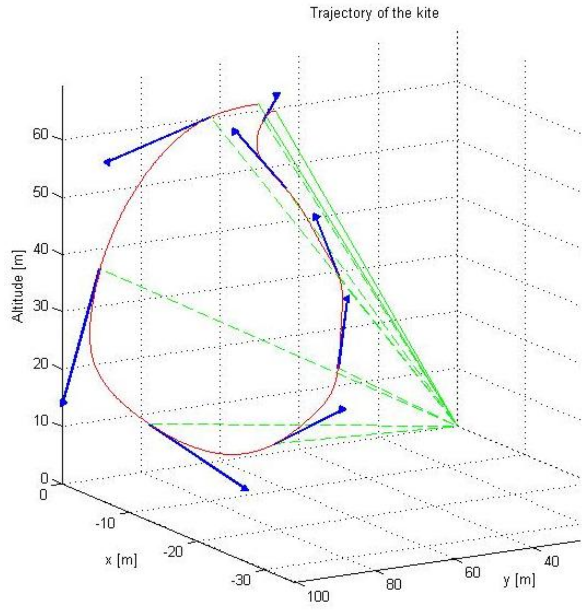

Figure 5.7: The ground station.

seem to go low. Also, at very high speeds of about 30 m/sec, the kite would start having elasticity problems. The structure would start having strong oscillations. Their frequency being of about 5 hertz, the only found way of avoiding them was to lower the speed of the kite.

5.3.3.3 The Landings

Without the crash proof concept, it would have taken between 5 and 10 prototypes to manage to do the first flight. The landings were every time very rough, nevertheless, the amount of reparation time due to crashes did not exceed 3 hours. Many problems came from the servos that resulted being low quality. Most of the reparation time was spent on changing propellers, about 10 were broken during the flight tests that lasted about one day and a half. For more information, please see the ”carnet de vol” section in the appendix.

5.4 Conclusion

This experiment allowed us to have a first outdoor experience that was a success. It gave to the team the opportunity to learn a lot about how to needs of real conditions flights, its organization and its problems. The following step will be to test the prototype in presence of wind, tests its performances in the longitudinal axis.

Chapter 6

General conclusion

This PhD thesis has proposed contributions to the development of new alternative renewable energy generation using wind. The original idea was very simple: replace the heavy and costly metallic infrastructure of a standard wind mill by a rope or a cable attached to a kite that will pull the rope to drive a dynamo which generates electricity. The motivation behind this idea is the reduction of cost as well as a reduction of the ecological footprint. Furthermore, the resulting system will be lighter and cheaper than actual wind turbines. Nevertheless, in order to prove that such alternative energy generation wind system could actually work, several steps had to be carried out. A deep study of the aerodynamical behavior of the system had to be performed to understand the system characteristics. Based on the obtained aerodynamical models, control strategies had to be proposed which will allow the system to track specific trajectories for generating energy or for staying in the air in absence of wind. In order to make sure that the proposed strategy works, many prototypes had to be designed and built to finally test the proposed control strategies and measure their performances. The objective of the present PhD work was therefore to carry out the development of the above necessary steps to obtain a reliable alternative wind electricity generation system.

Chapter I has presented a state of the art of the existing wind turbine energy generation systems, kite energy generation systems as well as other systems based on auto-giros and blimps.

Chapter II presented a study on aeronautical innovations based on the pioneers of flight. This study brought guidelines that allowed us to improve the speed of development of our project.

Chapter III described the first prototype that has been built during the PhD thesis. The prototype is basically composed of a wind tunnel and a wing attached to a generator. The aerodynamical model of the system has been obtained and two control strategy has been proposed. The control algorithm has been successfully validated in a real time experiment, the trajectory of the kite and the output power of the generator could be properly controlled in presence of strong wind changes.

Chapter IV presented the reverse pumping strategy which is a technique for increasing the kinetic energy of the kite by pulling the kite with a rope. This kinetic energy is then transformed into potential energy by gaining altitude. This technique allows to keep the kite airborne in total absence of wind. This chapter has discussed the constraints introduced into the aerodynamical model. The control strategy has been illustrated in numerical simulations and has been validated in the experimental setup.

Chapter V presented the development of an outdoor prototype. Such prototype is an extension of the indoors setup presented in Chapter III. Conditions outdoors are more complex than indoor because the wind has not constant velocity as in the wind tunnel. The experimental tests are encouraging but further development is still required.

Future work could address the following topics:

1) Autonomous landing and take-off of the kite depending on the wind conditions.
2) Test of an outdoor flight in strong wind conditions.
3) Development of the multi-kites systems
4) Development of other uses like pulling boats.

Chapter 7

Appendix

7.1 List of accidents

This list is a little sum up of the accidents the the author has experienced in model airplanes, UAV, paragliding and kite energy generation. This experience started about 20 years ago.

-Propeller, rotors and high speed turning devices: It can cut yourself. T-shirts, hair, shoelaces can also get stuck in.
-Batteries: The previous generation of batteries were contained in a metallic box (Ni-Cad, Ni-Mh). When the charge or discharge is not made properly, they can produce a lot of heat. The battery's inner pressure will rise until the battery will explode. Also, depending on the connectors you have, it might happen that the + and the - cables fit together. One should avoid those connectors.
- Electric cables, soldering: The cables need to be carefully treated, one should always remember that they have poor mechanical resistance. Make sure that no force or friction is exerted on them, make proper soldering, check often that they are doing fine.
- Dynema-like cables: It is a true underestimated danger. They have great mechanical resistance with respect to their diameter,therefore they can cut just like a razor blade. It can also burn the skin. If you do not need such mechanical resistance, you should rather use standard cables. No parts of the body should get in contact with these, specially in unexpected forces environments (wind gusts and aeroelastic aerodynamic surfaces like a paraglider for example). If you have to deal with a cable that is likely to move, use gloves and do not grab cables, but push them with palm of the hand. It will reduce risks of cutting fingers.
- Electric engines: They can get very hot. An other problem happens in the case of DC motors, depending on the kind of controller, as the last transistor before the motor burns

it may happen that it gives full power to the electric engine.
- Servos: depending on the quality of the servos, it might happen that the servo's motor starts heating. This might make the glue that holds the first gear loose its properties and looses adherence with the motor's axis. Be always sure that the forces and voltage respect the specification of the servo, that the cables are not long enough to make voltage drops. The gear might break if too much force is applied to the servo, if you don't have critical weight problems, use servos that have metallic gear.
- Receivers: make sure that the antenna does not move and that the electric engine and the controller controller does not generate interference. Prefer controllers with an opto-coupler.
- Glue: Glue can get really hot, specially fast epoxy. If you use these kind of resins, try to avoid big stacks of glue. As it will harden, it might get internal cracks due to the change of temperature, just like a Prince Rupert's drop. An other point is that depending on the glued material, it might look like it is fixed and as you pull it softly, it stays still, but with a very small shock, it will stop adhering. It happens sometimes with very flat non-rough surfaces.
- Duct tape: It might get old with the sun, and humidity.
- Velcro: It is as well a very nice material but it should be used with forces that apply on the axis of the surface, not orthogonal to it.
- Gyros: be sure that they do not take into account undesired rotations.
- Ground effect; might take you longer than expected to land your kite. As one wingtip goes close to one wall, its lift will increase, its drag decrease, it might provoque unexpected movements.
-Paragliding sails: The front wires tend to get longer with time: this will increase the angle of attack and might lead to stall. The junctions between the cables and the attaches are a great point of friction, verify the cable is not used in this particular point. Small insects, like crickets, often get in the paraglider and start eating it, make sure they don't eat your paraglider.
-Sand: if you fly near sand, be sure you have holes to make the sand go away. If you have a kitesurf-like structure, the latex inner later is often pierced by sand. If sand gets in the inflating pump, it will project sand with a very high speed to the latex that is in front of the intake. It will make small holes that will make the pressure go low.
-Animals: Animals have behaviors that are hard to predict. The two worse cases that were experienced were: - a seagull that started attacking the UAV. It would take height on top of the UAV, take a huge speed diving steeply like a pelegrine falcon, heading towards the UAV and would spread his wings to blow air to the UAV , maybe in order to make it loose control. The UAV was around one hundred meters away from the author but the force involved were so strong as the wings would be spread, the turbulence of the air was very clearly heard. - a horse was next to the paragliding takeoff site. As paragliders inflate during the takeoff, they make noise and a surface of around 25 m^2 seems to appears. The color of this wing was shiny yellow. It seemed that the horse got

afraid and the person that was on the horse was "ejected" from the horse as he started jumping.

7.2 Carnet de vol

These flight notes sum up the prototypes first flight's behaviors, the improvements and modifications made.

- First kite prototype (see figure 7.1), 03/2010:
  Flew in the wind tunnel of the Ecole Centrale Paris, after some tuning, it worked fine. At some point, The person that was helping pushed the speed of the wind tunnel much too high and the kite started shaking, broke most of its attachments and almost got aspired by the wind tunnel. If it had happen, it would have broken very expensive devices in the wind tunnel.

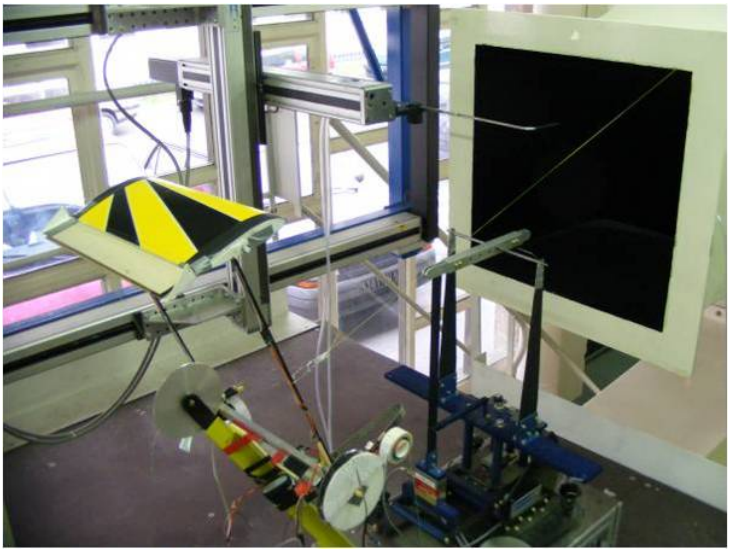

Figure 7.1: The first kite system in flight.

- Second kite prototype (see figure 7.1), 07/2010:
  The first flight was successful but was a bit unstable on the yaw axis. Cables were added between the wingtips and the main tether to damp the oscillation, the flight were then stable.

- Third kite prototype (see figure 7.1), 02/2011:
  First flight was very unstable due to excessive turbulence, lateral instabilities, The

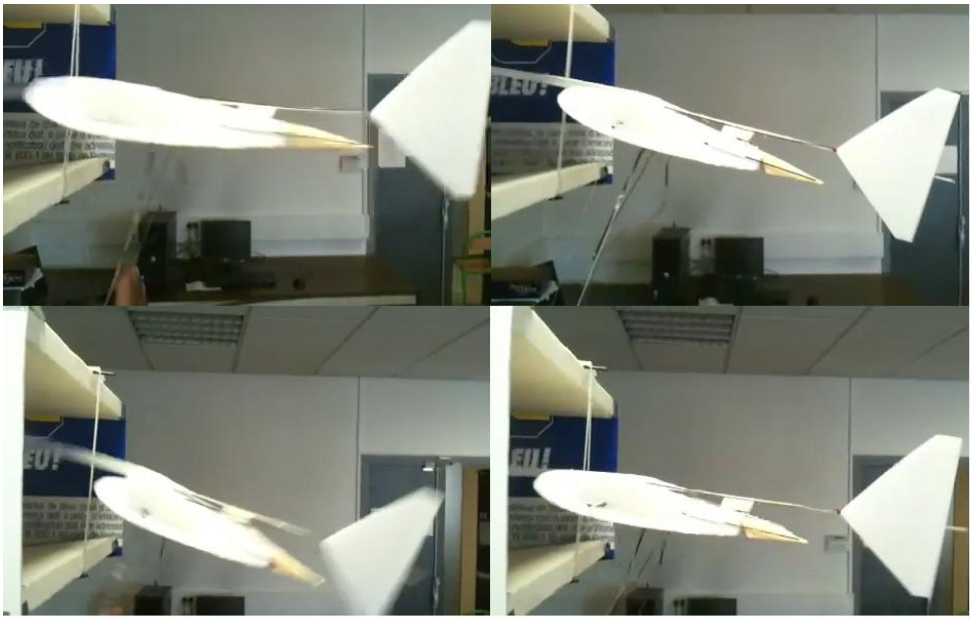

Figure 7.2: The second kite system in flight in the "air conditioner wind tunnel".

size of the rudder was changed, wiglets were installed, lateral strings were installed to stabilize roll. Poor results.

- Fourth kite prototype (see figure 7.1), 03/2011:
  First flight successful. The gyro was changed, which increased of stability. The system of AOA control, it increased of precision and response time. The prototype is still able to perform flights, he survived many crashes.

- First reverse pumping prototype (see figure 7.1), 04/2011:
  Flies well but we cannot see any change when it should accelerate, maybe due to wrong estimation of the drag. Some stall problems appear very suddenly at low speed.

- Second reverse pumping prototype (see figure 7.1), 04/2011:
  We can see an acceleration but the height is very hard to control manually. It seems that the structure is not stiff enough. And that the propulsion system generates a lot of drag as the engine turns off because the propeller keeps on turning.

- Magnus effect prototype (see figure 7.1), 06/2011:

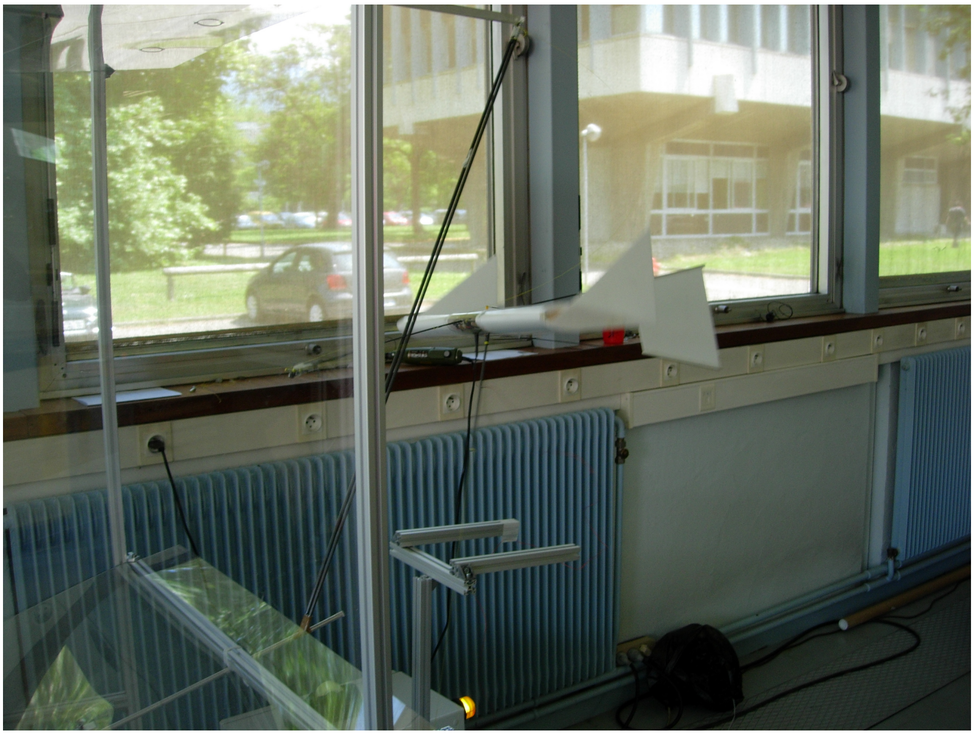

Figure 7.3: The third kite kite system in flight.

The prototype flew very well, since the very first test.

- Third reverse pumping prototype (see figure 7.1), 01/2013:
  The system accelerates, but the wings twists a lot, it cannot reach high speeds.

- Fourth reverse pumping prototype (see figure 7.1), 02/2013:
  The L/D ratio is not good enough, the carbon structure shakes and twists, as a consequence, the wing's angle of attack changes independently from the servo's output.

- Fifth reverse pumping prototype (see figure 7.10), 04/2013:
  The wings' angles of attack are now independent from the structure, the wings have been reinforced with carbon fiber. Flights were successful, even if it did not worked as well as planned.

- Outdoor model prototype (see figure 7.1), 08/2012:

  First flights: 5 crashes, the position of the center of mass is not enough advanced. The servos broke down due to excessive voltage that seems to have provoked too

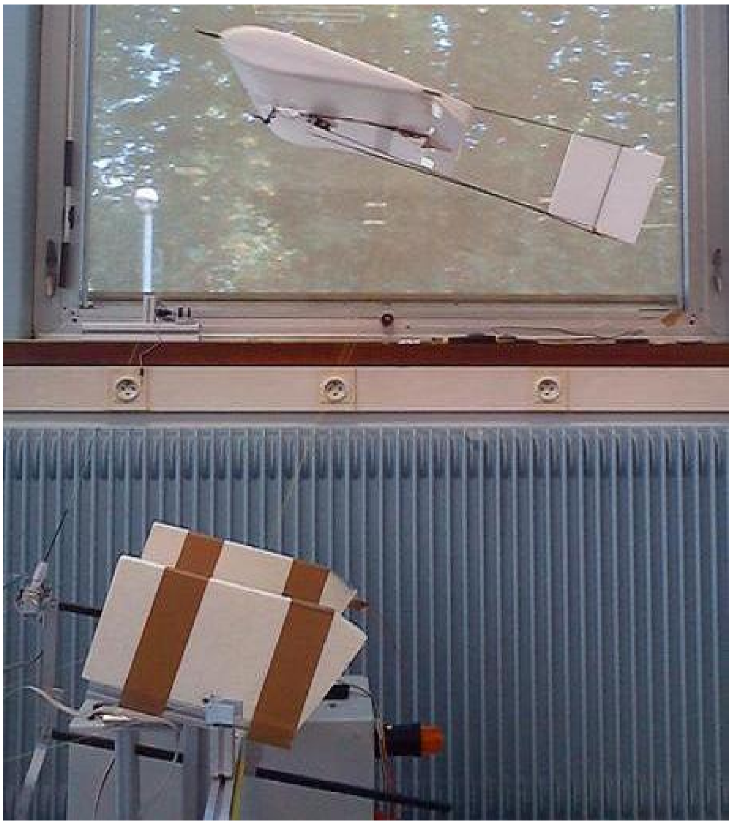

Figure 7.4: The fourth kite system in flight.

much heat. Some false contacts provoke dysfunctions. As we change the servo's voltage, the servo and the centre of mass position, the kite performs a beautiful controlled flight.

Second session of flights: 08/2011:
The aluminum structure had been twisted due to the rough landings, structure was changed. we experience takeoff crashes: as the model takes off, a strong twist of the structure makes a Dyneema cable get in contact with the fiberglass propeller. Dyneema wins! around 7 propellers were destroyed. The worst crash: due to the violent landings, the battery's attaches moved and the battery fell down from the kite as it was flying. As it reached the ground, it felt at a distance of two meters away from the author. He did felt a very scary vibration threw the ground, the weight of the battery was around 1.2 Kg and felt from a height of 20 m.

- The "small kite" (see figure 7.1), 06/2013:
  It flew very well since the first test.

Figure 7.5: The first reverse pumping prototype.

Figure 7.6: The second reverse pumping kiten.

Figure 7.7: The magnus kite system in flight.

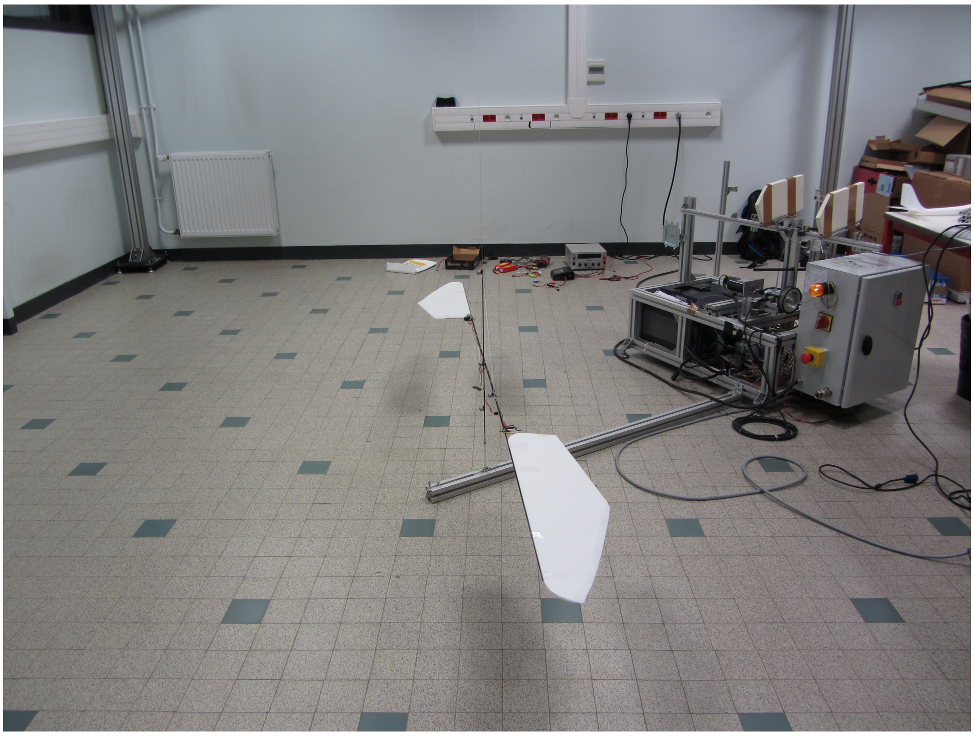

Figure 7.8: The third reverse pumping kite in the Vicon motion capture system.

Figure 7.9: The fourth reverse pumping kite in flight.

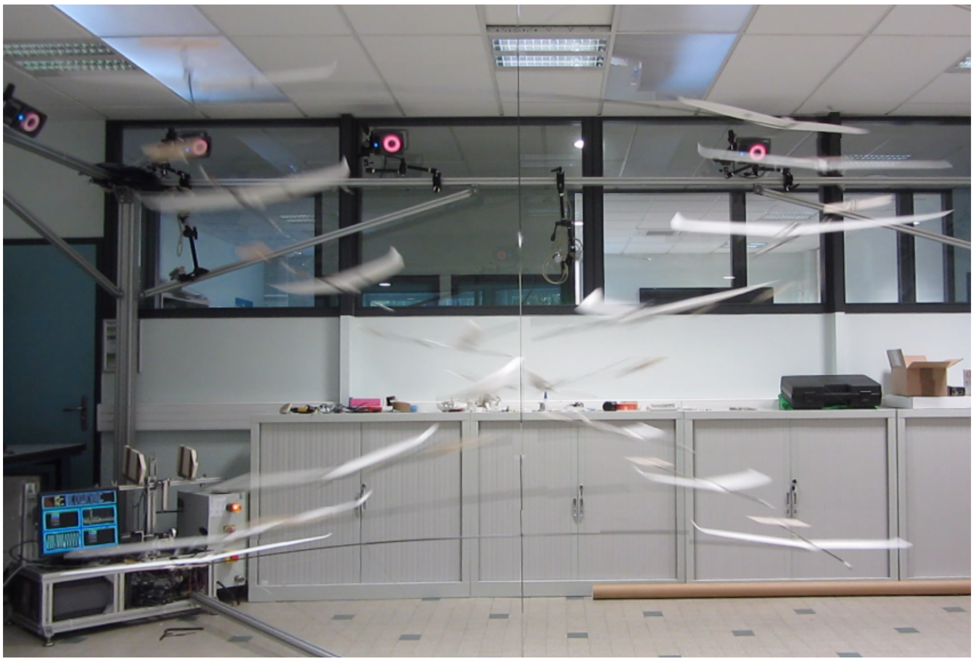

Figure 7.10: The fifth reverse pumping kite in flight, increasing its energy.

Figure 7.11: The outdoor model in flight in the park of the university.

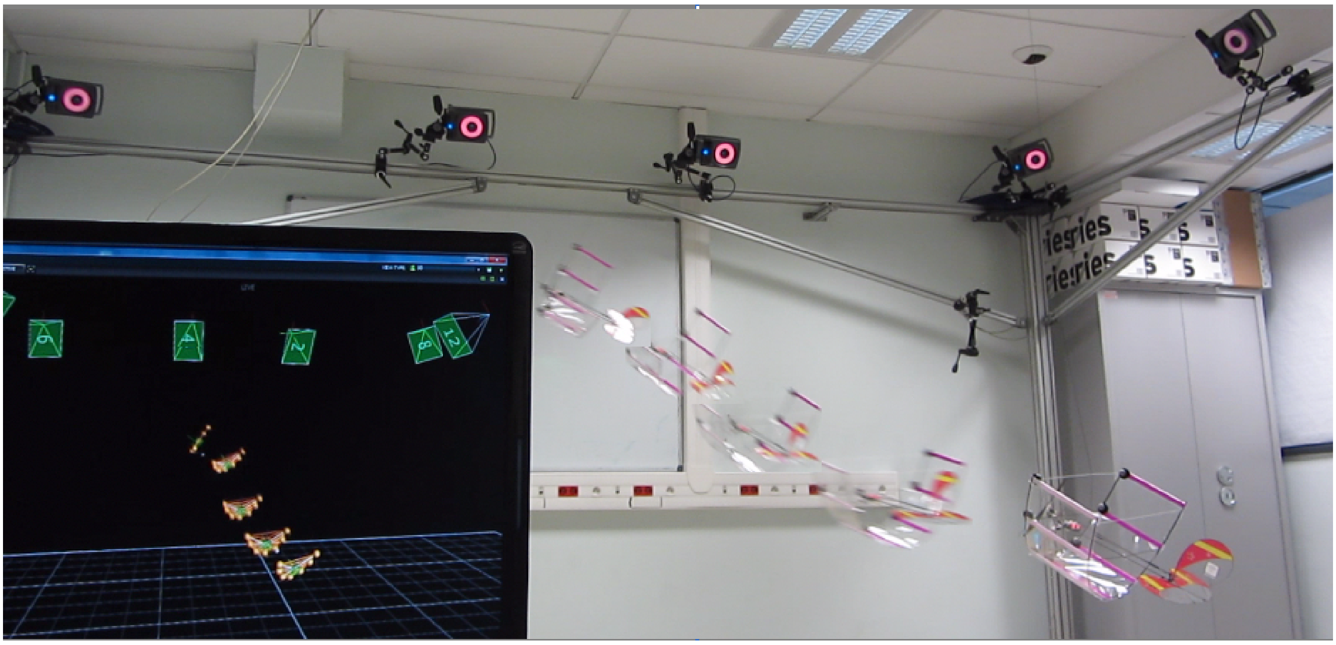

Figure 7.12: The "small kite" in flight, note on the left bottom the measurement of its position.

Bibliography

[1] http://www.gipsa-lab.grenoble-inp.fr/recherche /plates-formes.php?id plate-forme=70.

[2] American Wind Energy Association (AWEA). U.S. wind industry annual market report : year ending 2009. Washington, D.C., (2010).

[3] B. Wu, Y. Lang, N. Zargari and S. Kouro: Power conversion and control of wind energy systems. Wiley, IEEE Press series on Power Engineering, (2011).

[4] R. Thresher, M. Robinson, and P. Veers: To capture the wind. IEEE power and energy magazine, pages 34-46, (2007).

[5] L. Fagiano: Control of Tethered Airfoils for High Altitude Wind Energy Generation. PhD thesis, Politechnico di Torino - Doctoral School, (2009).

[6] http ://www.gl-garradhassan.com/en/highaltitudewind.php

[7] Miles L.Loyd: Crosswind kite power. Journal of energy, article no. 80-4075, (1980).

[8] U. Ahrens, M.Diehl, R. Schmell: Airborne wind energy, springer editions, (2013).

[9] http://www.makanipower.com/

[10] http://www.skywindpower.com/

[11] http://www.altaerosenergies.com/

[12] http://www.enerkite.com/Home.html

[13] http://www.kitepower.eu/

[14] http://www.ampyxpower.com/

[15] http://www.omnidea.net/

[16] http://www.skysails.info/english/

[17] http://homes.esat.kuleuven.be/ highwind/

[18] http://www.kitegen.com/

[19] M. Zanon, S. Gros, J. Andersson, and M. Diehl: Airborne Wind Energy Based on Dual Airfoils. IEEE Transactions on Control Systems Technology, (2013).

[20] M. Vukov, A. Domahidi, H.J. Ferreau M. Morari and M. Diehl: Auto-generated Algorithms for Nonlinear Model Predictive Control on Long and on Short Horizons. In Proceedings of the 52nd IEEE Conference on Decision and Control, Firenze, Italy, (2013).

[21] S. Gros, M. Zanon, and M. Diehl: A Relaxation Strategy for the Optimization of Airborne Wind Energy Systems. In Proceedings of the European Control Conference, Zurich, Switzerland, (2013).

[22] S. Gros, M. Zanon, and M. Diehl: Control of Airborne Wind Energy Systems Based on Nonlinear Model Predictive Control and Moving Horizon Estimation. In Proceedings of the European Control Conference, Zurich, Switzerland, (2013).

[23] K. Geebelen, A. Wagner, S. Gros, J. Swevers and M. Diehl: Moving Horizon Estimation with a Huber Penalty Function for Robust Pose Estimation of Tethered Airplanes. In Proceedings of the 2013 American Control Conference, Washinton DC, USA, (2013).

[24] S. Gros, R. Quirynen and M. Diehl: Aircraft Control based on Fast Non-linear MPC and Multiple-shooting. In Proceedings of the 51nd IEEE Conference on Decision and Control, Maui, Hawai, USA, (2012).

[25] S. Gros, H. Ahmad, K. Geebelen and M. Diehl: In-flight Estimation of the Aerodynamic Roll Damping and Trim Angle for a Tethered Aircraft based on Multiple-shooting. System Identification Conference, (2012).

[26] S. Gros, M. Zanon, M. Vukov, and M. Diehl: Nonlinear MPC and MHE for Mechanical Multi-Body Systems with Application to Fast Tethered Airplanes. In Proceedings of the 4th IFAC Nonlinear Model Predictive Control Conference, Noordwijkerhout, The Netherlands, (2012).

[27] J. Sternberg, J. Goit, S. Gros, J. Meyers and M. Diehl: Robust and Stable Periodic Flight of Power Generating Kite Systems in a Turbulent Wind Flow Field. In Proceedings of the 15th IFAC Workshop on Control Applications of Optimization, (2012).

[28] S. Gros, M. Zanon, and M. Diehl: Orbit Control for a Power Generating Airfoil Based on Nonlinear MPC. In Proceedings of the 2012 American Control Conference, Montreal, Canada, (2012).

[29] J. Gillis, J. Goos, K. Geebelen, J. Swevers and M. Diehl: Optimal periodic control of power harvesting tethered airplanes: how to fly fast without wind and without propellor?. In Proceedings of the 2012 American Control Conference, Montreal, Canada, (2012).

[30] J. Sternberg, B. Houska and M. Diehl: A Structure Exploiting Algorithm for Approximate Robust Optimal Control with Application to Power Generating Kites. In Proceedings of the 2012 American Control Conference, Montreal, Canada, (2012).

[31] H.J. Ferreau, B. Houska, K. Geebelen and M. Diehl: Real-time control of a kite-carousel using an auto-generated nonlinear MPC algorithm. In Proceedings of the IFAC World Congress, (2011).

[32] B. Houska and M. Diehl: Robustness and Stability Optimization of Power Generating Kite Systems in a Periodic Pumping Mode. In Proceedings of the IEEE Multi Conference on Systems and Control, Yokohama, Japan, (2010).

[33] B. Houska and M. Diehl: Optimal control of towing kites. In 45th IEEE Conference on Decision and Control, pages 2693-2697, San Diego, CA, USA (2006).

[34] M. Zanon, S. Gros, J. Andersson, and M. Diehl: Airborne Wind Energy Based on Dual Airfoils. IEEE Transactions on Control Systems Technology, (2013).

[35] M. Zanon, S. Gros, and M. Diehl: Rotational Start-up of Tethered Airplanes Based on Nonlinear MPC and MHE. In Proceedings of the European Control Conference, Zurich, Switzerland, (2013).

[36] M. Zanon, S. Gros, and M. Diehl: Rotational Start-up of Tethered Airplanes Based on Nonlinear MPC and MHE. In Proceedings of the European Control Conference, Zurich, Switzerland, (2013).

[37] K. Geebelen, H. Ahmad, M. Vukov, S. Gros, J. Swevers, and M. Diehl: An experimental test set-up for launch-recovery of an Airborne Wind Energy (AWE) system. In Proceedings of the 2012 American Control Conference, Montreal, Canada, (2012).

[38] U. Fechner, R. Schmehl: Design of a Distributed Kite Power Control System. 2012 IEEE Multi-Conference on Systems and Control, Dubrovnik, Croatia, 3-5 October 2012.

[39] J.H. Baayen, W.J. Ockels: Tracking control with adaption of kites. IET Control Theory and Applications. Vol. 6, No. 2, pp. 182-191, (2012).

[40] S.G.C. de Groot, J. Breukels, R. Schmehl, W.J. Ockels: Modeling Kite Flight Dynamics Using a Multibody Reduction Approach. AIAA Journal of Guidance, Control and Dynamics. Vol. 34, No. 6, pp. 1671-1682, (2011).

[41] E.J. Terink, J. Breukels, R. Schmehl, W.J. Ockels: Flight Dynamics and Stability of a Tethered Inflatable Kiteplane. AIAA Journal of Aircraft, Vol. 48, No. 2, pp. 503-513, (2011).

[42] J. Breukels, W.J. Ockels: A Multi-Body System Approach to the Simulation of Flexible Membrane Airfoils. Aerotecnica Missili and Spazio (AIDAA), Vol. 89, No. 3, pp. 119-134, (2010).

[43] P. Williams, B. Lansdorp, W.J. Ockels: Optimal Crosswind Towing and Power Generation with Tethered Kites. AIAA Journal of Guidance, Control and Dynamics, Vol. 31, No. 1, (2008).

[44] P. Williams, B. Lansdorp, W.J. Ockels: Nonlinear Control and Estimation of a Tethered Kite in Changing Wind Conditions, AIAA Journal of Guidance, Control and Dynamics, Vol. 31, No. 3, (2008).

[45] B. Lansdorp, R. Ruiterkamp, P. Williams, W.J. Ockels: Long-Term Laddermill Modeling for Site Selection. AIAA-2008-6690, AIAA Modeling and Simulation Technologies Conference and Exhibit, Honolulu, Hawaii, 18-21 August 2008.

[46] A.R. Podgaets, W.J. Ockels: Robust Control of Laddermill Wind Energy System. Wind Power Shanghai Conference, Shanghai, China, 1-3 November 2007.

[47] A.R. Podgaets, W.J. Ockels: Comparison of two mathematical models of the kite for Laddermill sail simulation. IAENG World Congress of Engineering Computer Science, San Francisco, CA, USA, 24-26 October 2007.

[48] A.R. Podgaets, W.J. Ockels: Flight Control of the High Altitude Wind Power System. 7th Conference on Sustainable Applications for Tropical Island States, Cape Canaveral, FL, USA, 3-6 June 2007.

[49] J. Breukels, W.J. Ockels: A multi-body dynamics approach to a cable simulation for kites. Asian Modelling and Simulation (AsiaMS2007), Beijing, China, 8-10 October 2007.

[50] U. Fechner, R. Schmehl: Model-Based Efficiency Analysis of Wind Power Conversion by a Pumping Kite Power System. In: U. Ahrens, M. Diehl, R. Schmehl (eds.) "Airborne Wind Energy". Springer, Heidelberg, (2013).

[51] U. Fechner, R. Schmehl: High level control and optimization of kite power systems. 8th PhD Seminar on Wind Energy in Europe, Zurich, Switzerland, 12-13 September 2012.

[52] P. Williams, B. Lansdorp, W.J. Ockels: Modeling of Optimal Power Generation using Multiple Kites. AIAA 2008-6691, AIAA Modelling and Simulation Technologies Conference and Exhibit, Honolulu, Hawaii, USA, 18-21 August 2008.

[53] W.J. Ockels: Patent 1004508, 12 November 1996.

[54] W.J. Ockels: Laddermill, a novel concept to exploit the energy in the airspace. Aircraft Design, 4:81âĂŞ97, (2001).

[55] B. Lansdorp and P. Williams: The laddermill - innovative wind energy from high altitudes in holland and australia. In Windpower 06, Adelaide, Australia, (2006).

[56] B. Lansdorp, B. Remes, and W.J. Ockels: Design and testing of a remotely controlled surfkite for the laddermill. In World Wind Energy Conference, Melbourne, Australia, (2005).

[57] M. Canale et al.: High Altitude Wind Energy Generation Using Controlled Power Kites, IEEE Transactions On Control Systems Technology, volume 18(2), pages 279-293, (2010).

[58] A.R. Podgaets and W.J. Ockels: Three-dimensional simulation of a laddermill. In Proceedings of the 3rd Asian Wind Power Conference, Beijing, China, (2006).

[59] R.Lozano Jr, J.Dumon, A.Hably, and M.Alamir: Control of a wind power system based on a tethered wing IFAC EGNCA, Bangalore, India, (2011).

[60] A.Hably, R.Lozano Jr, and J.Dumon, and M.Alamir: Observer-based control of a tethered wing wind power system: indoor real-time experiment, American Control Conference, Washington, USA, (2013).

[61] R.Lozano Jr, J.Dumon, A.Hably, and M.Alamir: Energy production control of an experimental kite system in a wind tunnel in presence of wind gusts ,IROS 2013, Tokyo, Japan, (2013).

[62] R.Lozano Jr, J.Dumon, A.Hably: Reverse pumping: theory and experimental validation on a multi-kites system. ICSTCC 2013, Sinaia, Romania, (2013)

[63] R.F. Verheul, J. Breukels, W.J. Ockels: Material selection and joining methods for the purpose of a high-altitude inflatable kite. AIAA 2009-2338, 50th AIAA/ASME/ASCE/AHS/ASC Structures, Structural Dynamics, and Materials Conference, Palm Springs, CA, USA, 4-5 May 2009.

[64] J. Breukels: An engineering methodology for kite design. PhD thesis, Delft University of Technology, (2011).

[65] A. Bosch, R. Schmehl, P. Tiso, D. Rixen: Nonlinear Aeroelasticity, Flight Dynamics and Control of a Flexible Membrane Traction Kite. In: U. Ahrens, M. Diehl, R. Schmehl (eds.) ”Airborne Wind Energy”. Springer, Heidelberg, (2013).

[66] J. Breukels, R. Schmehl, W.J. Ockels: Aeroelastic Simulation of Flexible Membrane Wings based on Multibody System Dynamics. In: U. Ahrens, M. Diehl, R. Schmehl (eds.) "Airborne Wind Energy". Springer, Heidelberg, (2013).

[67] A. Bosch, R. Schmehl, P. Tiso, D. Rixen: Dynamic nonlinear aeroelastic model of a kite for power generation. Accepted for publication in AIAA Journal of Guidance, Control and Dynamics, (2012).

[68] J. Breukels, W.J. Ockels: Analysis of complex inflatable structures using a multi-body dynamics approach. AIAA-2008-2284, 49th AIAA/ASME/ASCE/AHS/ASC Structures, Structural Dynamics, and Materials Conference, Schaumburg, IL, USA, 7-10 April 2008.

[69] P. Williams, B. Lansdorp, W.J. Ockels: Modeling, Simulation, and Testing of Surf Kites for Power Generation. AIAA 2008-6693, AIAA Modelling and Simulation Technologies Conference and Exhibit, Honolulu, Hawaii, USA, 18-21 August 2008.

[70] B. Lansdorp, W.J. Ockels: Design and construction of the 4kW groundstation for the laddermill. 7th IASTED International Conference on Power and Energy Systems (EuroPES 2007), Palma de Mallorca, Spain, 29-31 August 2007.

[71] P. Williams, B. Lansdorp, W.J. Ockels: Flexible Tethered Kite with Movable Attachment Points, Part II: State and Wind Estimation. AIAA-2007-6629, AIAA Modelling and Simulation Technologies Conference and Exhibit, Hilton Head, SC, USA, 20-23 August 2007.

[72] P. Williams, B. Lansdorp, W.J. Ockels: Flexible Tethered Kite with Movable Attachment Points, Part I: Dynamics and Control. AIAA-2007-6628, AIAA Modelling and Simulation Technologies Conference and Exhibit, Hilton Head, SC, USA, 20-23 August 2007.

[73] J. Breukels, W.J. Ockels: Tethered kiteplane design for the Laddermill project. 4th World Wind Energy Conference and Renewable Energy Exhibition 2005, Melbourne, Australia, 2-5 November 2005.

[74] A.Ilzhofer, B.Houska, and M.Diehl: Nonlinear MPC of kites under varying wind conditions for a new class of large-scale wind power generators, International Journal Of Robust And Nonlinear Control,volume 17, pages 1590–1599, (2007).

[75] A.MM Wellington: Mechanics of flight and aspiration, Proceedings of the International conference on Aerial Navigation, Chicago, (1893).

[76] L.Gastine: L' A.B.C. de l'aviation: Biplans et monoplans, Project Gutenberg EBook,(2010)

[77] T.D. Crouch & Peter L. Jakab: The Wright brothers and the invention of the aerial age, Nationnal geographic society, (2003).

[78] P.Almond : Aviation the early years, Getty images, (1997).

[79] Don Dwiggins: Man-powered aircraft, Tab Books, (1979).

[80] M.Grosser: Gossamer odysey, The thiumph of Human powered flight, Zenith press, (2004).

[81] Margaret Conner (2001): Frank Whittle and the invention of the Jet Engine, Airlife England.

[82] J.Golley: Hans Von Ohain: Elegance in flight, American Institute of Aeronautics and Astronautics, (1996).

[83] J.D.Anderson: Fundamental of aerodynamics, McGraw-Hill, (2001).

[84] W.R.Young: The Helicopters, Time-life, (1983).

[85] O.Lilienthal: Birdflight as the basis of aviation,(1911).

[86] Don Dwiggins: Man-powered aircraft, Tab Books, (1979).

[87] W.Johnson: Helicopter theory, Dover publications, (1980).

[88] http://garyconnery.com/

[89] J.H.Baayen: Automatic trajectory tracking control of kites, PhD of Delft University of Technology, (2011).

[90] M. Ahmed, A.Hably and S.Bacha: High Altitude Wind Power Systems: A Survey on Power Kites, The International conference on electrical machines, (2012): .

[91] M. Ahmed, A.Hably and S.Bacha: Power Maximization of a Closed-orbit Kite Generator System, 50th Conference on Decision and Control and European Control Conference (IEEE CDC-ECC), (2011).

[92] A.Furey and I.Harvey: Evolution of neural networks for active control of tethered airfoils, Advances in Artificial Life Journal, pages 746–755, Springer (2007).

[93] C. Novara, L. Fagiano, M. Milanese : Direct data-driven inverse control of a power kite for high altitude wind energy conversion, IEEE International Conference on Control Applications (2011), pages 240–245 .

[94] P. Williams, B. Lansdorp, W.J. Ockels: Flexible Tethered Kite with Movable Attachment Points, Part II: State and Wind Estimation. AIAA-2007-6629, AIAA Modelling and Simulation Technologies Conference and Exhibit, Hilton Head, SC, USA, 20-23 August 2007.

[95] P. Williams, B. Lansdorp, W.J. Ockels: Flexible Tethered Kite with Movable Attachment Points, Part I: Dynamics and Control. AIAA-2007-6628, AIAA Modelling and Simulation Technologies Conference and Exhibit, Hilton Head, SC, USA, 20-23 August 2007.

[96] G. Baldwin: Kite Power for Heifer Internationals Overlook Farm. PhD thesis, Worcester Polytechnic Institute, (2008).